(NASA-CR-148322) METHODS FOR TESTING HIGH VOLTAGE CONNECTORS IN VACUUM, MEASUREMENTS OF THERMAL STRESSES IN ENCAPSULATED ASSEMBLIES, AND MEASUREMENT OF DIELECTRIC STRENGTH OF ELECTRODES (District of Columbia G3/33

N76-27477
Hc $5.50

Unclas
44631

FINAL TECHNICAL REPORT

Methods for Testing High Voltage Connectors in Vacuum; Measurements of Thermal Stresses in Encapsulated Assemblies; And Measurement of Dielectric Strength of Electrodes in Encapsulants Versus Radius of Curvature.

Renate S. Bever, Principal Investigator

April 15, 1975 - April 15, 1976

NASA Grant #NGR 09-053-003, Supplement 1

District of Columbia Teachers College
1100 Harvard Street, N.W.
Washington, D. C. 20009

ACKNOWLEDGEMENT:

The author wishes to express her appreciation for help received and acknowledge her indebtedness to Mr. John L. Westrom, code 711.3; the following Goddard Space Flight Center Scientists and Engineers gave invaluable aid and advice: Dr. John Sutton, Code 325.1, Mr. Jesse F. Stern, code 325.1; Dr. John J. Park, code 764.3; Dr. Benjamin Seidenberg, code 764.3, Mr. Carrel Clatterbuck, code 764.3; and technicians Kenneth Young, code 711.3 and Elijah Tankisley, code 282.2.

For everythingthere is a seasen,
and a time for every matter under heaven:
a time to be born, and a time to die;
a time to plant and a time to pluck up what is planted;
a time to kill, and a time to heal;
a time to break dewn , and a time to build up;
a time to weep, and a time to laugh.

Ecclesiastes 3: 1-4

ABSTRACT

Newly Initiated Study:

Internal embedment stress measurements were performed, using tiny ferrite core transformers, whose voltage output was calibrated versus pressure by the manufacturer. Comparative internal strain measurements were made by attaching conventional strain gages to the same type of resistors and encapsulating these in various potting compounds. Both types of determinations were carried out while temperature cycling from $77^{o}C$ to $-50^{o}C$.

Continuation Studies:

1. Gas leakage tests on Reynolds connectors were performed.
2. Further Lapshear Adhesive Strengths testing was done on Thiokol Solithane 113, formulations 6 and 11.
3. A more generally applicable set of solutions to the Diffusion equation is presented than heretofore. These solutions are applicable to the case of thick potting compound-small void.
4. Extensive D.C. partial discharge testing was performed, mostly on the HEAO-A high voltage distribution board and also on condensors, up to 5000 volts.

Note: "Measurement of Dielectric Strength of Electrodes in Encapsulants Versus Radius of Curvature" was not carried out, on the advice of the NASA Technical Officer, Mr. John L. Westrom, Code 711.3

TABLE OF CONTENTS

Chapter I. Internal Embedment Stress and Strain.

Introduction:

In the course of potting electronic components or circuits the experimenter will occasionally be witness to the actual act of separation of the potting compound from a portion of the circuitry or to the opening up of a large crack as things are taken out of the curing oven. One can not help but wonder about the order of magnitude of internal embedment stresses as compared to the magnitudes of the adhesive forces and the tensile strengths. It was from such curiosity that both readings in the literature and some actual stress and strain measurements were undertaken.

Theory:

Reporting on stress measurements as a function of polymerization and subsequent temperature cycling is found in journal articles and contract documents. None was found summarized or explained in standard texts on strain gage uses. There are a few review articles [1], [2]. Many methods have been tried, among them embedding ordinary thermometer bulbs as transducers [3], affixing strain gages to either real or simulated circuit components [4,5,6,7,8,9,10], embedding ferrite-core transformers and measuring their output [11,12,13,20], potting so-called Oliphant washers and counting the number of temperature cycles to cracking [14].

The basic Mathematical theory is discussed by several authors. A place to start perhaps is basic Elastic Theory.[15]

The complete stress-strain relationships in a homogeneous, isotropic medium are that the strains e_x, e_y, e_z are given by

$$\frac{\Delta x}{x} = e_x = \frac{1}{Y}\left[\sigma_x - \mu(\sigma_y + \sigma_z)\right] + \alpha \cdot \Delta T \qquad (1)$$

$$\frac{\Delta y}{y} = e_y = \frac{1}{Y}\left[\sigma_y - \mu(\sigma_z + \sigma_x)\right] + \alpha \cdot \Delta T \qquad (2)$$

$$\frac{\Delta z}{z} = e_z = \frac{1}{Y}\left[\sigma_z - \mu(\sigma_x + \sigma_y)\right] + \alpha \cdot \Delta T \qquad (3)$$

if the material of linear expansion coefficient α is being simultaneously heated through ΔT degrees and stressed by $\sigma_x, \sigma_y, \sigma_z$ force/area in the three directions. Y is the linear Young's Modulus and μ is Poisson's ratio which tells by how much a material shrinks in the y or the z direction while being stretched in the x direction, for instance. It lies between 0.2 and 0.3 for most materials. From these basic relations one can draw some deductions.

a. For example, first let $\Delta T = 0$ and obtain an expression for k, the compressibility. Now, the definition of k is the following:

$$k = \frac{1}{\text{Bulk Modulus } B} = -\frac{1}{V} \cdot \frac{\Delta V}{\Delta P} = -\frac{\Delta V}{V} \cdot \frac{1}{\Delta P}$$

By putting $\sigma_x = \sigma_y = \sigma_z = -\Delta P$, where ΔP is applied pressure, V is volume and remembering that $\frac{\Delta V}{V} = \frac{\Delta x}{x} + \frac{\Delta y}{y} + \frac{\Delta z}{z}$

$$\therefore \quad k = \frac{3}{Y}(1 - 2\mu)$$

Substituting $\mu = 0.3$, one gets

$$k = \frac{3(0.4)}{Y} = \frac{1}{B} \qquad \text{or } Y \approx B, \text{ approximately.}$$

This means that for $\mu = 0.3$ materials the Bulk volume modulus is approximately equal to the Young's linear modulus.

b. Now if we permit a temperature change, but restrict the solid from expanding in all directions, basic thermodynamics gives that

$$\left(\frac{\partial P}{\partial T}\right)_V = \frac{\beta}{K} = \frac{3\alpha}{K}$$

since the thermal volume coefficient of expansion β is 3 times the linear one, α. Therefore,

$$\left(\frac{\partial P}{\partial T}\right)_V = 3\alpha B \cong 3\alpha Y \cong \left(\frac{\partial P}{\partial T}\right)_\ell \cdot 3$$

This means that a three-dimensionally restrained solid, while being heated, builds up approximately 3 times the internal pressure as a one-dimensionally restrained body if μ = 0.2 to 0.3.

What for instance exerts restraint? The potting container if made of rigid non yielding, thick-walled metal, would be a good example of two-dimensional restraint, most severe, because it keeps the entire size of the potting mass from doing what it wants. Resistors and other circuit components soldered parallel to each other between two printed circuit boards, perpendicular to the planes of the circuit boards in cordwood fashion represent one-dimensional restraint. Embedded components represent restraints because they keep the resin surrounding them from shrinking inward as much as it would like upon polymerizing or upon cooling, or if the adhesive forces are good, from expanding outward as much as it would like upon heating. The adhesion of the potting compound to the circuit components acts as a restraint.

Using equations (1), (2) and (3) one can make calculations as to the theoretical magnitude of these stresses. In the case of <u>one-dimensional restraint</u>, $e_x = 0$, $\sigma_z = 0$, $\sigma_y = 0$

$$\therefore 0 = \frac{1}{Y}\sigma_x + \alpha \cdot \Delta T$$

$$\therefore \sigma_x = -\alpha Y \cdot \Delta T$$

and also,

$$e_y = -\frac{\mu}{Y}\sigma_x + \alpha \cdot \Delta T$$

$$e_z = -\frac{\mu}{Y}\sigma_x + \alpha \cdot \Delta T$$

If one uses some plausible numbers for Epon 828, namely[23] $Y = 0.5 \times 10^6$ psi, $\mu = 0.3$, $\alpha = 50 \times 10^{-6}$ /°C, one gets

$$\therefore \sigma_x \cong 25 \text{ psi}/^\circ\text{C}$$

In the case of <u>two-dimensional restraint</u>, $e_x = e_y = 0$, $\sigma_z = 0$

$$\sigma_x = \sigma_y = \frac{-(\mu+1)\alpha Y \cdot \Delta T}{(1-\mu^2)}$$

$$\therefore \sigma_x \cong 35 \text{ psi}/^\circ\text{C}$$

<u>Three-dimensional restraint</u> means $e_x = e_y = e_z = 0$ and

$$\sigma = \frac{-\alpha Y \cdot \Delta T}{1-2\mu}$$

$$\therefore \sigma \cong 70 \text{ psi}/^\circ\text{C}$$

This would mean that Epon 828, if cooled through 100°C being prevented from shrinking by an embedded component would build up 7000 psi compressive pressure on it. On the other hand, a rubber of Y = 1000 psi and α = 300 x 10^{-6} /°C would only build up about 1 psi/°C compressive stress or one to two atmospheres if heated thru 20°C without permission to expand.

The above analysis assumes that the restraining agent is totally non-yielding. A more realistic point of view is that it does expand and contract some, much less than the resin. Therefore, the α that comes into play is (α plastic - α other). This leads essentially to the theory of some of the authors, such as Dewey and Outwater[16], whose expression for radial shrinkage pressures in cylindrical geometry is

$$P = Y (\alpha_{pl} - \alpha_{emb}) \cdot \Delta T \Big/ \frac{D^2 + d^2}{D^2 - d^2} + \mu$$

where D = diameter of the outside of the plastic cylinder and d = diameter of the embedded component.

A more complete analysis of effects on potted components is given by Baker [17], also by Frankland et al [18]. Here we have the one-dimensional restraint case as shown in the sketch below

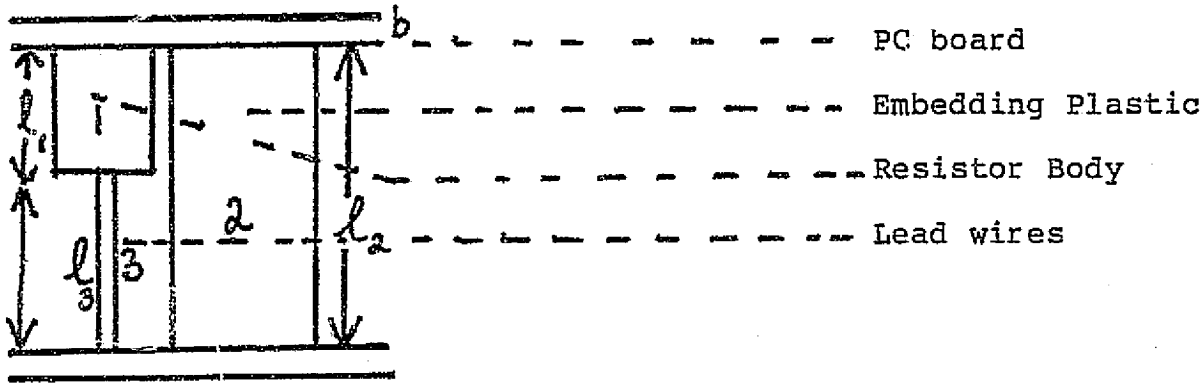

Therefore the net change in length

$$\Delta X_{net} = [\alpha_2 l_2 + \alpha_b l_b - \alpha_1 l_1 - \alpha_3 l_3]\,\Delta T$$

The stiffness of each material, S, is

$$S = \frac{\psi A}{l} \quad \text{lbs/inch} = \frac{1}{\text{Flexibility}}$$

where l is the length or thickness of each participant and A is the cross section.

The load in lbs is F

$$F = \sum_i^n \alpha l \Delta T \Big/ \sum_i^n \frac{l}{\psi A}$$

Therefore the stress in lbs/inch^2 in any one participant is

$$\sigma_1 = \frac{[\alpha_2 l_2 - \alpha_1 l_1 - \alpha_3 l_3]\,\Delta T}{\left[\frac{l_1}{\psi_1 A_1} + \frac{l_2}{\psi_2 A_2} + \frac{l_3}{\psi_3 A_3}\right] A_1} \qquad (4)$$

This equation, will be referred to again later when the treacherous behavior of elastomers like silicones and soft polyurethanes is discussed as found by Kerlee[19].

Method and Results:

Figures 1-5 are results with 3-dimensional compression measurements using the tiny ferrite-core transformers and excitation-read-out circuit discussed by Stucki, Dallimore et all[11,12,13], and marketed by International Technical Industries. The tiny transformers are sold already calibrated, output voltage versus pressure. The zero-setting for the tiny transformer output voltage is arbitrary, and there is no vernier control on this potentiometer, so that it is not possible to carefully reset it if it has been disturbed. The raw data of transformer output voltage versus thermocouple read-out voltage (indicating temperature) is presented for each potting compound in figures 1-4, namely Epon 828 in figure 1, Solithane 113, formulation 11 in figure 2, Sylgard 184 in figure 3 and sandfilled Sylgard 184 in figure 4. It must be remembered again that the "before potting" curves (crosses) are at an arbitrary voltage level with respect to the "after potting" curves on each graph. These graphs then give no information about the stresses set up during the curing of the encapsulants, but do show the stresses developed during temperature cycling. Whereas the "before" curves of the transducers are almost constant with temperature, the "after" curves rise more or less steeply as the resins are cooled from +77°C to -50°C. The unfilled Sylgard 184 is the exception, with before and after curves almost parallel,

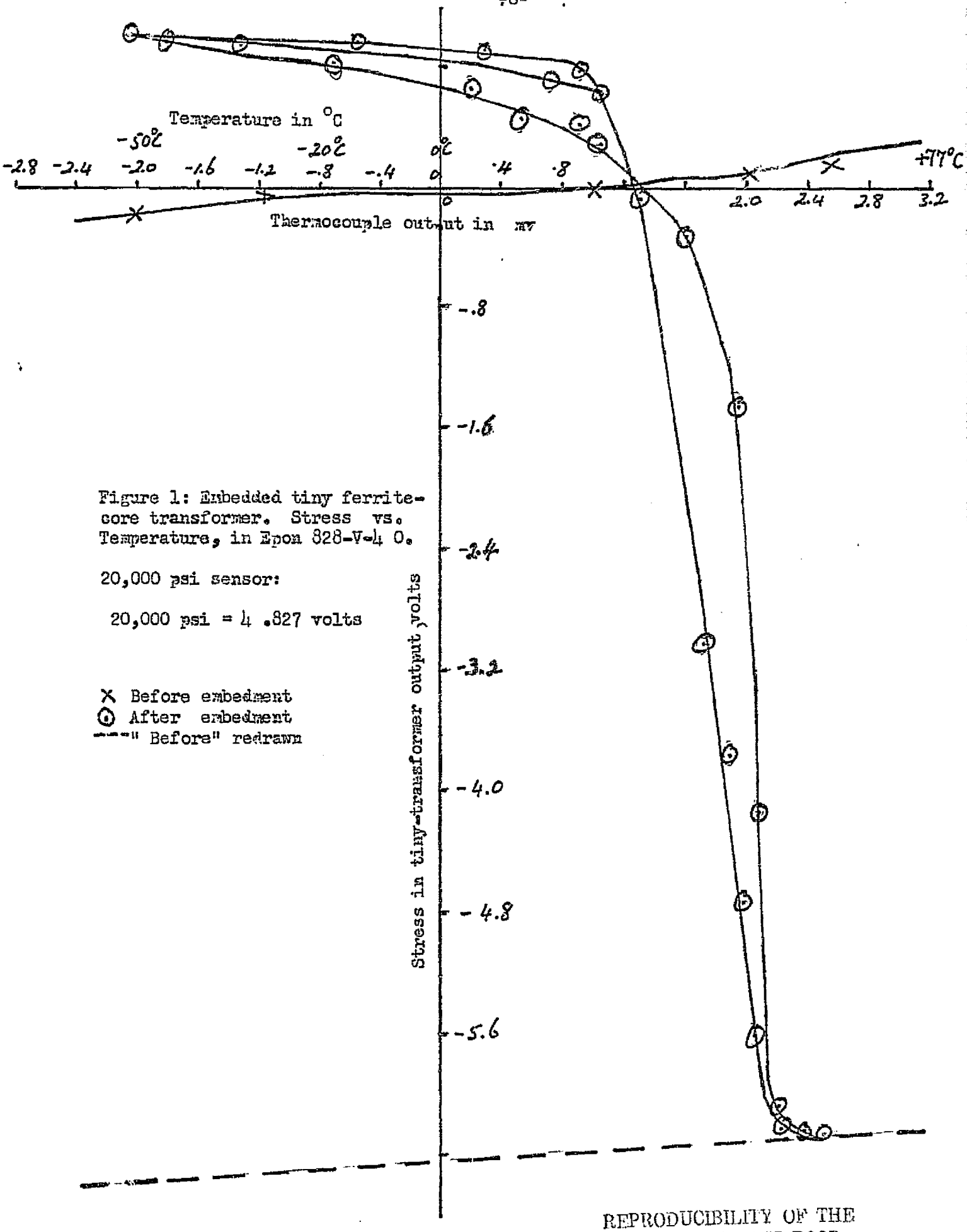

Figure 1: Embedded tiny ferrite-core transformer. Stress vs. Temperature, in Epon 828-V-4 0.

20,000 psi sensor:

20,000 psi = 4 .827 volts

× Before embedment
⊙ After embedment
- - - " Before" redrawn

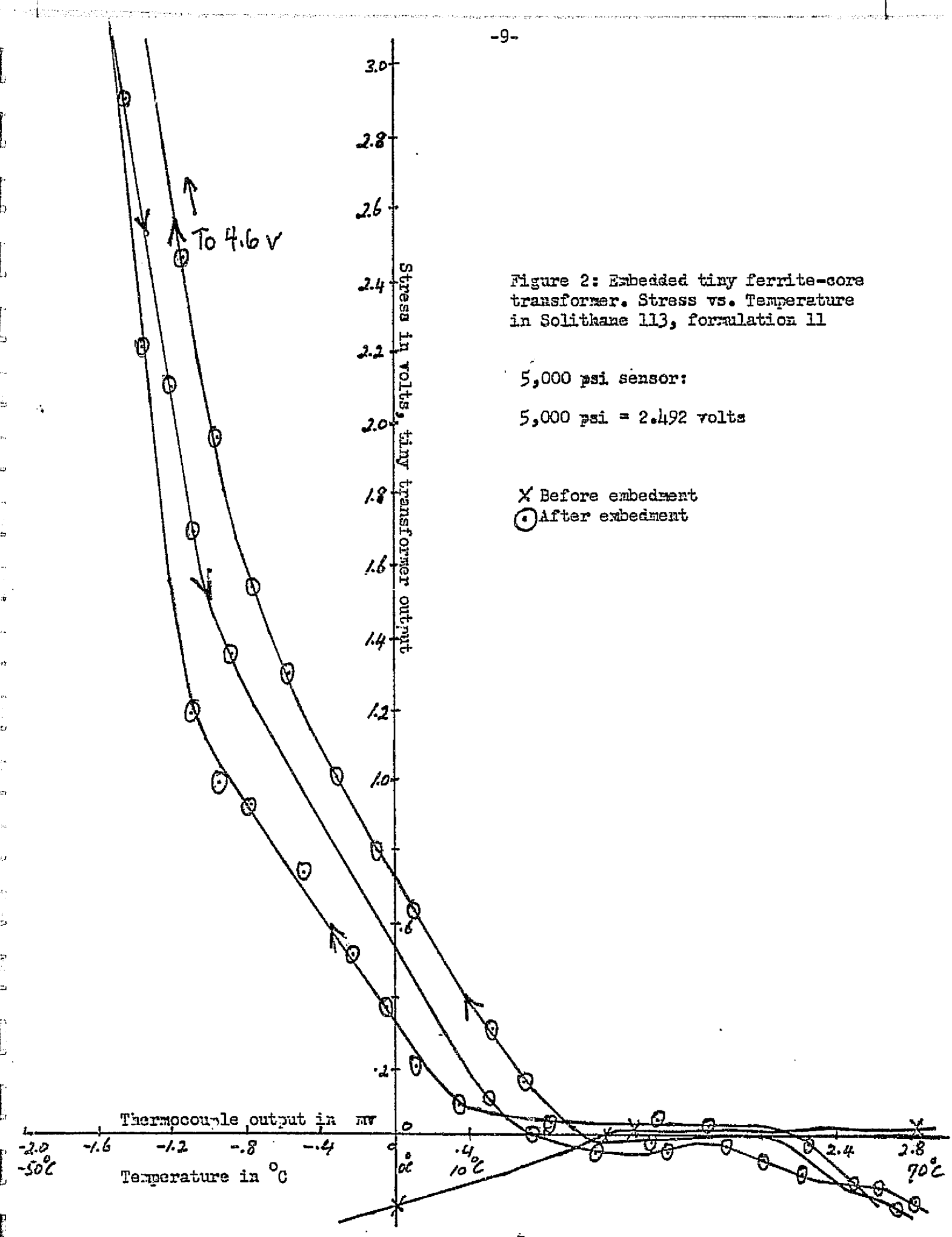

Figure 2: Embedded tiny ferrite-core transformer. Stress vs. Temperature in Solithane 113, formulation 11

5,000 psi sensor:

5,000 psi = 2.492 volts

X Before embedment
⊙ After embedment

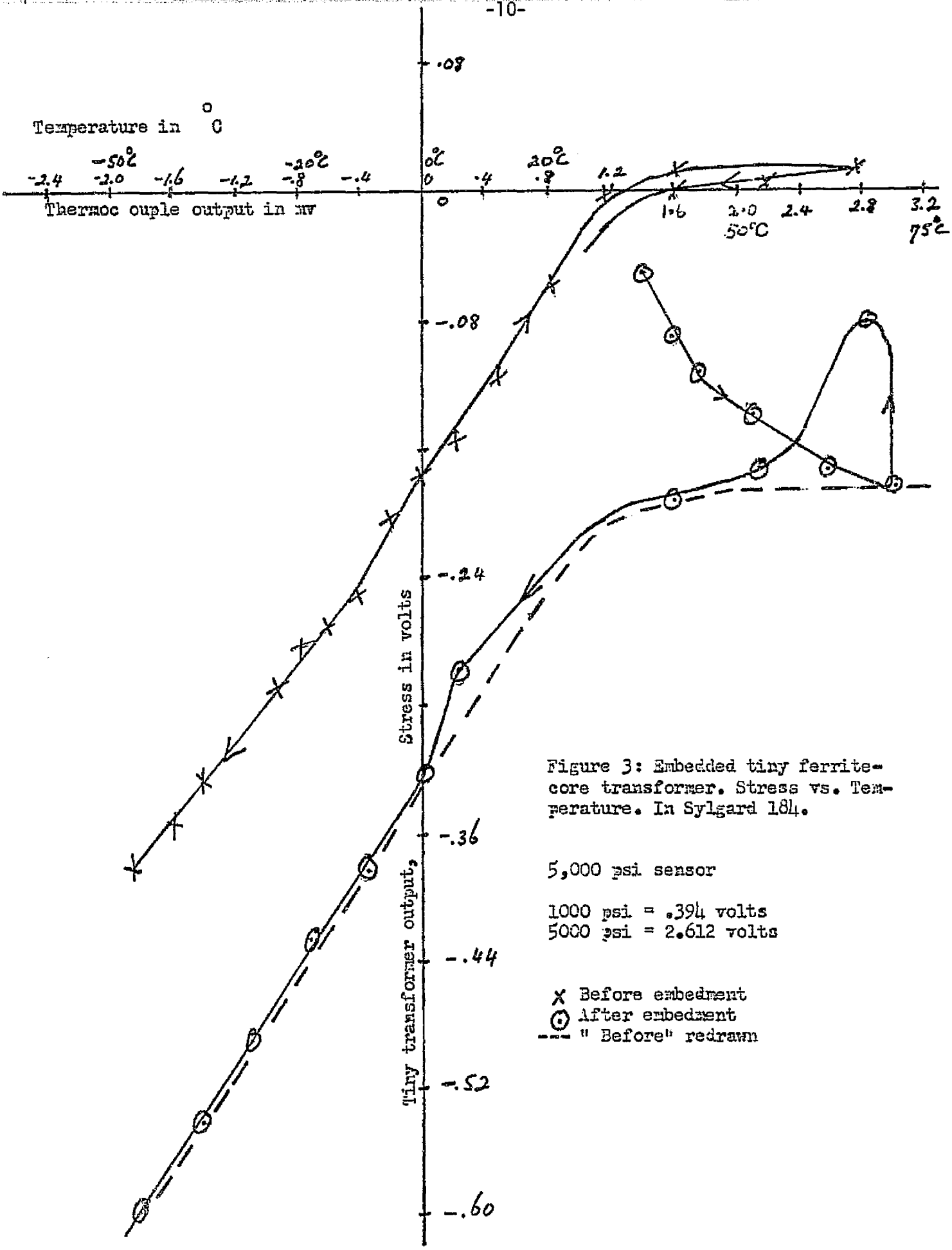

Figure 3: Embedded tiny ferrite-core transformer. Stress vs. Temperature. In Sylgard 184.

5,000 psi sensor

1000 psi = .394 volts
5000 psi = 2.612 volts

X Before embedment
⊙ After embedment
--- " Before" redrawn

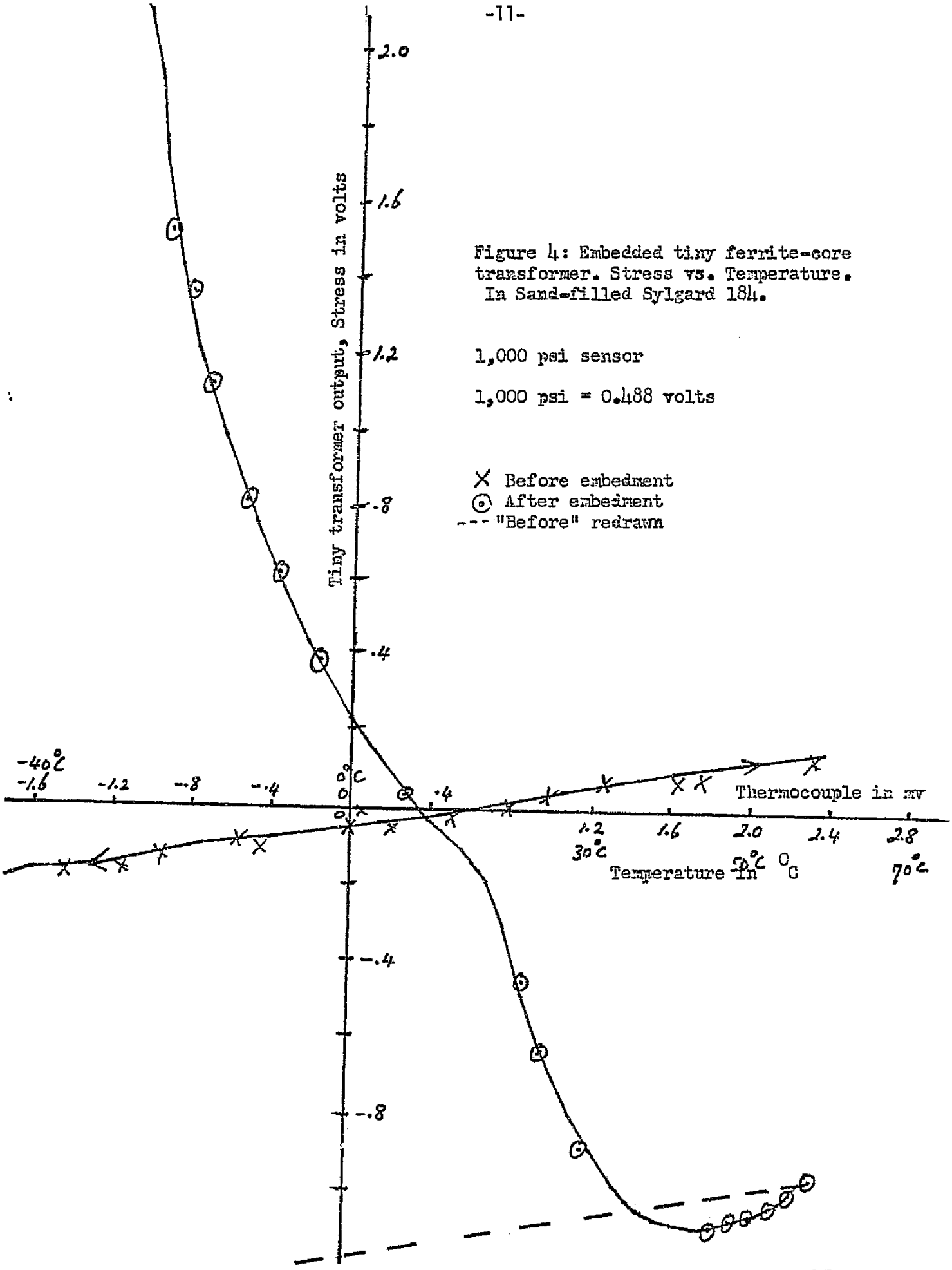

Figure 4: Embedded tiny ferrite-core transformer. Stress vs. Temperature. In Sand-filled Sylgard 184.

1,000 psi sensor

1,000 psi = 0.488 volts

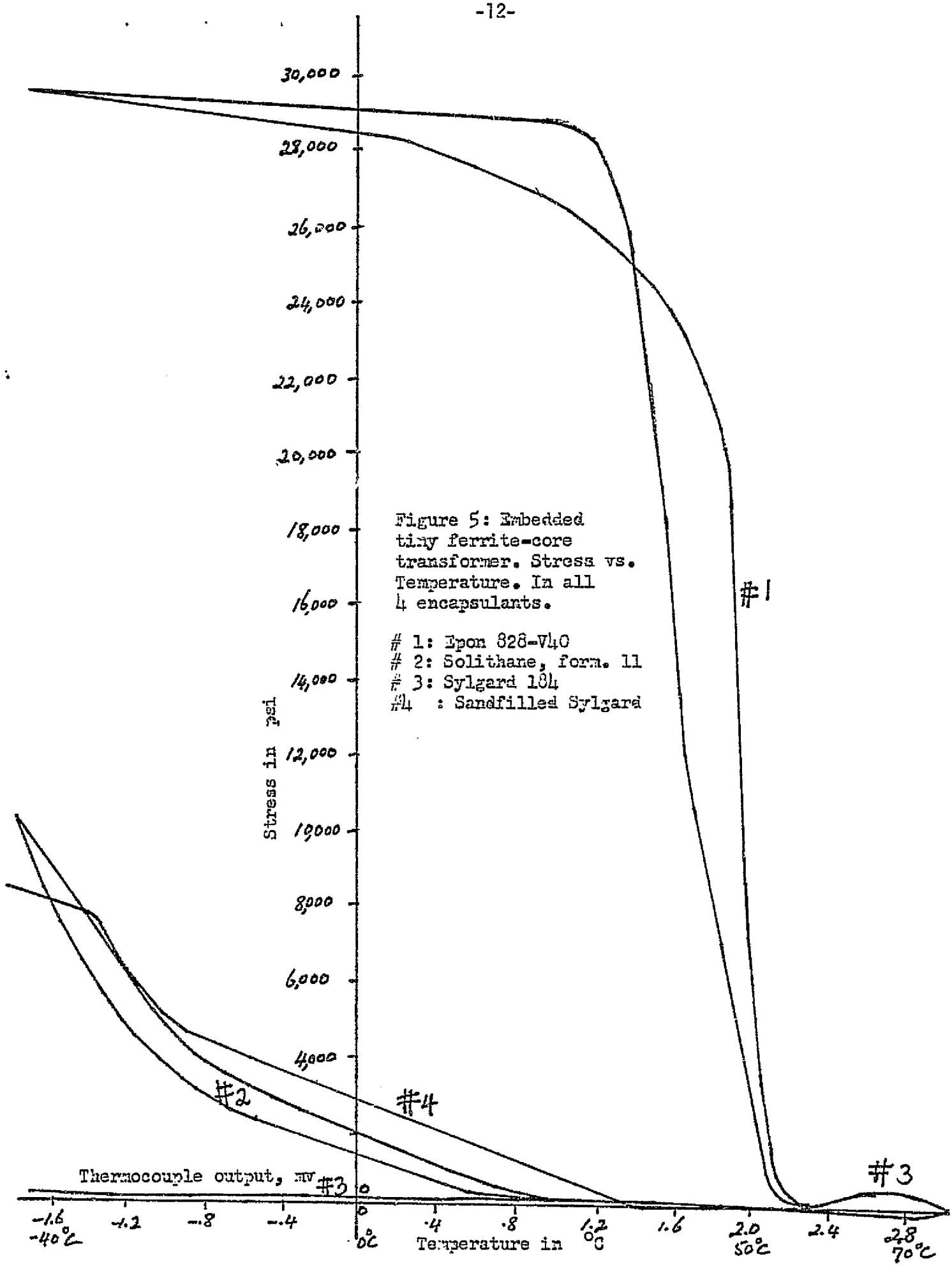

Figure 5: Embedded tiny ferrite-core transformer. Stress vs. Temperature. In all 4 encapsulants.

1: Epon 828-V40
2: Solithane, form. 11
3: Sylgard 184
#4 : Sandfilled Sylgard

meaning very little stress set up by temperature cycling. There is a hysteresis at the high-temperature end of the run, amounting to about 250 psi and quite reproducible on successive cycles.

To obtain figure 5, the "before" curves were arbitrarily moved down to the "after' level at the high temperature end, subtracted out, and the pressure calibration supplied by the manufacturer applied. Figure 5 then, shows compressive stress versus temperature for all 4 encapsulant systems tested. The Epon 828 epoxy rises very steeply to about 30,000 psi during a narrow cooling range from about 50°C to 40°C and then increases little beyond that high stress value with further cooling. The unfilled Sylgard exerts practically zero-stress on this comparative scale. The filled Sylgard, sand-impregnated, however, is quite another matter, rising gradually and fairly linearly to a compressive stress of about 8000 psi by the time it has been cooled to -50°C. The Solithane, formulation 11, rises even more steeply to a stress of 10,000 psi, having its steepest slope at the coldest temperature as though worse is yet to come. The slope behavior, in a very rough approximation, depends on the temperature at which the glass transition of the resin occurs: The Epon 828 epoxy becomes glassy and hard, already considerably above room temperature, the Solithane approaches glass transition not too far below the -50°C limit of the cold run, whereas for the Sylgard even at -50°C a second order transition is not anywhere "in sight" yet. What is disturbing and surprising, however, is the actual magnitude of the -50°C compressive stresses developed: 30 000 psi for the Epon 828 and 10,000 psi for the Solithane 113,

formulation 11. Remember that 1 atmosphere is 15 psi, so this would amount to 2000 atmospheres.

Figure 6 to 12 show comparative strain measurements. A BLH strain gage was mounted longitudinally on the outside of a Caddock resistor MG721, 50 megs, 1%, of cylindrical geometry, and this was then potted in a cylindrical vial of very thin polyethylene, in the various resins. The only exception was figure 8, which was obtained from a strain gage mounted on the inside of a hollow steel cylinder with ends closed off to keep the embedding resin out of the hollow cylinder. Because of that cylinder's much larger O.D., it was then potted in a proportionately scaled up polyethylene container, actually a pint container. To return to the above mentioned resistors for mounting the strain gages, they were chosen by accident, so to speak. After very discouraging tries with flat, ceramic slab resistors that were too difficult to stretch and compress, and which therefore were insensitive to the effects of potting stresses, the experimenter used the above mentioned resistors with great enthusiasm, when these actually showed significant and fairly reproducible strain effects, both due to the initial curing of the resins and due to temperature cycling. It must be emphasized what has meaning here and what does not. There the "before" and "after" relative positions of the curves on any one figure do have meaning. The BLH 1200 Wheatstone bridge and straingage read-out instrument is a well regulated instrument with precision verniers on the zero-setting dials that can be reset to the same value if disturbed between the "before" and "after" runs. The strain gage, of course,

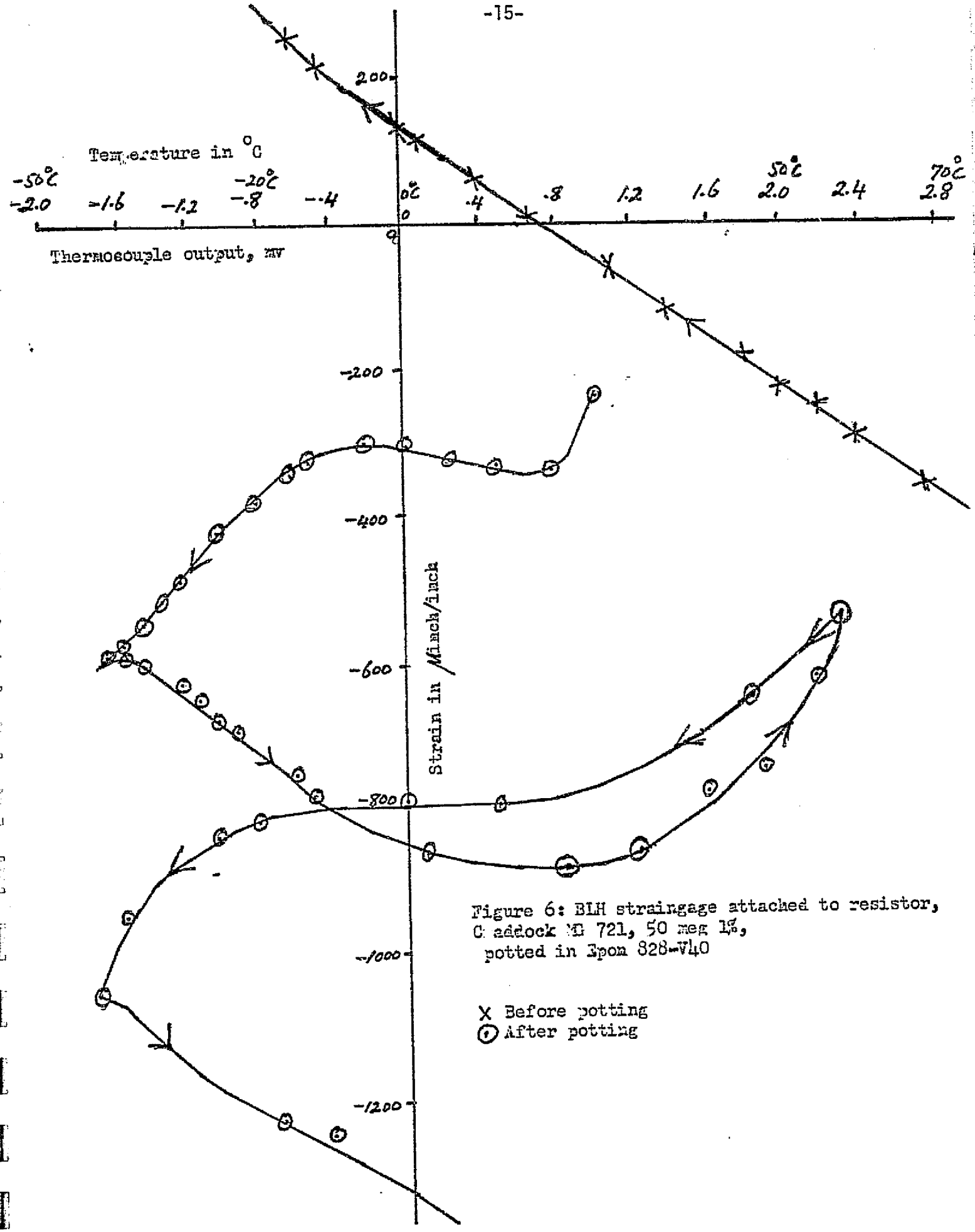

Figure 6: BLH straingage attached to resistor, Caddock MG 721, 50 meg 1%, potted in Epon 828-V40

X Before potting
⊙ After potting

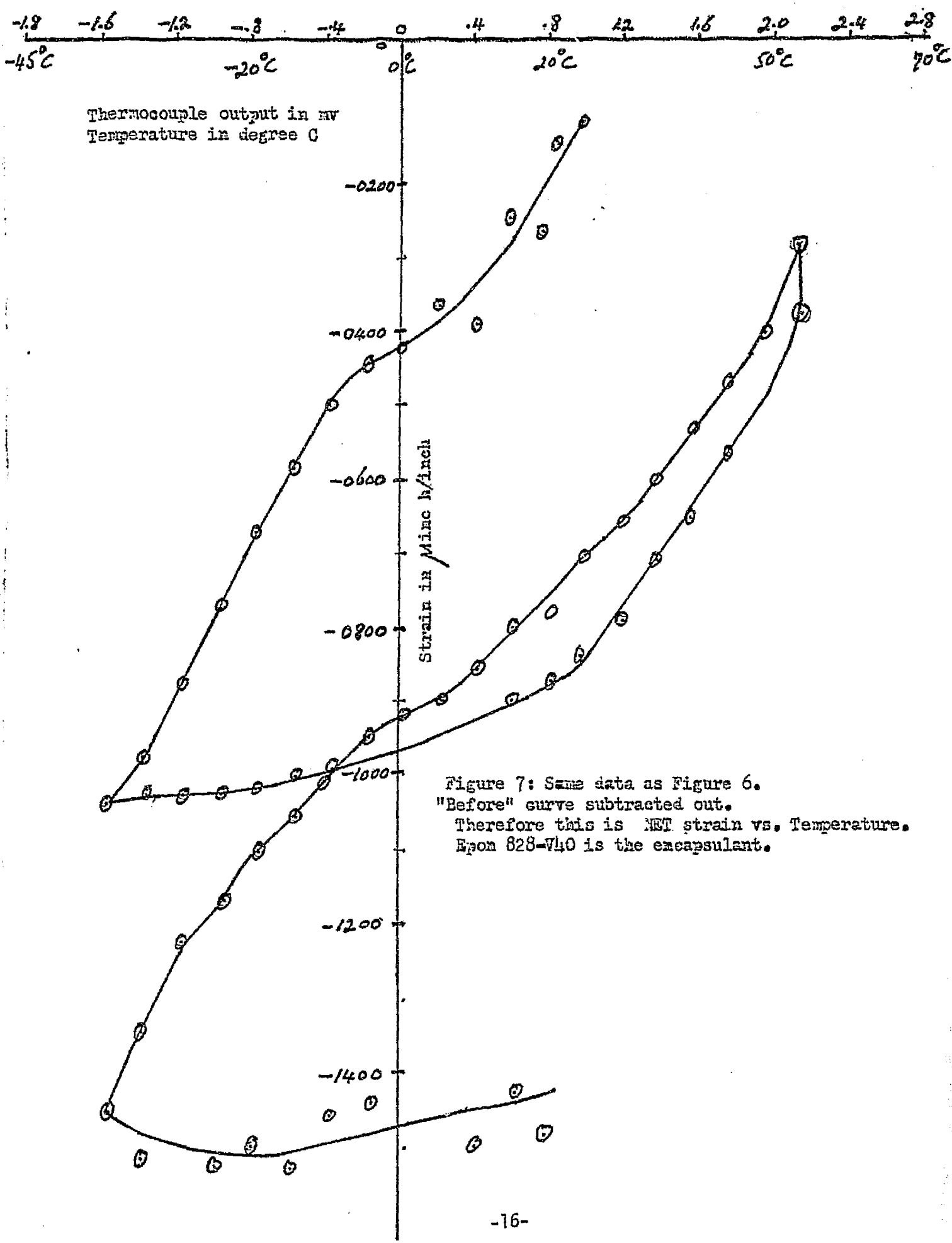

Figure 7: Same data as Figure 6.
"Before" curve subtracted out.
Therefore this is NET strain vs. Temperature.
Epon 828-V40 is the encapsulant.

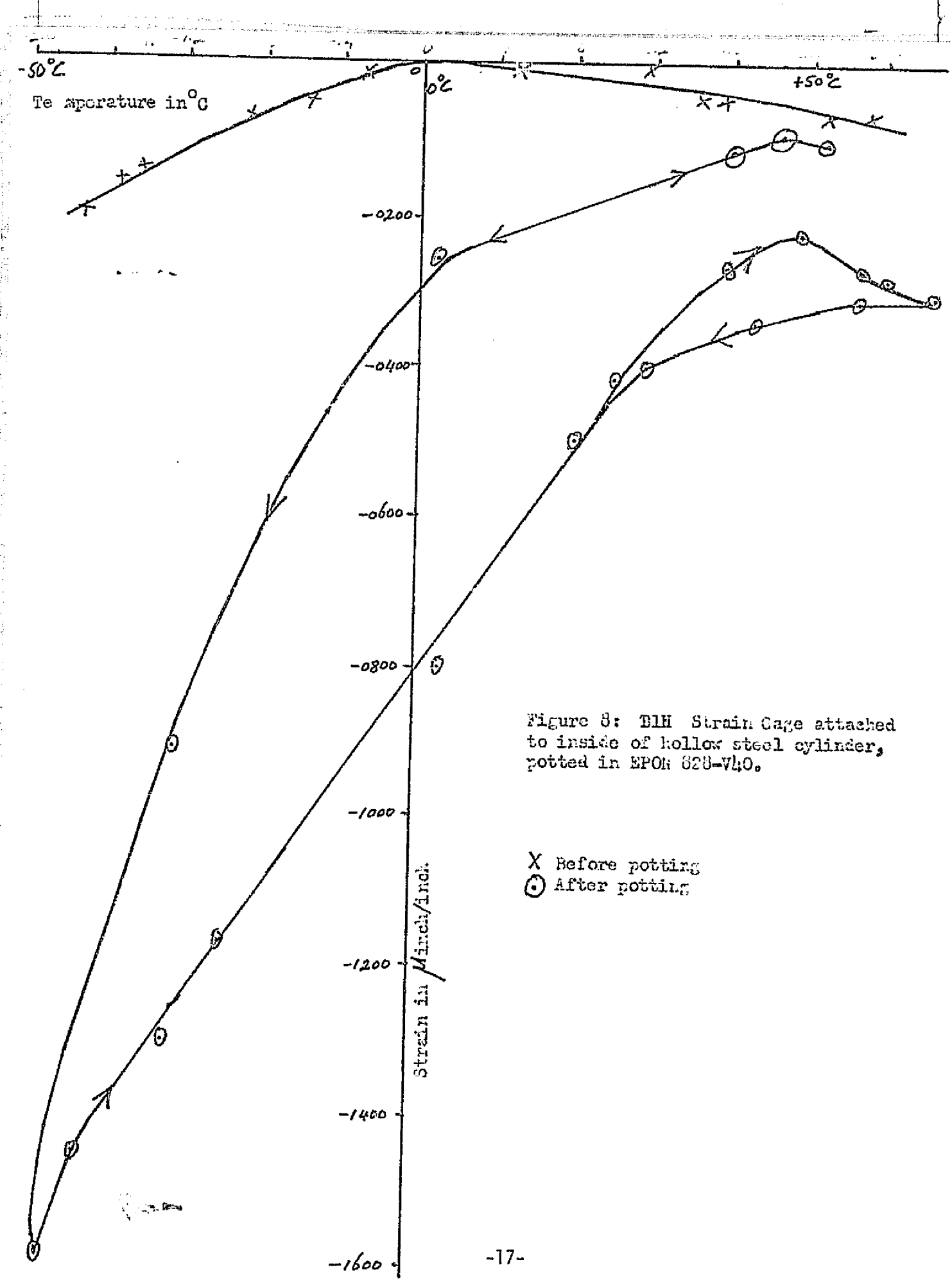

Figure 8: BLH Strain Gage attached to inside of hollow steel cylinder, potted in EPON 828-V40.

X Before potting
⊙ After potting

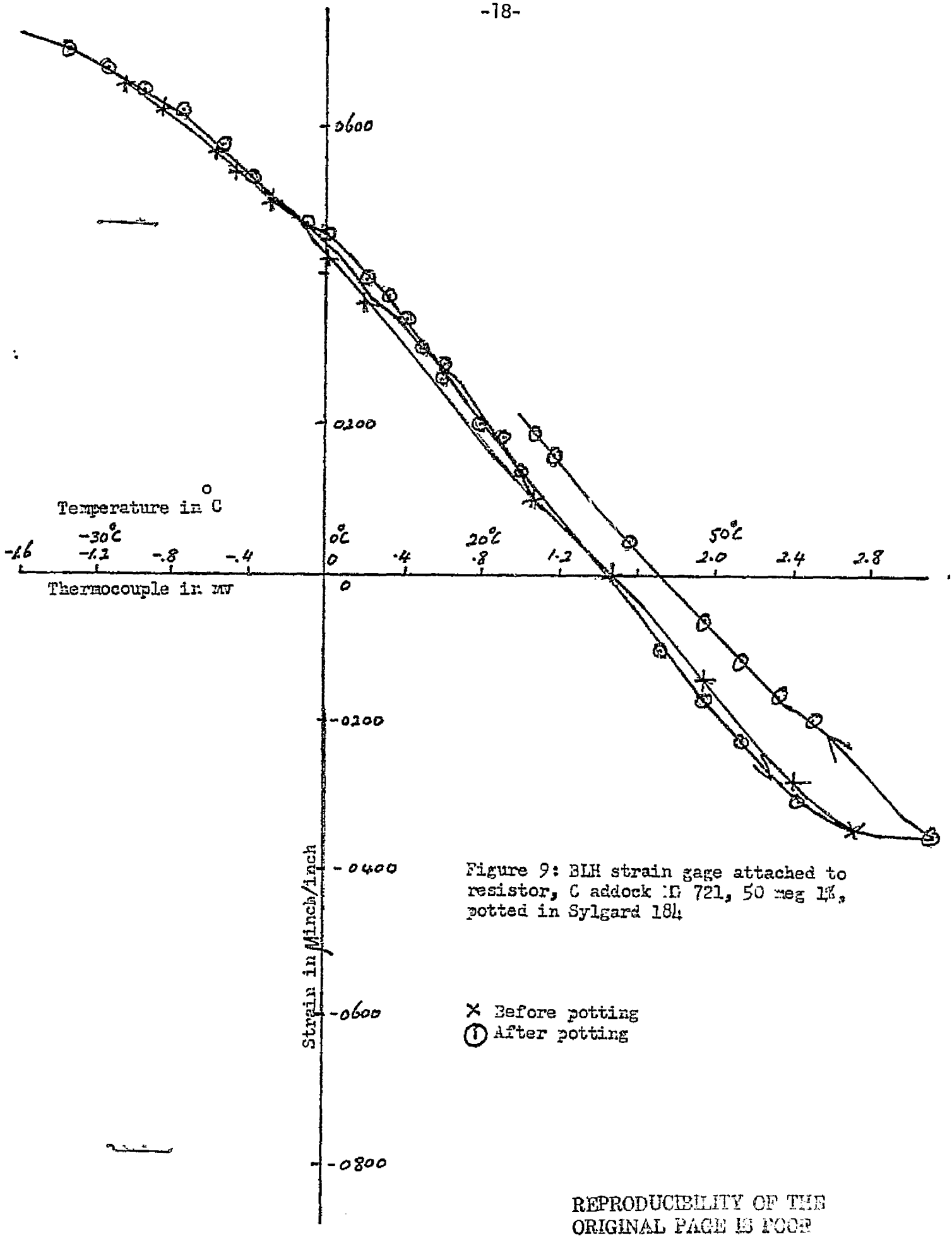

Figure 9: BLH strain gage attached to resistor, C addock ID 721, 50 meg 1%, potted in Sylgard 184

× Before potting
① After potting

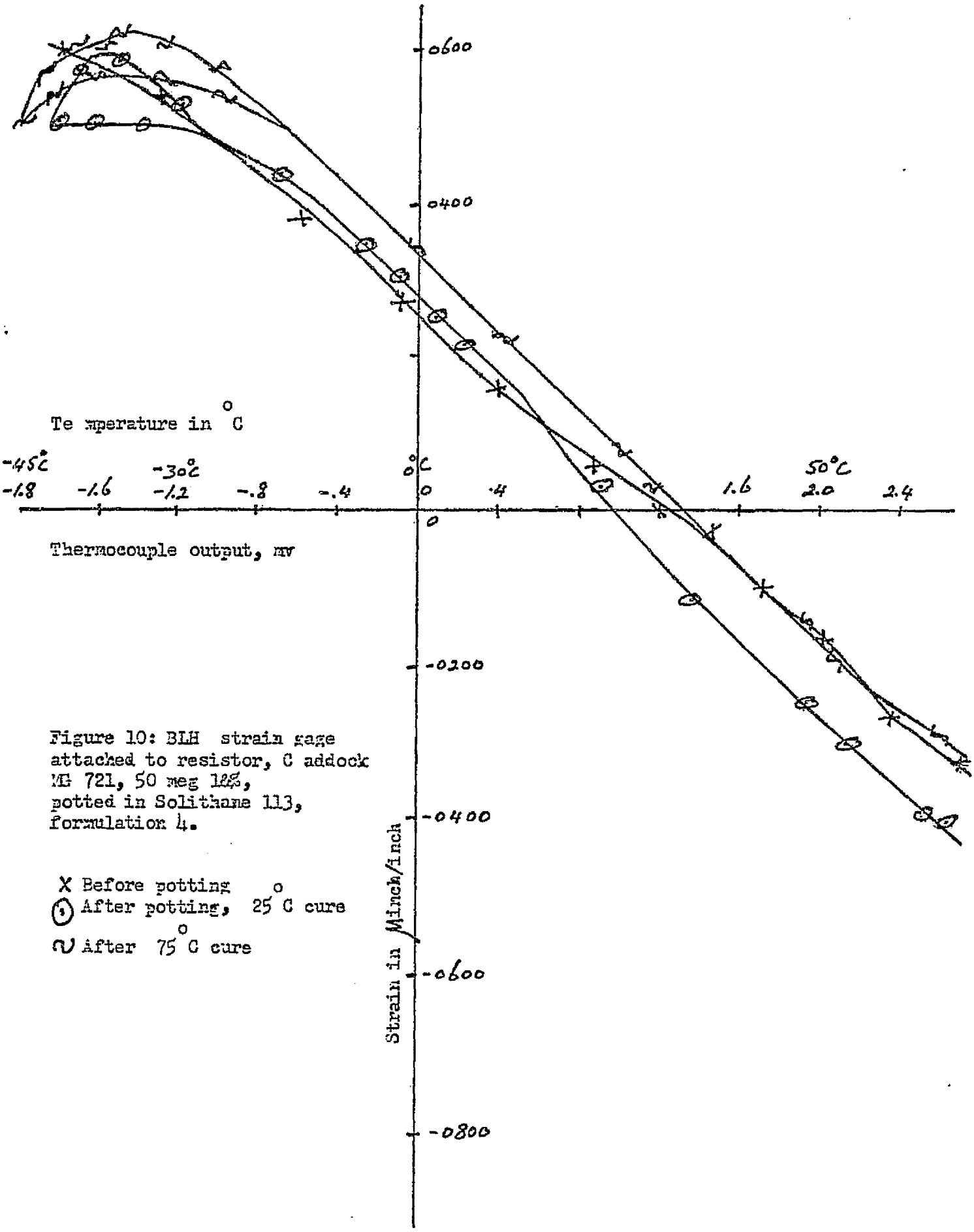

Figure 10: BLH strain gage attached to resistor, C addock MG 721, 50 meg 1%, potted in Solithane 113, formulation 4.

X Before potting
(1) After potting, 25° C cure
∿ After 75° C cure

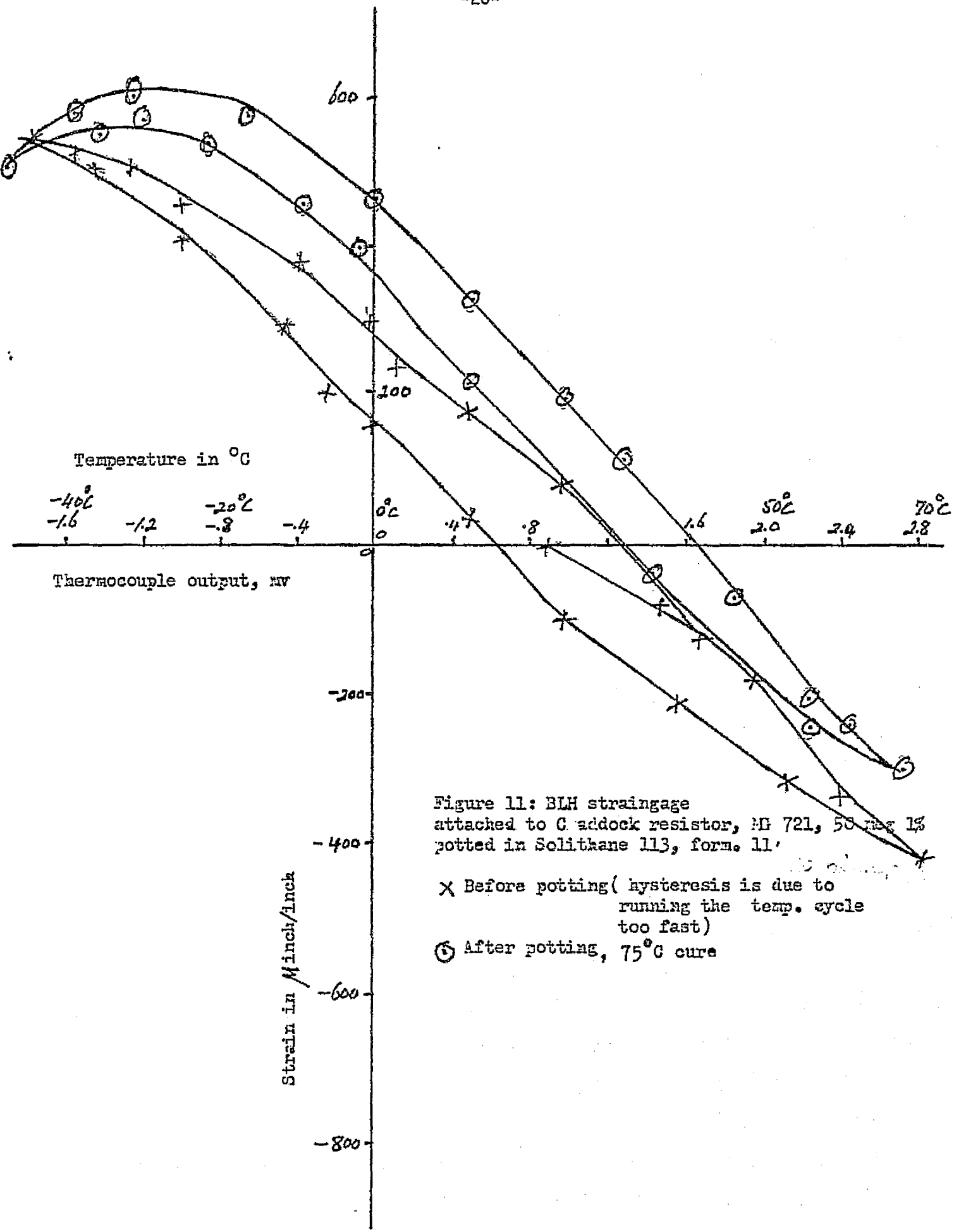

Figure 11: BLH straingage attached to C addock resistor, MG 721, 50 meg 1% potted in Solithane 113, form. 11.

× Before potting (hysteresis is due to running the temp. cycle too fast)

⊙ After potting, 75°C cure

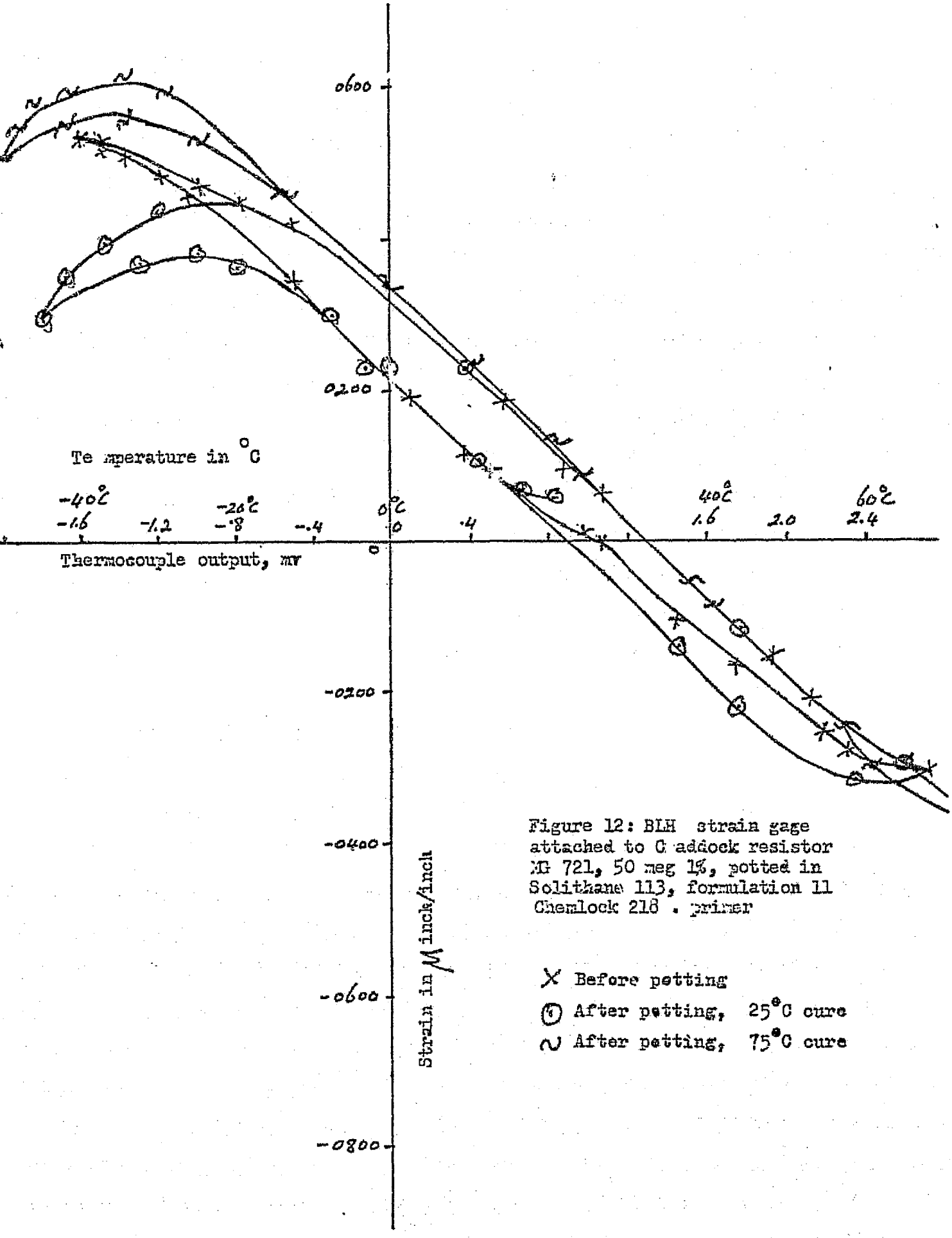

Figure 12: BLH strain gage attached to C addock resistor MF 721, 50 meg 1%, potted in Solithane 113, formulation 11 Chemlock 218 . primer

X Before potting

① After potting, 25°C cure

② After potting, 75°C cure

also responds to both tension (+) and compression (-). The absolute value of the strains depends, of course, on what the strain gage is attached to, what its geometry is and what the geometry of the potting vessel is. The resistor with strain gage attached should be placed in a hydraulic pressure vessel, and calibration be obtained of strain of that particular resistor with attached gage, versus pressure, in psi. From this calibration of micro inch/inch versus psi more absolute information about the behavior of any one potting compound could be deduced. As the experiments with strain gages were originally carried out, the results were purely comparative. It was not until the end of this test series that a hydraulic pressure vessel became available and several stress-strain calibration runs were made in hydraulic oil, on these Caddock resistors with strain gage attached.

A point that needs belaboring is the question as to why not at least a half-bridge for temperature compensation was used, not to speak of a four-arm bridge to cancel out bending effect. Actually, a half-arm bridge was first used, several times, with the disturbing results that the "before potting" runs showed no temperature compensation whatsoever. The longitudinal gage elongated with cooling while the transverse gage contracted. This was totally puzzling until it was realized that the inside of the resistor is actually a spiral metal ribbon wound as a spring which coils tighter when being cooled and thus gets longer. It was then decided to use a single gage as a quarter-bridge and every time take a "before" and "after" temperature cycle. The two curves can then be subtracted if

desired to give the net effect of temperature cycling when the unit is embedded in the resin.

Figure 6 shows strain gage data thus obtained with Epon 828 as the potting resin. It turns out to be a beautiful example of a thermal ratchet. Due to the large compressive forces exerted by the Epon 828 there seems to be permanent deformation of the strain gage or resistor at the -50° end. Warming and doing the cycle over again gives the same shape of cycle, but displaced to more negative values of strain. Figure 7 is the same data with the net strain plotted, the "before" curve having been subtracted out. The Epon 828 was then repeated, but this time potting a hollow, thin-walled steel cylinder with strain gage inside to keep the resin from pressing directly upon it. The general shape of the strain-temperature loop is the same, but the thermal ratchet effect has disappeared. Note also that just the curing effect alone, without temperature cycling causes compressive strains, and the "after" curves lies below the "before" one. Moreover, the temperature cycling produces a pronounced hystesis effect. See Figure 8.

By contrast, Figure 9 of resistor potted in Sylgard 184 has the "before" and "after" potting curves superimposed, which means very little stress, until the Sylgard has been heated to the highest temperature of 77°C, following which there seems to be a relatively small constant tensile strain. Figure 10 is for Solithane formulation 4, and both Figures 11 and 12 are for Solithane formulation 11. The "before" and "after" curves here have the same slope and almost coincide (but not quite) until the

temperature reaches about -20°C. Then the "after" curve bend downward showing compressive response. One point which at first examination seems minor is that the "after" curves either coincide when Chemlok 218 primer is used or lie above the "before" curves. When the Solithane has been further heat-cured at 150°F the "after" curves lie further above. This means that the curing for some reason causes the Solithane to exert tensile forces on the resistors. Perhaps this is the reason why, as the Solithane was taken from the curing oven, breaking away of it from the embedded resistor was observed several times. The loss of adhesion was then always followed by a cracking apart of the Solithane along the axis of the cylinder like splitting a log. No such difficulties were ever encountered with the Epon 828 or the Sylgard embedments. A resistor with strain gage was encapsulated in Solithane, formulation 11, this being done asymmetrically in a mold of cubical shape to see if the potting vessel geometry caused the above named effects. The results were negative, as seen in Figure 13, which looks just like the graphs obtained with the concentric cylinder geometry: after curing, the resistor is under tension rather than compression, and a net compressive strain does not appear until the sample has been cooled below 0°C.

Figures 14 and 15 are calibration graphs of stress versus strain of the same type of Caddock resistors with the same type of strain gages attached as the ones that were actually potted. The calibration was carried out in hydraulic oil in a custom built pressure vessel, equipped with well insulated electric

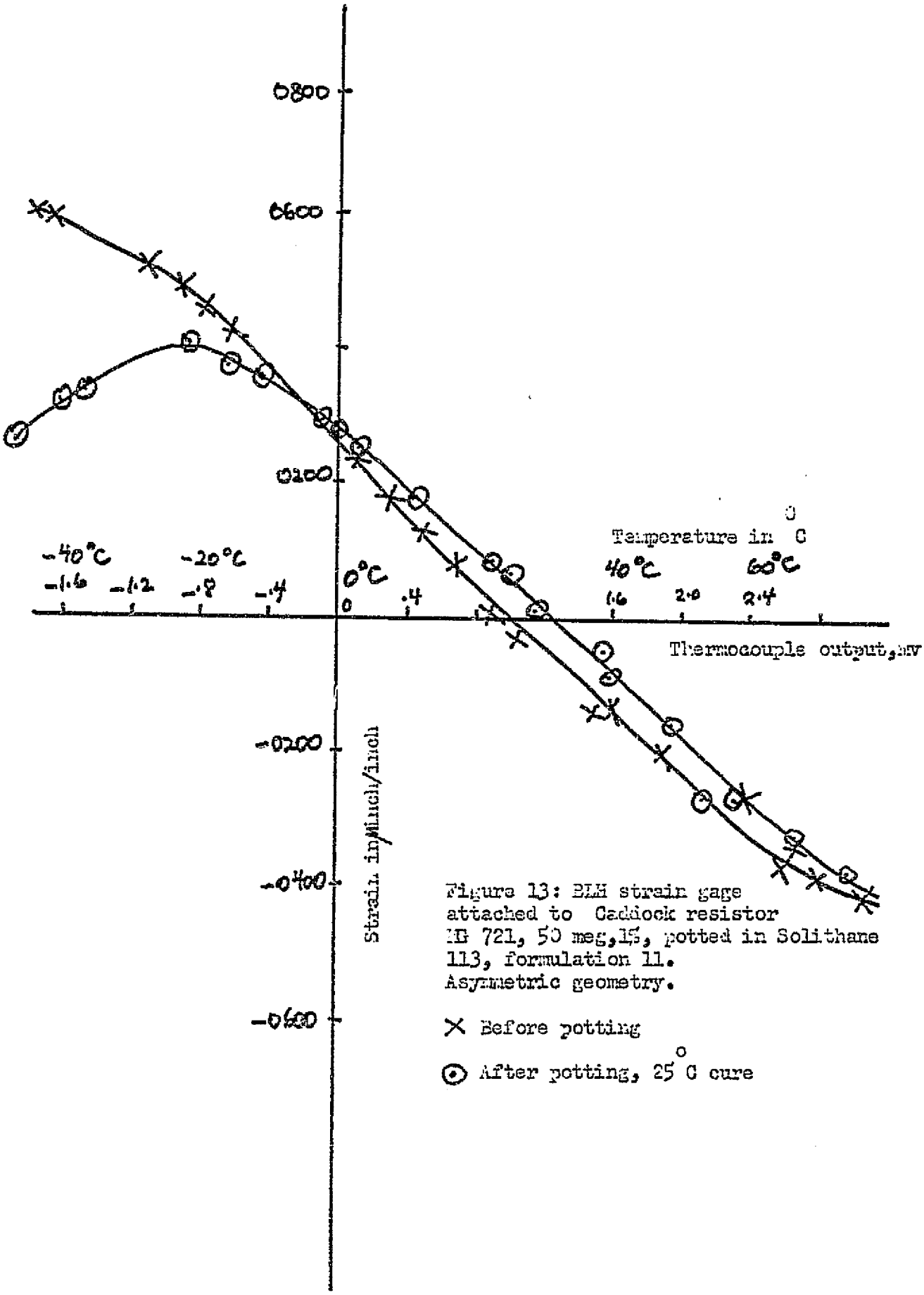

Figure 13: BLH strain gage attached to Caddock resistor MG 721, 50 meg, 1%, potted in Solithane 113, formulation 11. Asymmetric geometry.

× Before potting

⊙ After potting, 25°C cure

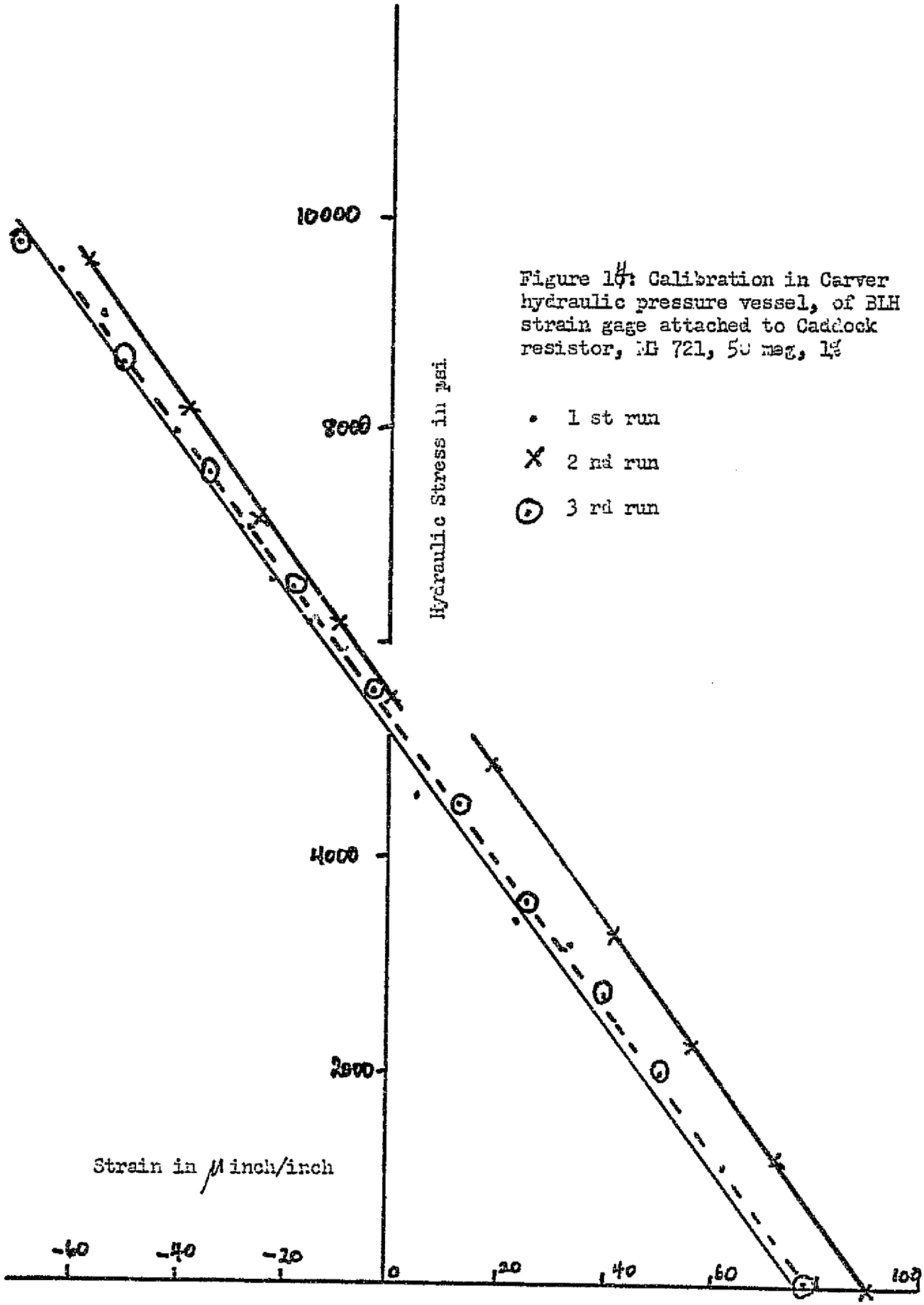

Figure 14: Calibration in Carver hydraulic pressure vessel, of BLH strain gage attached to Caddock resistor, MG 721, 50 meg, 1%

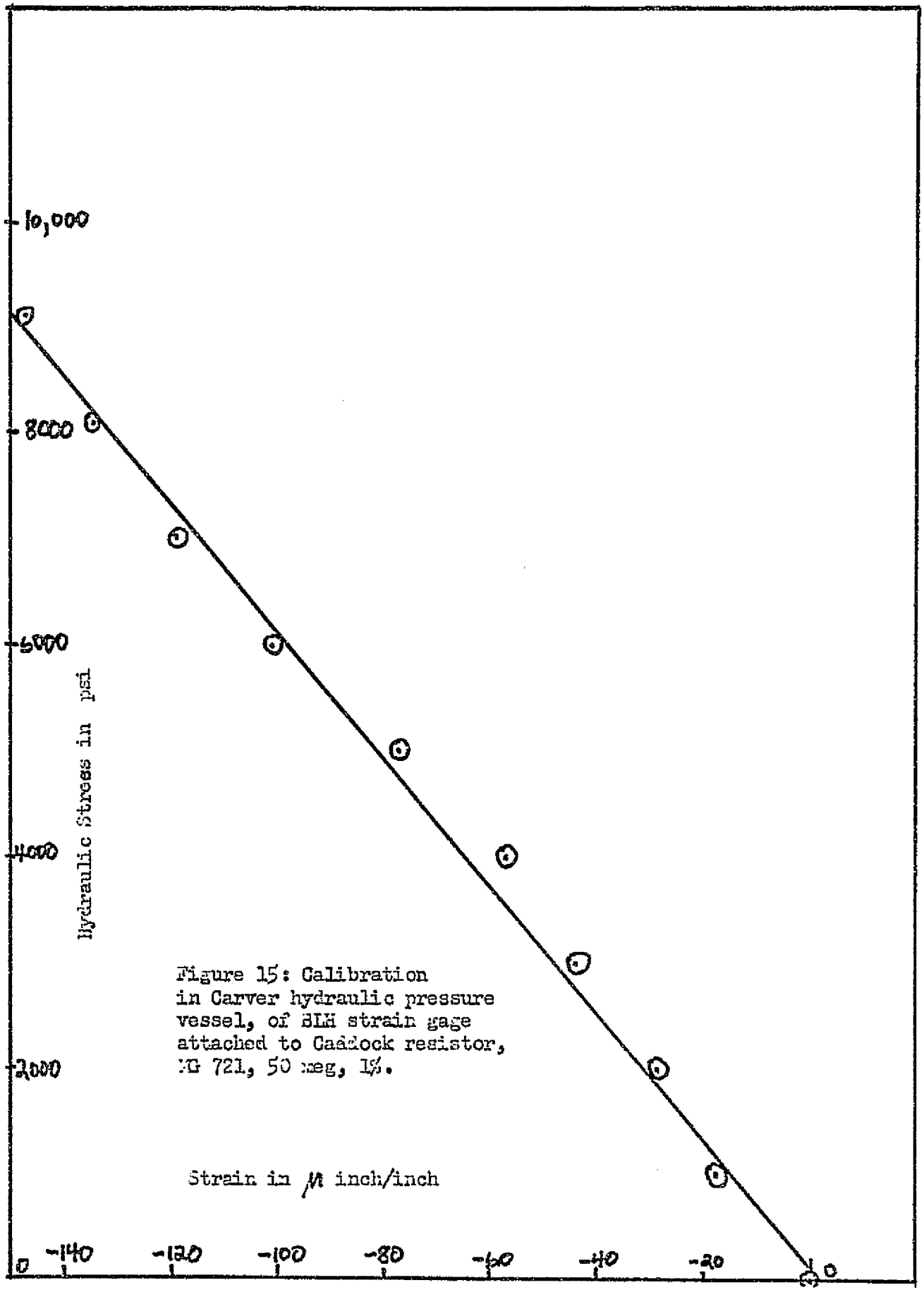

Figure 15: Calibration in Carver hydraulic pressure vessel, of BLH strain gage attached to Caddock resistor, MG 721, 50 meg, 1%.

feedthroughs. The calibration was carried out up to 10,000 psi after ascertaining that there were no electric leakage currents between the feedthroughs. The two resistors calibrated have almost identical slopes of 61 and 68 psi of stress per 1 microinch/inch of strain. This gives one confidence that this calibration is valid for the actually potted resistors.

Now this calibration was carried out in the hopes of checking on the high values of embedment stresses obtained from the tiny ferrite transformer transducers and obtaining a lower stress value from the BLH strain gages. But the contrary was found to be the case: the BLH strain gage on resistor method gives about twice the magnitude for compressive stresses as found with the ferrite toroids! In Figure 7 for Epon 828 there is a change of 900 microninch/inch as the embedment is cooled from 25°C to -45°C. This amounts to 55,000 psi by the above calibration as opposed to 31,000 psi by ferrite toroid transformer. In Figure 13, for Solithane, 11, between 0°C and -50°C the difference of strain of 300 microinch/inch means 18,000 psi as compared to 10,000 psi with the transformers. The much higher stress with the Caddock resistors may be due to the fact that its response is due to both compressive hydrostatic pressures perpendicular to the circular ends of the resistor and in addition, to shear forces parallel to the cylindrical surfaces of the resistor, which is not included in the fluid calibration. The compressive forces perpendicular to the cylindrical surface produce little effect as seen in Figure 16. Another discrepancy that needs explaining away is the fact that in the case of the

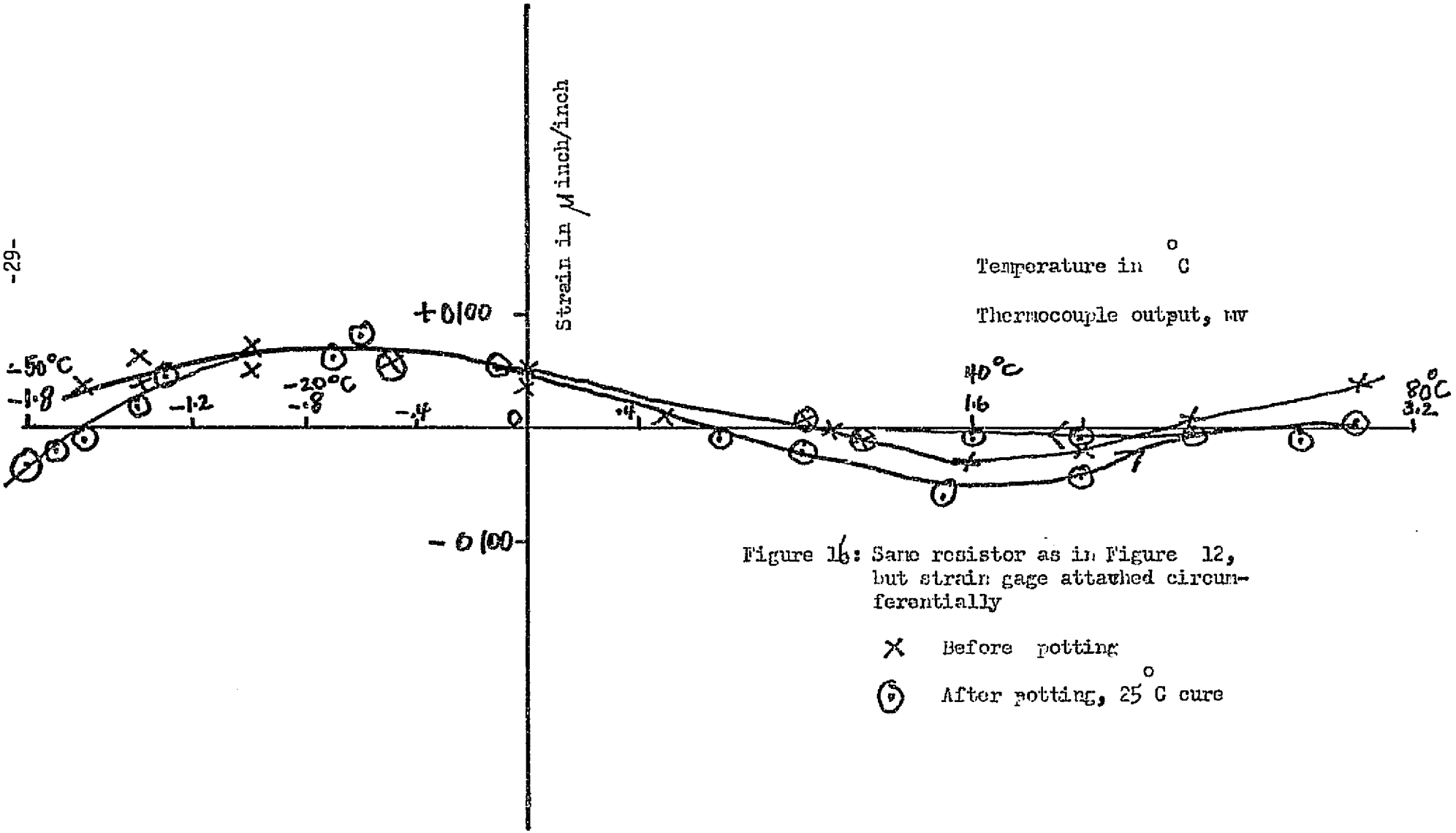

Figure 16: Same resistor as in Figure 12, but strain gage attached circumferentially

X Before potting

(9) After potting, 25° C cure

Epon 828 the measured stresses are so much higher than the calculated ones in the theory section, or a calculated 5,500 psi between 25°C and -50°C. What the theory does not take into account, however is that one goes through the glass transition temperature for Epon 828 in this temperature interval which causes a drastic change in the physical characteristics of the material.

A further concern is that wrong conclusions might be drawn from the stress measurement results on Sylgard. The higher compressive stresses in the sand-filled Sylgard than in the unfilled do not mean that this would cause breaking away or greater cracking tendencies. The higher stresses are due to the much higher value of the elastic modulus of the now much less deformable composite. Stress depends on the product $Y \cdot \alpha \cdot \Delta T$. By contrast it might erroneously be thought that the soft pure Sylgard exerts absolutely zero pressure. It must be realized that pressures of one or two atmospheres that the Sylgard might build up is only 15 or 30 psi and is undetectable in the way these measurements were carried out. Kerlee[19] reports that in tests on solder joints in Cordwood modules during temperature cycling the solder joints failed quickest when the potting material was unfilled silicones or polyurethanes, especially if the entire assembly was constrained by rigid, lateral side-boards. This brings 2-dimensional constraint into play across the entire cross section area of the potting with corresponding larger forces in the 3rd direction, to be counteracted by the

lead-wires of relatively small cross section areas A_i as in equation (4). And, of course, the thermal coefficient of expansion of unfilled silicone rubber is enormous, 300 x $10^{-6}/^{o}C$ and thus from equation (4) in the theory section one can see why Kerlee's results can happen. It may also be that when the container walls are yielding as in the present experiment and the only constraint is a small embedded foreign object, then the soft materials can easily deform around the small foreign body, thus registering little force. This is quite different from the forces brought into play when the entire mass of the elastomer is constrained.

Placing the doubly refracting Solithane and Epon 828 moldings between crossed polaroids showed marked localized colored fringes around the periphery of the embedded objects. This finding of localized uneven stresses agrees with the summary by R. E. Keith[4] in his review article " that processing shrinkages and the related internal stresses are <u>not</u> isotropic, but are strongly influenced by such factors as the shape and position of the mold, processing conditions and the geometry of the circuit being embedded." It can, also, be concluded from the measurements that the materials that show strong adhesion also build up high internal stresses upon temperature cycling, and visa versa. Whether the adhesive forces win or the internal break-away stresses win is hard to predict from this data. A comparative test like the Oliphant washer test might give more directly applicable answers for choosing materials from the point of view of comparative thermal shock resistance.

A related test is the hexbar test for cracking tendencies. This was actually carried out on Selithane, formulation #6, (100 gm resin, 120 gm curing agent-softer) and formulation #2,(100 gm resin,80 gm curing agent-harder). This tests their cracking tendencies due to internal stresses near the embedded object, namely a large hexagonal brass nut with sharp edges and sharp threads. The nuts were suspended by string near the centers of rigid-walled medicine vials of about 100cc capacity. Six samples of each formulation were prepared in the usual sequence: warming both resin and catalyst to 140°F, mixing, degassing the mix under vacuum until no gas bubbles emanated, then pouring under vacuum, then curing under atmospheric pressure at 140°F. The twelve vials showed no cracks when the curing was finished.

The twelve vials were then arranged at random in a Tenney environmental chamber, cooled to -50°C, left at that for 1 hour., then taken out and placed at random into an oven already at 100°C, left ther for 1 hour and then taken out to room temperature.

After this one temperature cycle a very interesting picture presented itself. Of the six samples of #2 formulation, 5 had developed beautiful cracks. Around the outside circumference each of the 5 hexnuts had caused 1 cleavage cracking plane emanating from one sharp edge and bisecting the 120° angle as though drawn with a precision protractor.,. It probably occured as the Selithane tried to shrink on cooling and encountered the sharp edges of the hexnut that did not want to shrink nearly as much.The sharp edges thus pressed into the Selithane with very large forces as predictable from Figures 1-16. In compound #2 the tear strength was not comparatively great enough to withstand, and so the Selithane was literally cleaved by the sharp edge along the 120° angle bisector, much as a gem cutter cleaves a stone by placing a sharp cleavage tool appropriately and giving a sharp blow on it. The formulation #6 showed no cracks as detectable with the naked eye. In #2 there also were cracking planes emanating from the sharp ends and threads of the nuts.

After letting the samples stand for 10 days in a room in which the daily temperature varied only from 32°C to 21°C

a) Two of the #6's also showed small cracks originating at one of the hexagonal edges

b) The cracking planes in the #2's had grown greatly some began to show cracks originating from a second edge around the circumference.

It can be concluded that

a) The cracks in Solithane are clearly caused by the cleaving propensity of sharp edges on an embedded object or of an embedded object on which adhesion is poor. In other words the entire object then tries to pry the Solithane apart.

b) The cracking or cleavage planes are determined by the location and direction of the causative sharp edgesn , not some prefered direction of alignement of the polymer chains.

c) Some formulations like #6 have a more favorable tear strength/ internal stress ratio than others and thus are less likely to crack . But even these seem to reveal some cracks as these grew large enough to be seen.

d) It would be interesting to experiment with another set of tests, comparing #2 Solithane with an entirely different polyurethane such as Adiprene.

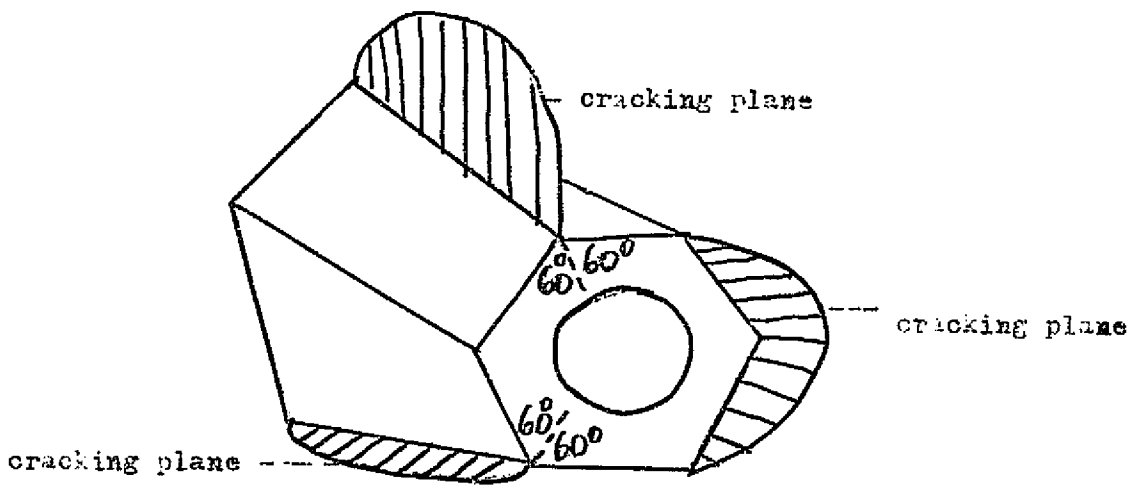

Conclusion:

More careful work could be done using a 4-arm-bridge with 2 strain gages attached to the inside of a hollow steel cylinder, similar to the one used for Epon 828. More sensitive ferrite core transformers could be obtained to get better data on Sylgard.

On the whole the strain behavior observed with the BLH foil strain gages is consistent with what would be expected from the stress measurements using the tiny ferrite transformers. In other words, for the same materials both methods show sharp changes in behavior at the same temperatures. Moreover, the results and curves obtained with the ferrite toroids are very similar to the curves shown by their inventors, used in similar potting compounds [11, 12, 13]. For all but the Sylgard silicone rubber the stresses developed at -50^{0}C are very formidable. The underlying reason is that even though the potting compounds are plastics, they nevertheless have very definite volumes that they wish to occupy at definite temperature. When this is prevented by embedding foreign objects with different physical constants, or by using thick-walled, rigid-walled potting containers ther. enormous internal stresses are developed which might crush the foreign objects if they happen to be fragile, or which might cause pulling away from the walls even though every step was taken to enhance adhesion. This will be discussed again the the chapter on Potting.

Chapter II. Continuation Studies

a. Reynolds Connector Gas Leakage Test

b. Adhesion Studies

c. Improved Mathematical Theory for Diffusion and Permeation.

a. Gas Leakage Tests on Reynolds Connectors, Series 600:

Two possible methods for trying to determine gas leakage rate from the Reynolds connectors, series 600, have already been described previously[24]. This is copied here again:

A: Open the connector in the vacuum jar while it is up to atmospheric pressure. Mate it. Pump down to as good a vacuum as possible. Wait for the desired length of time t. Valve off the jar and immediately open the connector while observing the sudden increase of pressure on a Pirani gage. With a connector assembled at GSFC that had been opened and closed many, many times, this gave a change of pressure Δp of 8 microns when t was 1/2 hour and a change Δp of 3 microns for t = 5 hours and no discernible Δp for t = 16 days. The volume of the vacuum jar was about 1000cc. Thus the 8 micron change meant that the internal volume of the mated connector, Vcon, is about 0.01cc, which agrees with information from the Reynolds Company. The attempt to discern Δp upon opening becomes more and more inaccurate the more gas has leaked out.

B. A much faster method is to attach a Helium leak detector to the vacuum jar. This must be caliberated with a standard leak. Fill the jar up to atmospheric pressure with Helium, while the connector is open. Pump down for 2 hours, then read the apparent leak rate due to remaining residual Helium in the jar. Again fill the jar up to atmospheric pressure with Helium, mate the connector, pump down for 2 hours again, read the leak rate again. The difference of the two leak rates is due to the mated connector leaking He into the jar. For the same connector as in Method A we thus obtained a leak rate of 1.3×10^{-7} atmospheric cc/second. Using the equation that $p = 76 \exp\left(-\frac{\text{Leak rate}_o \cdot t}{Vcon}\right)$ one can calculate that it would take 4 days to leak down to 10 torr and 6.25 days to leak down to 1 torr. Hence, there would be 2.25 days duration within the corona region.

$$2.3 \times \text{Ln}\ \frac{76}{p} = \frac{+\text{Leak Rate}_o \times t}{.012cc}$$

$$t = \frac{.012 \times 2.3}{\text{Leak Rate}_o}\ \text{Log}\ \frac{76}{p}$$

The Method B, although more elegant, had to be discarded because filling the entire jar initially at atmospheric pressure with Helium gas caused problems such as dissolving of helium in materials of the vacuum chamber, notably the red silicone rubber gaskets and O-rings. This was later given off as an everlasting virtual leak.

Table I below gives results using Method A. One had to wait 1/2 hour to 1/6 hour before opening the connector the first time. It was assumed that the pressure inside the connector at that time was still atmospheric or 760 torr. Subsequent pressures inside the

connector were then calculated from a direct ratio of the pressure change dp or $P_c = \frac{760 \times dp\ later}{dp\ original}$

This should of course approximately agree with p_c calculated from Boyle's Law, namely $p_c = \frac{1100\ dp}{0.012}$ and it does.

Table II then shows calculations done with those connectors on which the original data looked good enough. These calculations extrapolate, using the mass flow equation stated at the top of Table II, how long it would take for the connector to leak down to pressures of 100 torr, 10 torr, 1 torr. Thus one calculates on the mass flow assumption that it would take of the order of 100 hours or 4 days to leak down to 1 torr. One torr means one has gone through the corona region for these connectors. Now actually, when one plots the data of Table I on semilogarithmic paper, Figure 17, several of the curves bend upward as though the leakage rate did go slower after getting to the pressures of about 100 torr, than would be expected from the law of mass flow. This is fully to be expected. After the pressure gets down low enough for the mean free path of a molecule to be of the order of the internal dimensions of the containing connector, molecular flow takes over, and this will result in much slower leakage.

It was attempted to test in this region experimentally, but without success, at least as far as a direct pressure test was concerned. This was because if one tried to detect the resulting pressure change in the 1100 cc vacuum jar when the tiny bit of gas contained in the Reynolds connector of volume

Table I: Gas Leakage Test On Reynolds Connectors

Connector# & Description V_c=(.01 + 20%)cc	Time Interval	dp on opening into 1100cc jar, in microns	Calculated $p_c = \frac{760(\text{dp later})}{(\text{dp orig.})}$ Inside Connector
#1			
Assembled at	1/2 hr.	10 microns	760 torr
GSFC. Seal:	1/2 hr.	8	760
Solithane.	16 days	1.8	150
2" cable potted	6 days	1.5	125
at far end.	1.5 hr.	7	590
	5 hr.	3	250
#2			
Assembled at	1/2 hr.	7	760
GSFC. Seal:	15 days	0.4?	20?
Solithane.			
Long cable not			
sealed at far			
end.			
#3			
Factory assem.	1/6 hr.	7	760
Connector at	17 hr.	2	217
both ends, far	5 hr.	2.5	270
end sealed	63 hr.	1 ?	110?
with male conn.	1/6 hr.	7	760
#4			
Factory assem.	1/6 hr.	5 ?	760
Connector at	41 hr.	1-2	150
both ends, far			
end sealed with			
male connector			
#5			
Factory assem.	1/6 hr.	9	760
2" cable, far	1/6 hr.	9	760
end sealed	1 hr.	7	590
with Epon 828	21 hr.	1.5	127
	1/6 hr.	10	760
	4-1/4 hr.	3.5	295
#6			
Factory assem.	1/6 hr.	8	760
Epoxied shut	91 hr.	1 ?	95 ?
at end of	10 hr.	3.5	330
shrink tubing.	13 hr.	2.5	240

Table II: Calculations on Reynolds Connector Gas Leakage Tests Assuming $p = 76 \exp \frac{(-\text{Leak Rate}_o \cdot t)}{V_{conn}}$

Connector #	Leak Rate$_o$ = $\frac{14 \times 10^{-3} \text{ cc}}{t \quad \text{hr}}$	t_1 to 100 torr = $\frac{2.8 \times 10^{-2} \log 76}{\text{Leak Rate}_o \quad p}$	t_2 to 10 torr = 2.14 t_1	t_3 to 1 torr = 3.27 t_1
#1	1.5×10^{-3}	19 hr	41 hr	62 hr
#3	0.8×10^{-3}	35 hr	75 hr	115 hr
#5	0.9×10^{-3}	31 hr	66 hr	100 hr
#6	0.9×10^{-3}	31 hr	66 hr	100 hr

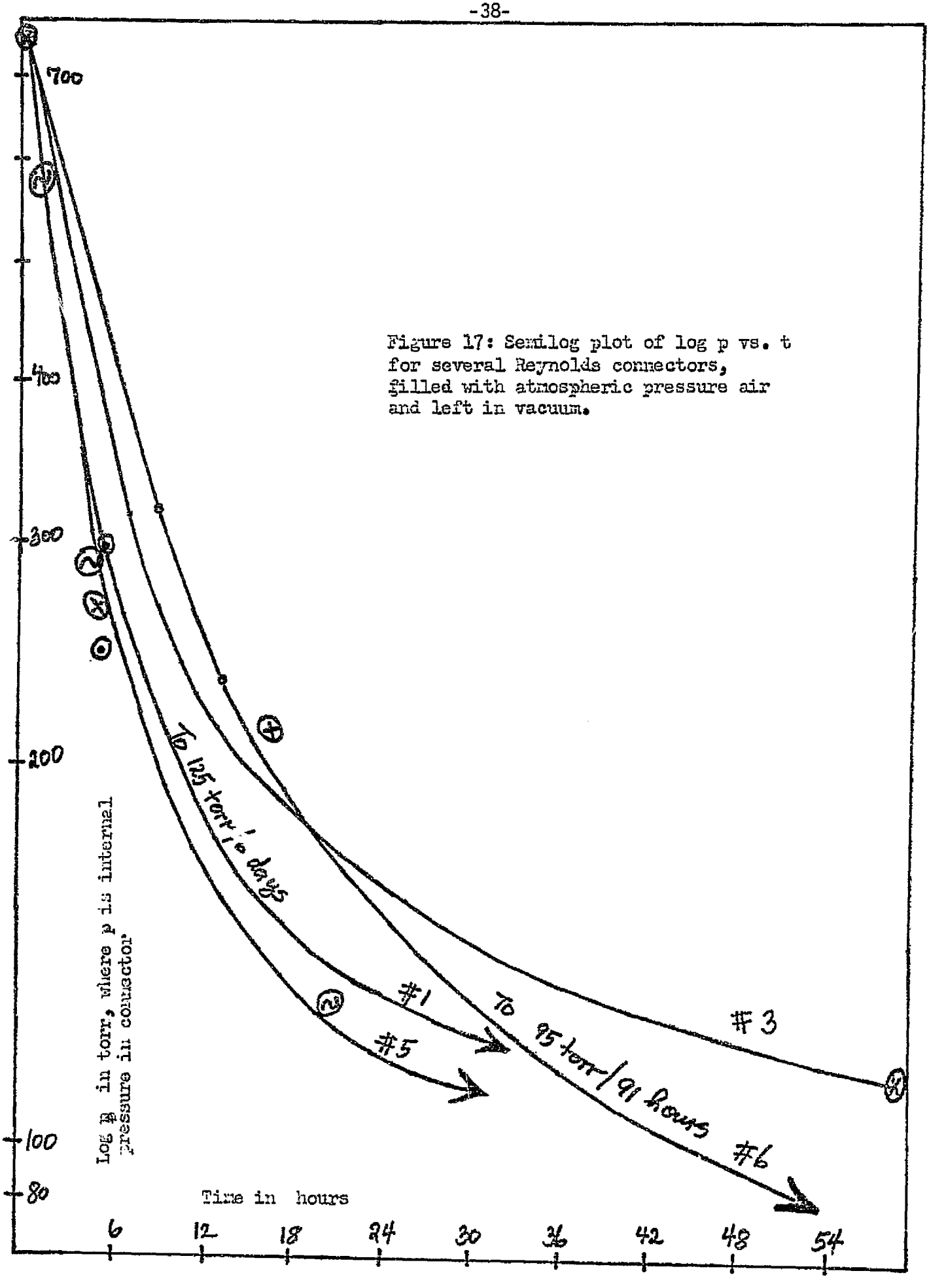

Figure 17: Semilog plot of log p vs. t for several Reynolds connectors, filled with atmospheric pressure air and left in vacuum.

0.012 cc at 1 torr or even 10 torr is dumped into the jar, one has to use an ionization gauge for measurement. This is a hot filament gauge. As soon as the jar is valved off from the pump to get ready for the measurement, the pressure rises enough and continuously due to outgasing to conceal the dp when the connector was opened, no matter how fast one tried to work. A cold gauge suitable in these low pressure ranges would be an Alphatron Gauge, but it was not available.

It was decided to use an indirect method, as follows:
C: After all, if the electrical noise count data reported earlier[24] is correct, and it is believed that it is, then as the connector leaks down from atmospheric pressure the count rate of noise counts should increase as the connector approaches the internal pressures of the corona region, namely between 10 torr to 2 torr for this type of connector. Only when its pressure has fallen below 1 torr should one expect the noise count to become zero, at a sensitivity of 2.5×10^{-14} coulombs. So by monitoring the noise count continuously after filling the connector at atmospheric pressure, closing it, and then immediately pumping down the surrounding jar down to a vacuum (only 10^{-3} torr for the system used) and keeping it at vacuum, one should be able to get an indication of the time it takes for the connector to leak down below the corona region. This was carried out for one connector and it took approximately 5 to 6 weeks for the connector to become quiet, as shown in Table III.

TABLE III

Connector filled at 760 torr, in 10^{-3} torr chamber
Noise count vs time at 2.5×10^{-14} coulomb sensivity
using "Rocket" preamplifier.

Date	Total Counts/5 minute intervals
July 10, 1975	18, 23, 18
July 11,	10, 11, 20, 10, 12
July 15,	4, 16, 4, 11, 6
July 17,	25, 46
July 22,	27, 7
July 24,	11, 10
July 25,	14, 11
July 29,	7, 7
July 30	6, 11, 4, 5, 7
August 4	14
August 7	8, 12, 6, 18
August 11	6, 3
August 12	4, 3
August 15	0, 0, 0
September 1	0, 0, 1, 0

Cold Temperature Test on Reynolds Connectors:

All previous tests were conducted at room temperature. It was decided to run the following test at - 30°C. Since the connectors leak gas quite rapidly as shown in the previous pages, and if placing them at cold temperatures should make the tight fitting of the diallyl phthalate shoulders against the silicone rubber O-rings less tight, then one would have a situation where continuous gas discharge would occur, when the internal pressure of the connectors attained between 2 and 10 torr. Three connectors terminated with male panel connectors were mounted into a Tenney environmental chamber, splice and terminus of male connecter solid potted with Epon 828. The test was run for almost 3 days. The current was monitored with an electrometer on the 10^{-8} ampere scale. At the end of almost 3 days the current did not change as far as could be detected, namely less than $1/100 \times 10^{-8}$ ampere. The experimental conditions are summeriz - ed in Table IV below.
Perhaps to be more conclusive the test should have been kept running for a longer time, perhaps one or two weeks.

Table IV: Cold test on 3 Reynolds connectors.

April 6,1976:

1 pm :	Pressure in environmental chamber	= 1 torr
	Temperature	= - 30°C
	Applied voltage	= 2500 volts

April 8,1976 :

10 a m :	Pressure in chamber	= 1 torr
	Temperature in chamber	= - 36°C
	Voltage	= 2500 volts

Current remained less than detectable, that is , less than 0.01×10^{-8} amp.

Conclusion:

Contrary to initial expectations it was found that the Reynolds connectors leak gas, quite rapidly at first, and then much more slowly, more slowly than would be predicted from an exponential decay type of relationship. Although it only takes a few days to leak down to 100 or 200 torr, it took 6 weeks for the connector to leak down below 1 torr. Incidentally, in correspondence with Reynolds Industries, Inc. a letter was received June 2, 1975, in which the following paragraph appeared, quoted below:

> "The series 600 connector interface does not rely upon the entrapment of air to withstand rated voltage at altitude. The use of silicone "O" rings creates a mechanical dielectric seal; therefore, the connector interface is not intended to be leak tight."

b.) Adhesion Studies:

Most of the following tables were already reported in the Goddard document X-711-75-221, but not in the Final Technical Report preceding the present one. The data on S elithane is therefore repeated here.

Tests were also performed on the NT Industries conformal coating material NT114, composed of silicone rubber and polyimide, 25% solid in a solvent. On glass-epoxy circuit board the adhesive strength was of the order of 1400 psi by lap shear testing. However, to the other substrates, namely solder on beryllium copper, sandblasted solder on beryllium copper, and etched teflon, the lap shear adhesive test gave less than 200 psi!

It is felt that lap shear testing is not the appropriate method here. The NT 114 neither has the opportunity to properly get rid of the solvent from under the lap joint, nor does water vapor have a good chance to get to the adhesive under the overlap to help cure it. Peel testing needs to be done here, but this has not been implemented yet.

TABLE Va

Lap Shear Strength of Thiokol Solithane 113, Formulation 4
100 gm resin, 100 gm hardener.

(A) Adherent: 60-40 Solder, Electro-plated on Beryllium Copper

Adhesive Thickness: 0.010 inches ±.002

Surface Treatment	Standard Deviation psi	Lap Shear Strength psi
Ultrasonic Clean with Freon TF	±25	90
Vapor Degrease Trichloroethane	±15	95
Alcohol Spray	±5	110
Vapor degrease with Trichloroethane, sand blast with Black Beauty grit, vapor degrease	±15	160
Vapor degrease with Trichloroethane, prime with thin coat of Epon 828/V-40. Primer used	±65	355 Cohesive Failure

(B) Adherent: Glass Epoxy Board

Adhesive Thickness: 0.010 inches ±.002

Vapor degrease with Trichloroethane, grit blast Black Beauty grit, vapor degrease	±30	215
Vapor degrease with Trichloroethane	±40	220

(C) Adherent: Ferrite

Adhesive Thickness: 0.010 inches ±.002

Ultrasonic clean, hand sanded on 400 grit SiC paper, Ultrasonic clean with Freon TF (Johnson)	±15	60
Repeat above (Clatterbuck)	±20	60
Ultrasonic clean only	±20	100

(TABLE Va - Cont'd)

(D) Adherent: Porcelain

Adhesive Thickness: 0.010 inches ±.002

Data very poor despite many tries. Perhaps the heavy cutting grease from the diamond saw is never quite removable.

Surface Treatment	Standard Deviation psi	Lap Shear Strength psi
Vapor degreased, Trichloro-ethane	±30	30
Vapor degreased, Trichloro-ethane, Bon Ami scrubbed, washed, dried, vapor desgreased	±65	75
Ultrasonic clean Freon, Bon Ami scrubbed, washed, dried, ultra-sonic clean Freon	±50	80

TABLE Vb

Lap Shear Strength of Thiokol Solithane #11

Thiokol C113 Resin: 100g, C113-300 hardner: 44g, TIPA: 6g
All samples ultrasonically cleaned with Freon-TF.

	Adherent Surface Treatment	Adhesive Thickness Inches	Standard Deviation psi	Lap Shear Strength psi
I.	No Primer Used:			
	60-40 Solder on Be-Cu	0.010	±96	576
II.	Chemlock 218 Primer: Thinned 50%-50% with MIBK			
	60-40 Solder on Be-Cu	0.010	±152	850
	Sandblasted Glass Balls, 60-40 Solder on Be-Cu	0.010	±195	1070
	Porcelain	0.010	±88	416
	Etched Teflon	0.010	±23	292
III.	Epon 828 Epoxy Primer: Thinned 50%-50% with Methyl Alcohol			
	Etched Teflon	0.010	±12	365
		0.020	±10	360
	Porcelain	0.020	±45	590
	60-40 Solder on Be-Cu	0.010	±70	780
	Sandblasted 60-40 Solder on Be-Cu	0.010	±130	860

TABLE Vc

Lap Shear Strength of Thiokol Solithane #6

Thiokol C113 Resin 100g, Thiokol C113-300 hardner 120g.
All samples were ultrasonically cleaned with Freon TF

Adherent Surface Treatment	Adhesive Thickness Inches	Standard Deviation psi	Lap Shear Strengtn psi
Adherent: 60-40 Solder, Plated on Beryllium Copper.			
Woolsey Metalast 919/920 Primer	0.020	±20	130 Cohesive Failure
Woolsey Metalast 919/920 Primer	0.010	±28	165 Cohesive Failure
Adherent: Etched Teflon			
Woolsey Metalast 919/920 Primer	0.020	±4	132 Cohesive Failure
Woolsey Metalast 919/920 Primer	0.010	±10	131 Cohesive Failure
Adherent: Sandblasted Glass-Epoxy Board			
Woolsey Metalast 919/920 Primer	0.020	±14	81 Cohesive Failure
Woolsey Metalast 919/920 Primer	0.010	±15	151 Cohesive Failure

c) Improved Mathematical Theory for Diffusion and Permeation.

In the previous annual report[37] and GSFC document X-711-75-221[24] permeation coefficient measurements were reported for several potting compounds. The equations presented were stated to be approximate solutions to the diffusion equation, and were applicable for the steady state case, in the long-time situation, for the geometry of thin permeation wall and large void. The experimental permeation chambers were built accordingly with about 0.2 cm thin wall and cavity of volume 32 cm^3. The permeation constants obtained this way are held to be correct.

The above-stated conditions for the approximate equations to hold really means that the parameter H, which is the ratio of the amount of penetrating gas in the wall to that in the cavity volume V be small. The ratio H can be written as KAl/V, where A is the cross-section area and l is the thickness of the wall, and $K = C/C_g$, where C and C_g denote the concentration of penetrant in the wall and the volume V respectively when the two phases are in equilibrium. At one atmosphere of pressure this is the same as slubility S in units of cm^3(STP) cm^{-3}per atmosphere.

Unfortunately, when the approximate equations, especially (7) and (8) in the aformentioned X-document are used to make calculations for thick-walled, small - void cases, such as a bubble deep in a potting compound, then they do not hold and give wrong predictions of time intervals for diffusion. The exact equations are infinite series and are difficult to put in usable form. A recent (1975) article on "Transient Diffusion Through a Membrane Separating Finite and Semiinfinite Volumes" [38] by J.A. Barrie, H.G. Spencer, and A. Quig was found,and the salient portion of that article is here with presented:

Consider a wall of cross sectional area A and thickness l separating penetrant at pressure p in the finite volume V from penetrant at pressure p_c, which is constant. This is shown in the figure below

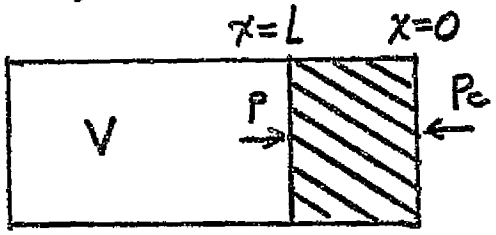

In general $p \neq p_c$, and either may be zero; the pressure in V as a function of time t is required. The diffusion equation and boundary conditions are as follows:

$$\frac{\partial^2 C}{\partial x^2} = \frac{\partial C}{\partial t} \qquad (1)$$

$$C(l,0) = C_o \; ; \; C(x,0) = C_i \; ; \; C(0,t) = C_c \qquad (2)$$

$$D\left(\frac{\partial C}{\partial x}\right)_{x=l} = -\frac{l}{H}\frac{\partial C(l,t)}{\partial t} \qquad (3)$$

K and H have already been defined on the previous page. Equation(3) relates the change in the concentration in the volume V to the rate at which penetrant diffuses into the face at x=l. The concentration C_i is initially uniform throughout the membrane. Using the Laplace transformation method the solution for C can be expressed as

$$C(x,t) = C_c + 2\sum_{n=1}^{\infty} \frac{(C_i - C_c)(H^2 + Q_n^2)\sin Q_n + (C_o - C_i)HQ_n \sin(Q_n x/l)\exp(-DQ_n^2 t/l^2)}{(H + H^2 + Q_n^2)\, Q_n \sin Q_n}$$

This equation is number (4)

The Q_n are the non-zero, positive roots of $Q \tan Q = H$ (5)

So, the first step in the application of what follows is the solution for the Q's for a given parameter H.

To illustrate, one considers five special cases of the initial and boundary concentrations designed I, II, III, IV, V, which occur often in experiments. Of these I to IV correspond to a uniform initial con-

centration of penetrant C_i in the wall whilst V is an example of a corresponding non-uniform initial concentration. In what follows, p^X with X = I,....,V denotes the pressure of penetrant in the volume of the void.

(I) The wall is initially free of penetrant; the initial pressure in V is p_o, and a constant zero pressure is maintained on the other side of the membrane so that $C_i = C_c = 0$; $C_o \neq 0$ and from equation (4)

$$C = 2C_o \sum_{n=1}^{\infty} \frac{H \sin(Q_n x/l) \exp(-DQ_n^2 t/l^2)}{(H+H^2+Q_n^2) \sin Q_n} \qquad (6)$$

This result is also obtained by transformation of the corresponding solution for heat flow in a slab. Evaluating C at x=l and defining the Henry's law solubility as $S = C/p$, one obtains for the pressure of penetrant in the void volume

$$\frac{p^I}{p_o} = \sum_{n=1}^{\infty} A_n^I \exp(-DQ_n^2 t/l^2) \qquad (7)$$

where

$$A_n^I = \frac{2H}{H+H^2+Q_n^2} = \frac{2\cos Q_n \sin Q_n}{Q_n + \cos Q_n \sin Q_n} \qquad (8)$$

(II) The membrane is first equilibrated with penetrant to establish a uniform concentration throughout; the pressure on the surface x=0 is reduced to zero and maintained constant so that $C_i = C_o \neq 0$; $C_c = 0$. Proceeding as in case (I) one obtains

$$\frac{p^{II}}{p_o} = \sum_{n=1}^{\infty} A_n^{II} \exp(-DQ_n^2 t/l^2) \qquad (9)$$

where

$$A_n^{II} = \frac{2(H^2 + Q_n^2)\sin Q_n}{(H+H^2+Q_n^2)Q_n} = \frac{2 \sin Q_n}{Q_n + \cos Q_n \sin Q_n} \qquad (10)$$

$$= \frac{2H^2}{Q_n \sin Q_n (H+H^2+Q_n^2)}$$

(III) The wall is equilibrated with penetrant as in (II); the pressure on the surface x = 0 is maintained constant whist that in the void is reduced to zero initially so that $C_i = C_c \neq C$; $C_o = 0$ and the pressure p^{III} in the void is given by

$$1 - \frac{p^{III}}{p_c} = \sum_{n=1}^{\infty} A_n^I \exp(-DQ_n^2 t/l^2) \qquad (11)$$

Thus the function $(1-p^{III}/p_c)$ decays with time at exactly the same rate as the function p^I/p_o.

(IV) The wall is initially free of penetrant; the initial pressure in the void is zero and a constant pressure is maintained on the surface x =0, so that $C_i = C_o = 0$; $C_c \neq 0$ and

$$1 - \frac{p^{IV}}{p_c} = \sum_{n=1}^{\infty} A_n^{II} \exp(-DQ_n^2 t/l^2) \qquad (12)$$

and the function $(1 - p^{IV}/p_c)$ decays at the same rate as p^{II}/p_o.

Equations (7),(9),(11), and (12) may be represented by the single equation

$$f^X(p) = \sum_{n=1}^{\infty} A_n^X \exp(-DQ_n^2 t/l^2) \qquad (13)$$

where

$$f^X(p) = p^X/p_o \quad \text{for cases X = I and II}$$

and

$$f^X(p) = (1 - p^X/p_c) \quad \text{for cases X = III and IV}$$

Also

$$A^I = A^{III} \quad \text{and} \quad A^{II} = A^{IV} .$$

For large t the first term of the summation dominates, and $f^X(p)$ decays exponentially with time so that

$$\ln \left[f^X(p)\right] = \ln A_1^X - DQ_1^2 t/l^2 . \qquad (14)$$

Further if H is sufficiently small, $\tan Q_1 \simeq Q_1$, $Q_1^2 \simeq H$ and equation (14) becomes

$$\ln \left[f^X(p)\right] \simeq \ln A_1^X - DHt/l^2 \qquad (15)$$

where $A_1^I = A_1^{III} = \frac{2}{2 + H}$ and $A_1^{II} = A_1^{IV} = \frac{2(1 + H)}{2 + H}$ (16)

Remember there H is small.

(V) Finally, a special case is considered of a non-uniform initial concentration C_i in the wall at $t = 0$;

$C_i = x/l\ C_o$; $C_c = 0$.

This means a linear concentration gradient is established in the wall at t=0 . By the Laplace transformation one gets that

$$C = 2C_o \sum_{n=1}^{\infty} \frac{H^2 \sin(Q_n x/l) \exp(-DQ_n^2 t/l^2)}{(H + H^2 + Q_n^2)Q_n^2 \sin Q_n} \qquad (17)$$

and

$$\frac{p^V}{p_o} = \sum_{n=1}^{\infty} A_n^V \exp(-DQ_n^2 t/l^2) \qquad (18)$$

where

$$A_n^V = \frac{2H^2}{(H + H^2 + Q_n^2)Q_n^2} = \frac{2 \sin^2 Q_n}{(Q_n + \cos Q_n \sin Q_n) Q_n} \qquad (19)$$

For large t the first term dominates giving as before simple exponential decay. Since from equation (5), $Q_1^2 < H$, then in general $A_1^V > A_1^I$ and will be close to unity .

If one, in addition looks at the situation for small H in this case, one gets as previously $\tan Q_1 \simeq Q_1$, $Q_1^2 \simeq H$.

Now if one substitutes this in equation (18) one gets the approximate relation that

$$\frac{p^V}{p_o} = \exp(-DHt/l^2)$$

But $H = KAl/V$; this leads to

$$\frac{p^V}{p_o} = \exp(-DKA/lV)$$. But KD is the permeability P .

$$\frac{p^V}{p_o} = \exp(-P\,A\,/\,l.V)$$. This is essentially equation 8

on page 21 in the previously reported theory[24], in units of $\frac{cm^3 \cdot cm}{cm^2 \cdot sec. \cdot 1 \text{ atmosphere}}$, which only holds for large time, thin wall, large void. The general theory thus reduces to the oversimplified situation previously given. This may however not in general be used. Using the proper equation (14) for case III of diffusion from an atmospheric pressure bubble into the vacuum of space, assuming the wall to be saturated with air to start with, and using the previously measured[24] $\underline{P}$ of $43 \times 10^{-9} \times 76 \frac{cm^3(STP) \cdot cm}{cm^2 \text{ sec} \cdot 1 \text{ atmosphere}}$ and assuming(?) a solubility of 2 $cm^3 \cdot cm^{-3}$/ 1 atmos. for silicone rubber, one can calculate for a cubical bubble 0.33 cm on a side, 1.0 cm under the surface to drop in pressure from 76 cm to 1cm of Hg pressure . This gives about 20 days of time instead of 5 days as previously calculated[24]. The difference between the two calculations would get worse the thicker the wall and the smaller the void.

One must use the more general equations presented in this report. These require a separate knowledge of solubility and diffusion constant, rather than their product $\underline{P}$. Experimental time runs with thick walls are planned for the same cylindrical units as used in the previously reported experiments[24]. The data obtained from these will then be attempted to be curve-fitted onto the theoretical curves by a computer program in the hope of extracting D and K for silicone rubber for diffusion of air.

It might be mentioned that for a polydimethylsiloxane silicone rubber by Dow Corning a permeation constant for CO_2 at 30°C has been reported which is another order of magnitude larger(!) than the one measured in the previous X document[24] for air at 25°C.

CHAPTER III

ELECTRICAL "NOISE" MEASUREMENTS

Introduction:

Electrical noise or partial discharge measurements were carried out on various circuit components or parts of circuits by a nuclear counting technique. both to see if this method would be a valid one, and to select the "quiet" configurations and capacitors for use in extremely sensitive X-ray detection equipment on the HEAO-A satellite. All the work was done with D.C. applied voltage.

The so-called "noise pulses are corona or partial discharge pulses: "a type of localized discharge resulting from transient gaseous ionization in an insulation system when the voltage stress exceeds a critical value. The ionization is localized over only a portion of the distance between the electrodes of the system"[27]. The discharges may be in a void filled with gas or oil inside a potting compound, they may be in inclusions, or they may be along a surface, or about sharp points or edges into the surrounding medium.

It is impossible to go into the detailed discussion as in the excellent book by F Kreuger[25], but some important points might be brought out here: If the void is filled with gas, then Paschen s curve regulates the inception voltage and extinction voltage as a function of pressure-electrode spacing. Ionization of atoms can occur at a few volts whatever the ionization potential of the given species of atoms is (e.g. 13 electron

volts for Hydrogen), but self-sustained gas discharge with cold cathode requires several hundred volts at least, even at the Paschen minimum.

A.C. versus D.C. testing:

The equivalent circuit of a void in a dielectric is given in Figure 18. The recurrence of internal discharges as a function of applied A.C. voltage is shown in Figure 20 [26]. As applied voltage v_a across the entire sample rises, so does the voltage across the cavity, v_c. When this reaches the breakdown voltage U^+ a flow of free charge occurs in the cavity, causing a drop in v_c, so that when the discharge extinguishes, v_c across the cavity is down to V^+. All this occurs in about 10^{-7} seconds [25]. If total applied voltage to the specimen, v_a, is still on the rise, then the v_c will increase again also, until it reaches U^+ again, and there will be another discharge. The field across the cavity is determined by the superposition of the main applied electric field causing fixed polarization charges in the dielectric lining the cavity walls and the field of the free surface charges at the inside of the cavity walls, left behind just after the last discharge. Just after the last discharge these fields counteract one another. A qualitative picture of the situation is seen in Figure 19. Just after discharge, the polarization charges and free charges adjacent to one another on the same wall almost neutralize one another until the increasing applied voltage makes the polarization charges increase in quantity again and predominate

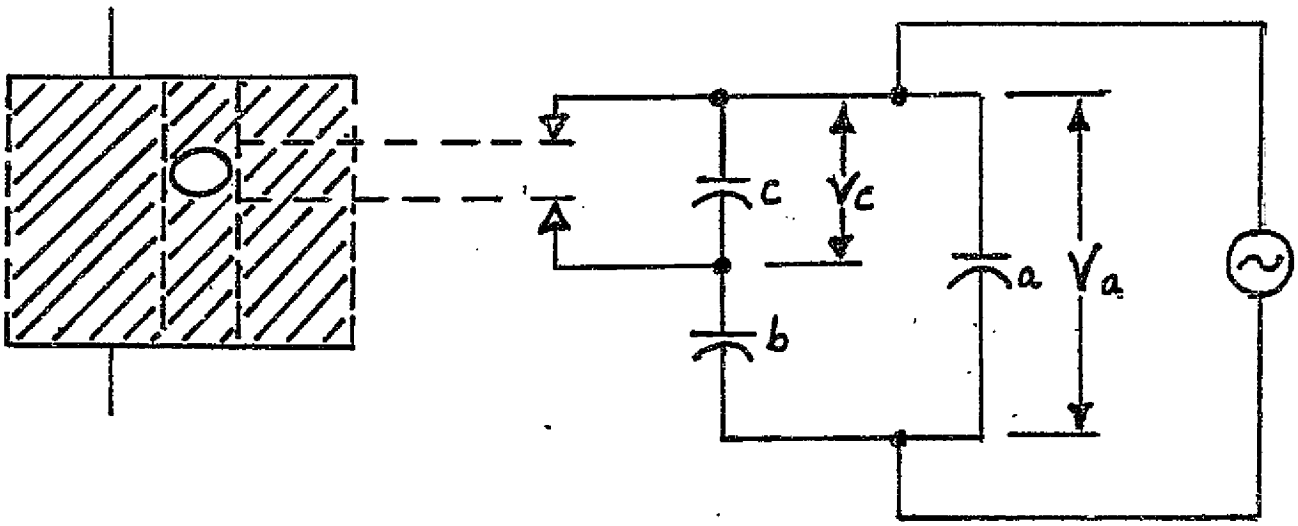

Figure 18: Left: Dielectric with void
Right: Equivalent circuit for AC partial discharge testing

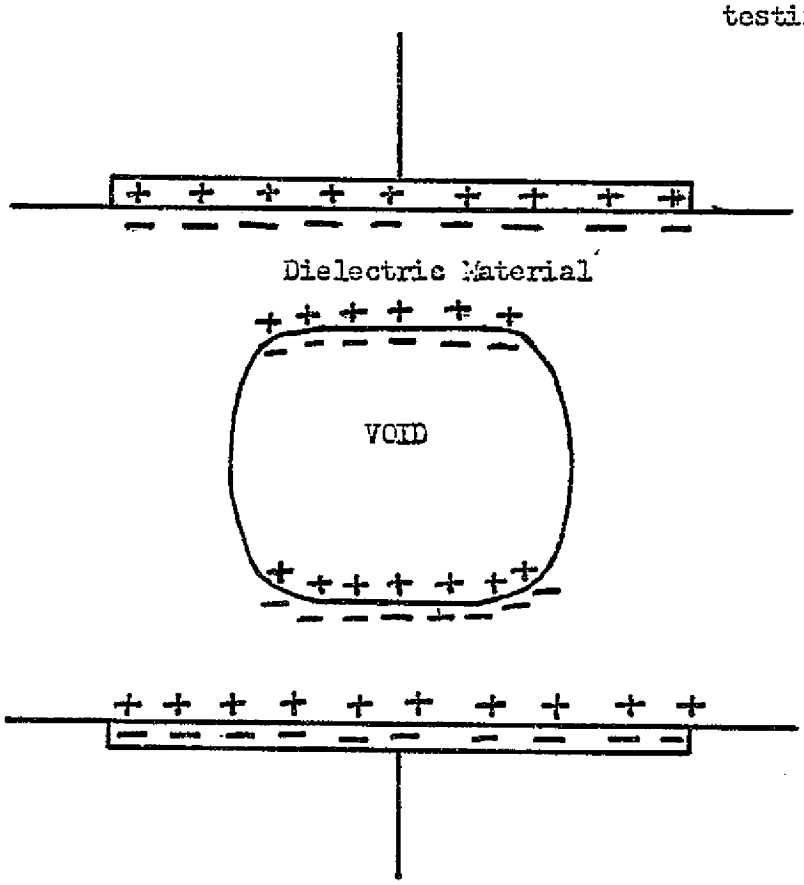

Figure 19: Charge distribution in a cavity just after discharge

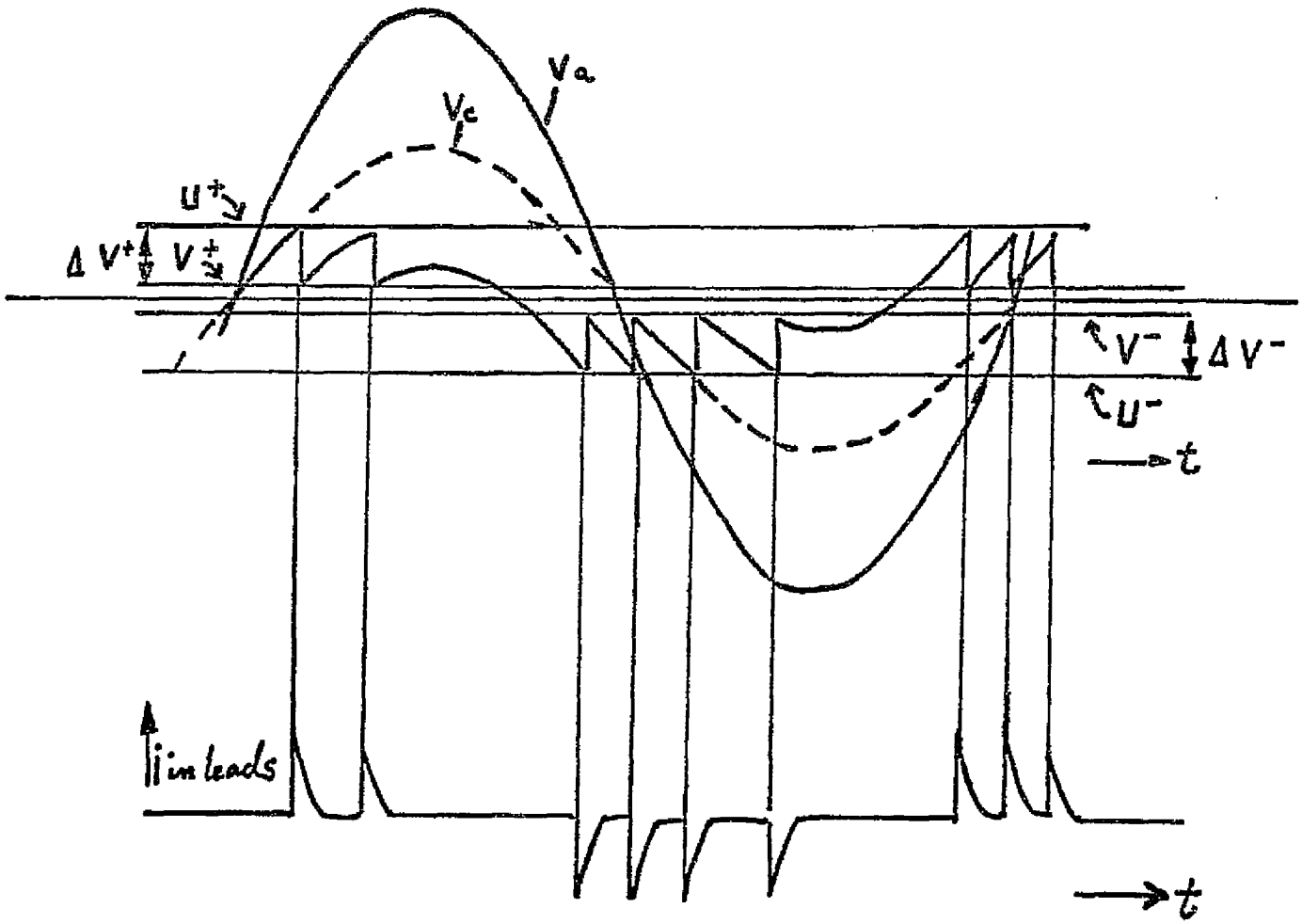

Figure 20: AC partial discharge testing.
Applied waveform v_a, voltage across the cavity v_c
and current in the leads i, as a function of time t.

again until their field causes another breakdown of the cavity or a second pulse. In the D.C. case, however, one has to wait until more polarization charges in the dielectric medium lining the cavity are placed there by conduction through the dielectric. Since the conductivity of a good dielectric is very low, this takes a long time. Hence, at applied electric fields at which a sample begins to show regularly spaced pulses at A.C voltages, discharge pulses at D.C. voltages are few and far between, and might in fact be missed altogether. Also, the violently alternating A.C. voltages drive the dielectric test sample much harder than the quiescent D C. voltage, making breakdown of flawed regions inside the dielectric more likely. For these several reasons, the observable onset of discharge pulses occurs at higher voltage for D.C. than for peak A.C. applied voltage. Moreover, the pulses on D.C are irregularly occurring with time rather than synchronized with the applied A.C. frequency. Observation on D C. must therefore be made with a storage oscilloscope and nuclear counters. (The equivalent circuit of the test sample on D.C. testing can be pictured as having high resistances parallel to C_b and C_a in Figure 18.) Ripple voltages superimposed on direct voltage will increase the D.C. discharge repetition frequency[25].

In short, D.C. measurements are much more difficult and more time consuming to make, especially where random interference pulses from disturbances on the electric lines or from electromagnetic waves despite shielding, can easily be mistaken for discharge pulses. On the other hand. D.C. measurements are much

less destructive to the sample than the violent A.C. oscillations which drive the sample quite hard and dissipate much energy in it. In general, samples should be tested under the same conditions under which they will be used.

Detection Methods:

The four basic circuit arrangements for carrying out partial discharge measurements are shown in Figure 21a, b, c. d, taken from ASTM D 1868-73[27]. In association with these, 3 questions arise:

(1) What is the detection impedance Z that translates the small current surges in the test specimen leads into measurable voltage pulses?

(2) What type of preamplifier is used and what are its input characteristics and its own noise levels, so as to permit the tiny. fast voltage pulses to pass thru without attenuation or obliteration?

(3) What is the circuit sensitivity of the 4 different curcuit arrangements shown? Circuit sensitivity is defined as the fraction of the terminal corona-pulse voltage that appears across the detection impedance Z for measurement.

Each of these is discussed below.

(1) a. Use a resistor R in parallel with a small capacitance C. The voltage pulse across this combination is unidirectional, of shape shown in Figure 22a. In the case of this investigation the RC was actually the feedback network of a charge-sensitive operational amplifier, the C acting as an integrating capacitor for the charge.

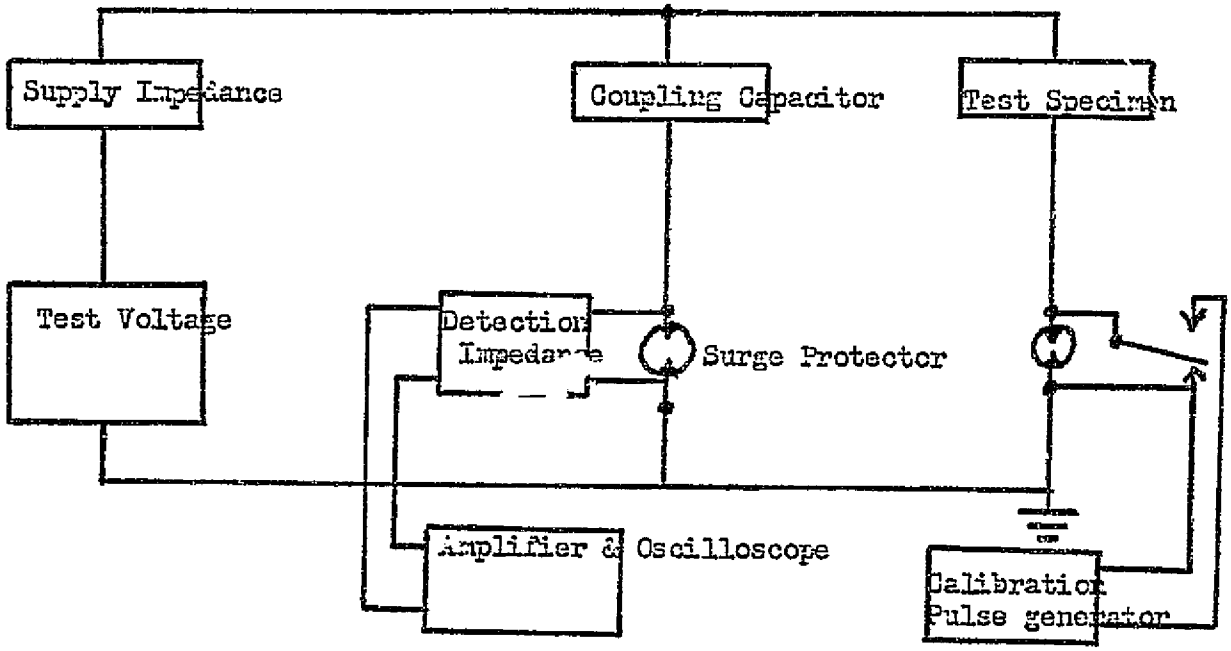

Figure 21, circuit a)

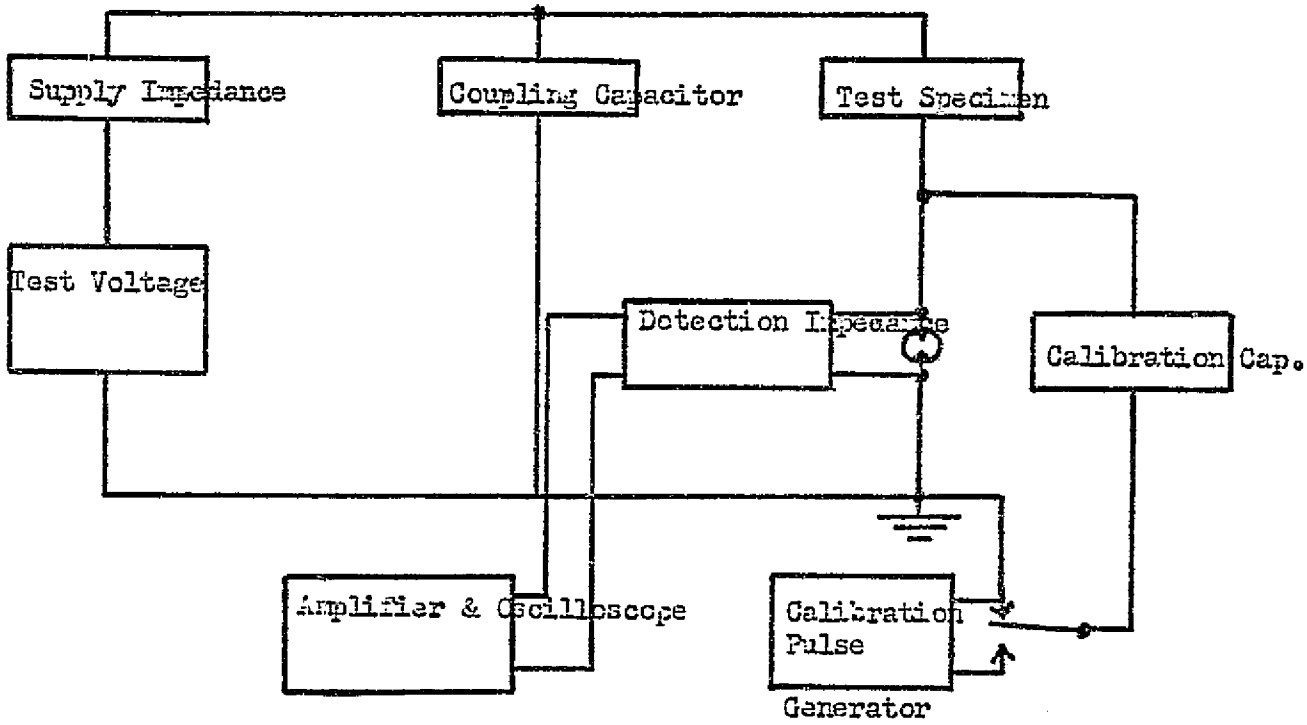

Figure 21, circuit b)

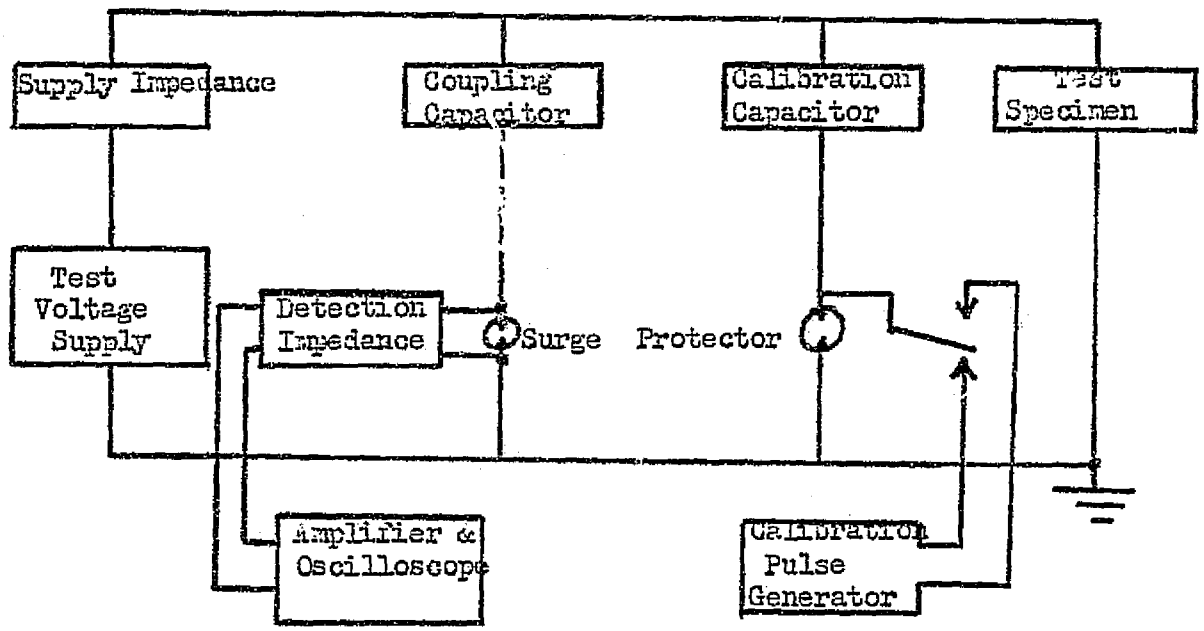

Figure 21, circuit c)

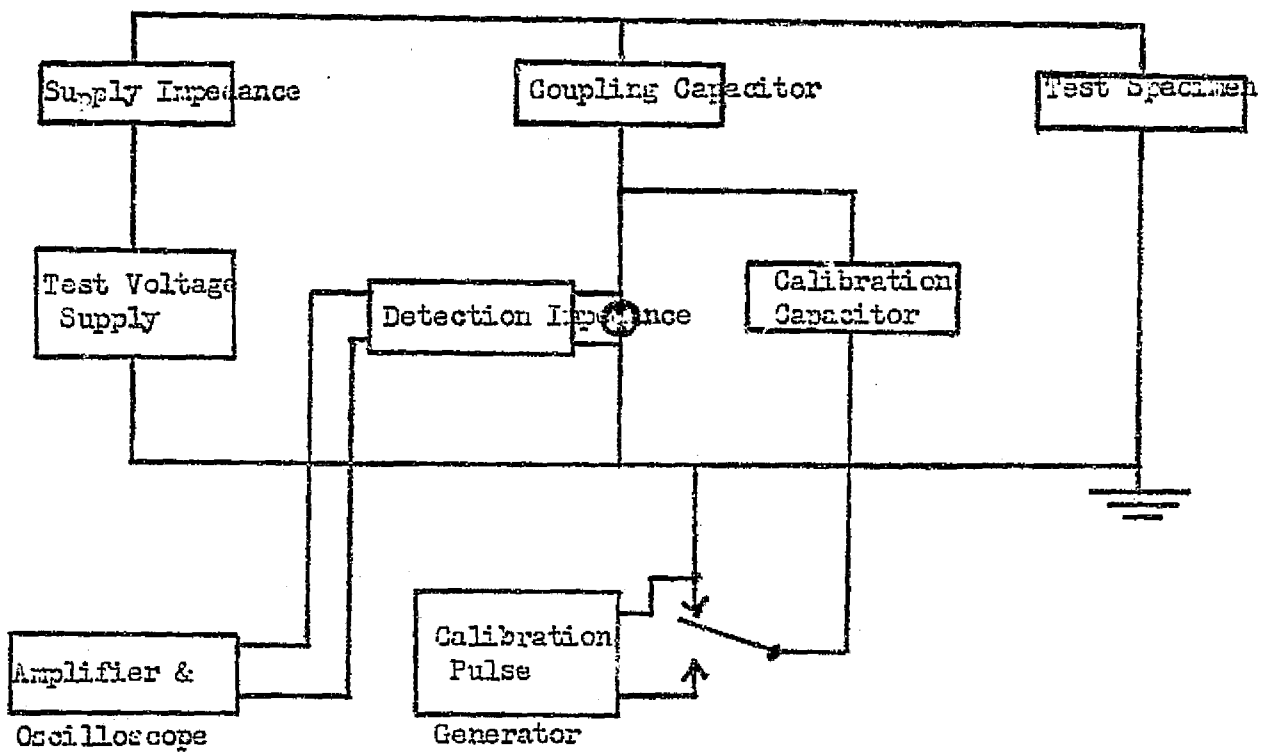

Figure 21, circuit d)

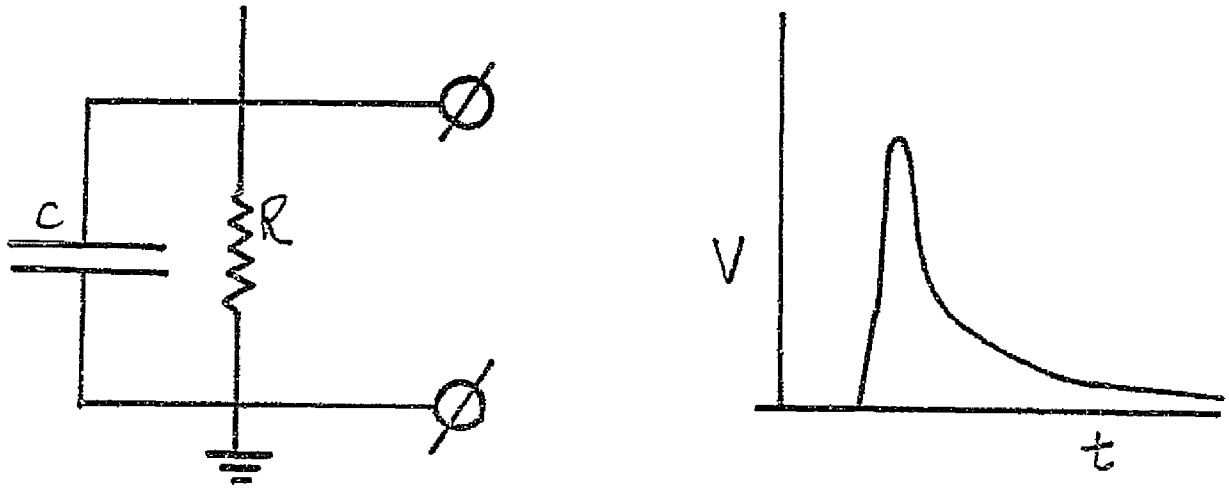

Figure 22 a) : R C as detection impedance & resulting output waveform

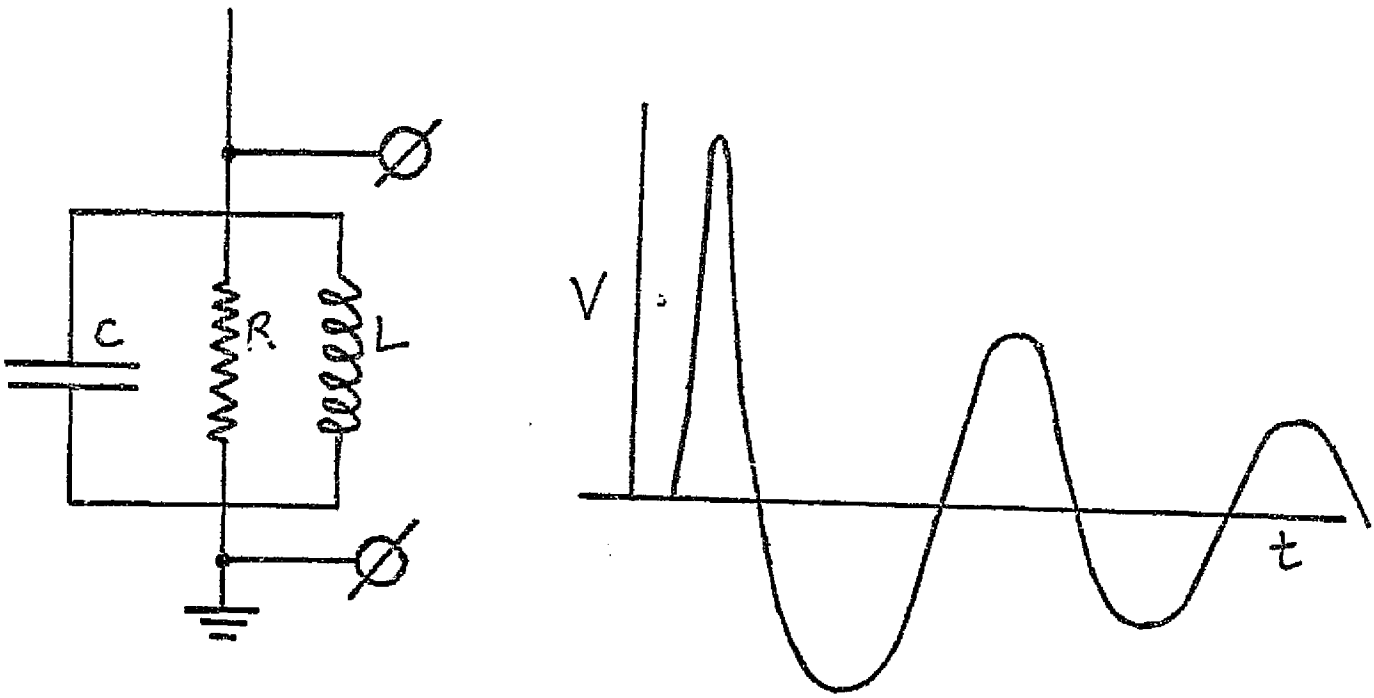

Figure 22 b) : C R L as detection impedance & resulting output waveform

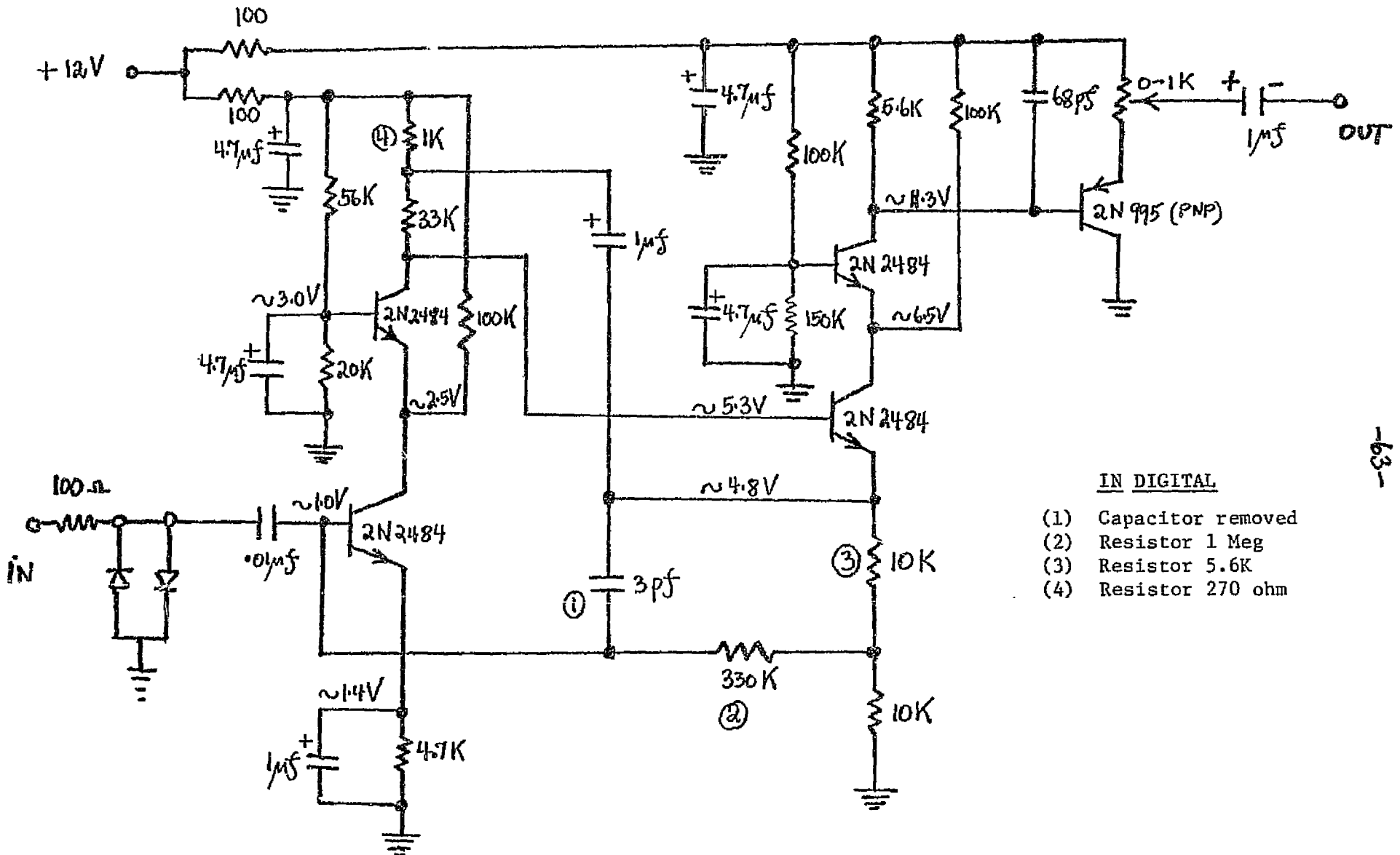

IN DIGITAL

(1) Capacitor removed
(2) Resistor 1 Meg
(3) Resistor 5.6K
(4) Resistor 270 ohm

Figure 29: Charge Sensitive Preamplifier
(Courtesy, Mr. Karageorge, Mr. Birsa, GSFC)

-63-

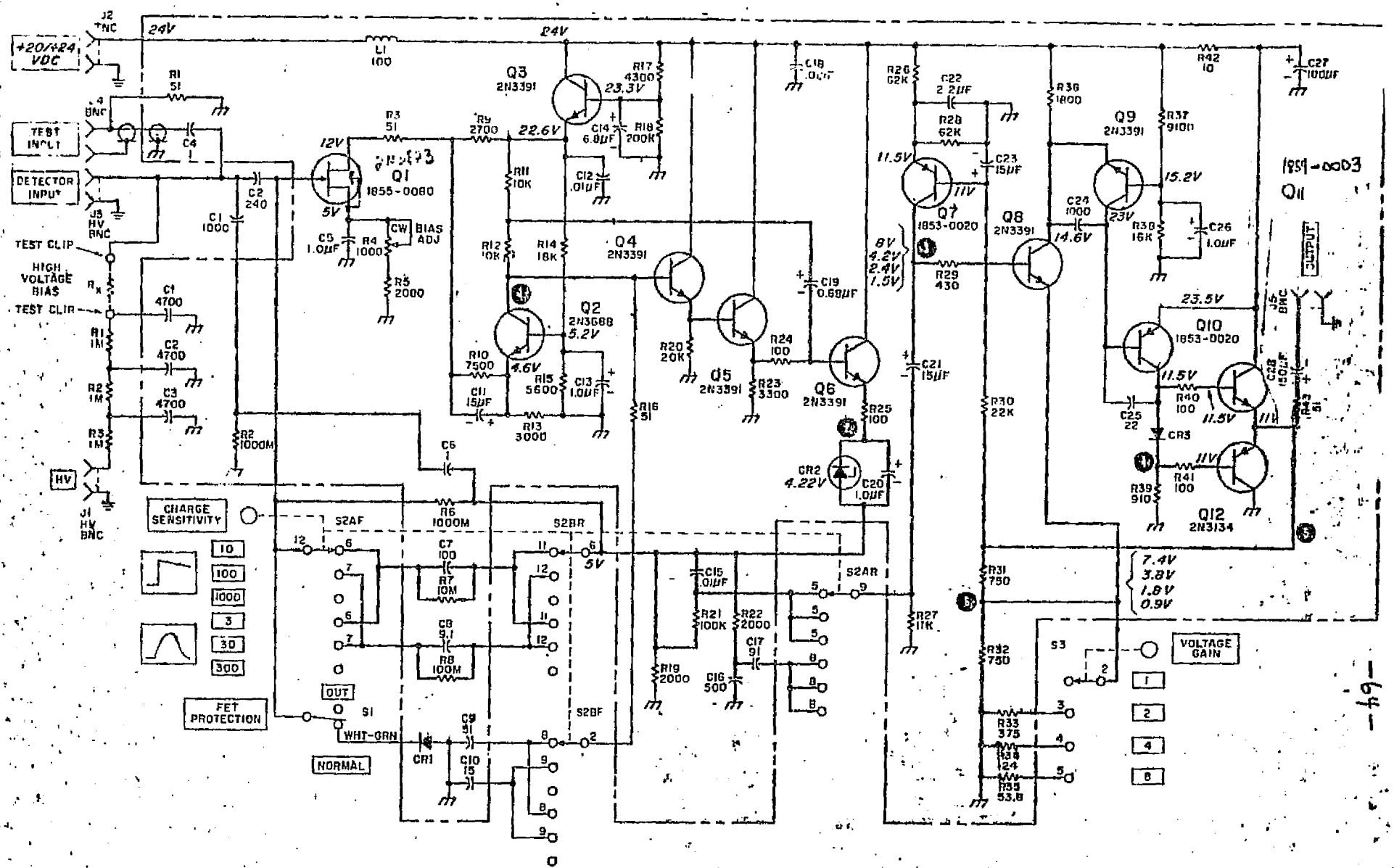

FIGURE 24: Hewlett Packard Preamplifier 5955C

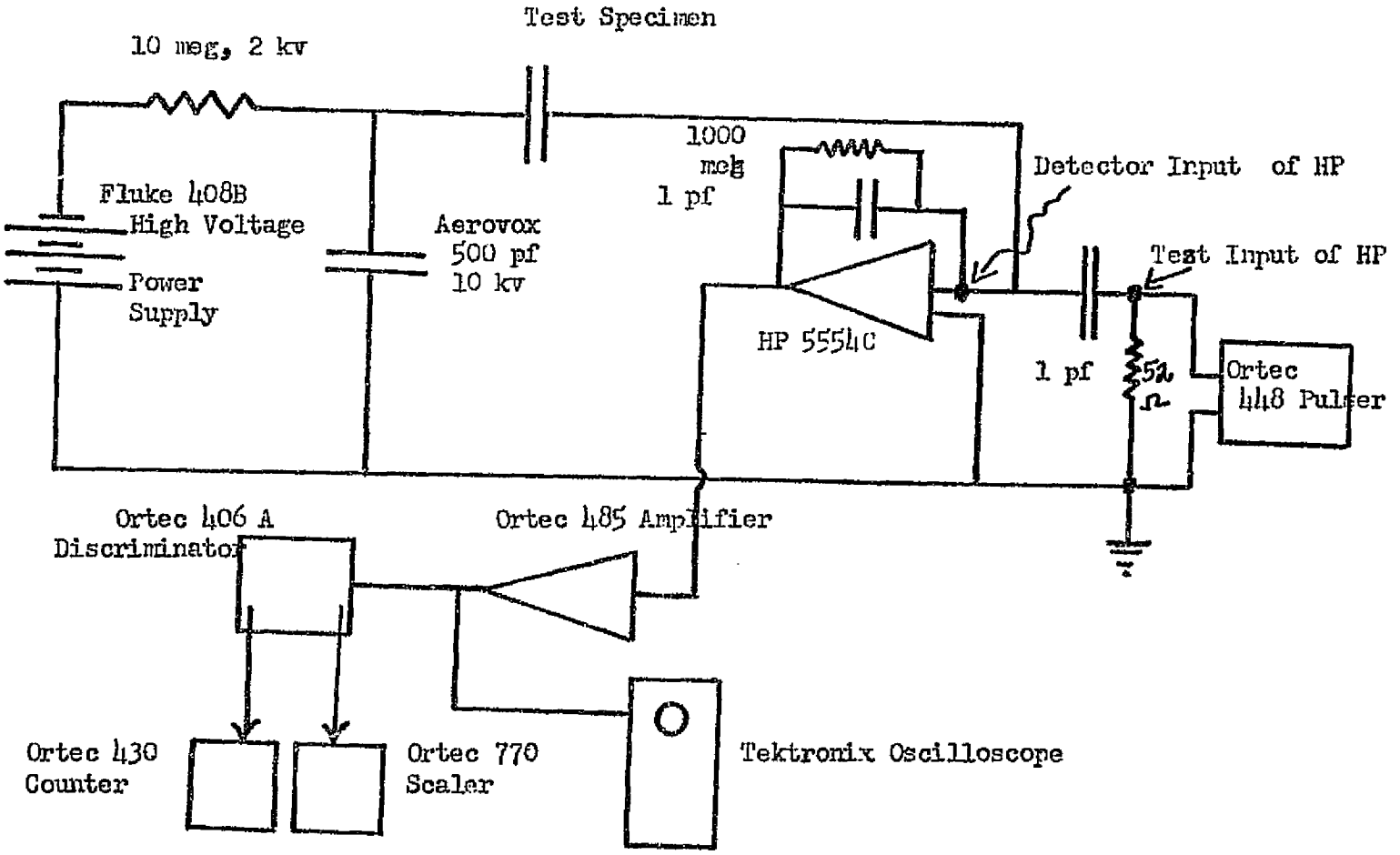

Figure 25: Partial Discharge Circuit for D.C. Capacitor Testing

b. Use an LCR circuit as seen in Figure 22b. The corona impulse sets off shock oscillations, the first negative half of which is integrated and amplified

(2) In our investigation two different preamplifiers were used. the so-called "Rocket" preamplifier with circuit diagram as shown in Figure 23 was used in the Reynolds connector study reported earlier[24] . A Hewlett Packard preamplifier 5554A was used for most of the studies in this report. Circuit diagram is reproduced in Figure 24. It has a FET input stage and is very quiet, its own noise level corresponding to 5×10^{-15} coulombs pulses. It seemed to give a greater count rate than the Rocket preamplifier, especially for very small discharges of the order of 10^{-14} coulomb, even when both preamplifiers were calibrated separately under the exact same circuit conditions.

(3) This brings one to the question of calibration method and circuit sensitivity. The truest calibration would be obtained if the calibrating signal via the calibration capacitor would be injected into the high voltage side of the coupling capacitor as in Figure 21c. In our case it was injected at the low voltage end of the coupling capacitor as in Figure 21d. The sensitivity that is useful is defined as the smallest discharge in picocoulombs that can just be detected. The "raw" calibration at the low voltage end then has to be multiplied by a factor $f = \frac{C_{cc} + C_t + C_s}{C_{cc}}$ if connections are made as in Figure 21d which is the way the Reynolds connector measurements were carried out earlier. In that case the factor f was very close to the value of unity.

If connections are made as in Figure 21 b, which was the case for the capacitor testing, then the factor f is $f = \frac{C_{cc} + C_t + C_s}{C_{cc} + C_s}$ which might amount to the value of 2 or 3 depending what the values of the coupling capacitance C_{cc} and test capacitance C_t and stray capacitance C_s are. In other words the sensitivity as calibrated "raw" might have been set at 2.5×10^{-14} coulomb, but is actually only 5×10^{-14} coulomb if C_{cc} is 1000 pf and C_t is 1000 pf. The experimental arrangement as used for the capacitor testing is shown in Figure 25, the Reynolds connector arrangement having been shown in the earlier report. Alternately, one could calculate what the different "raw" calibrations would have to be in order for all the actual sensitivities to be the same, and then do a new "raw" calibration before each condenser is connected into the circuit.

RESULTS:

The results of extensive partial discharge testing are shown in the following sets of tables. Unfortunately, such testing results of various and sundry circuit components and circuit portions can not be made into a coherent, logical sequence in which the end result is one newly discovered physical constant. The individual tables have to be laboriously scrutinized by the reader to arrive at conclusions.

The counts are reported per 5 minute time interval. The first number gives the total counts, followed after a comma by the number of "big" counts, of charge content greater than the upper window limit. Thus, if corrected circuit sensitivity is 2×10^{-14} coulomb, and the window is 2×10^{-14} to 20×10^{-14} coulombs, then a count rate of 16,3 means 16 total counts of all charge content above 2×10^{-14} coulomb, of which 3 are "biggies" of charge content greater than 20×10^{-14} coul. Moreover, many samples were observed for several successive 5 minute intervals and the average of the last two observations is reported here. Or the last two observations are reported separately. This is because it was found again and again that for voltages not too far above corona inception, the count rate generally decreased with time and leveled off into a more or less steady count rate, after about ten minutes of steadily applied voltage. This investigator feels that it is this leveled-off, steady count rate which is of importance for predictions of long-term behavior rather than the more copious burst of counts one observes just after applying electrical stress. In any case, the reader needs to be aware of

the fact that with this type of measurement a single 5 minute observation is meaningless, and that trends with time need to be observed.

Test 1: HEAO-A high voltage distribution circuit, in vacuum at 10^{-7} torr.

This circuit consisted essentially of seven parallel filter sections or "channels" as shown in Figure 26. The seven high voltage feedthroughs going through the aluminum shielding box (shown at the right side of the figure) were initially not sandblasted, but the single high voltage feedthrough coming from the high voltage power supply was sandblasted. The contents inside the shielding box were solid potted with 93-500 Dow Corning silicone rubber after application of 92-019 primer. Outside of the box the 8 high voltage feedthroughs were not encased in potting. Since application of high voltage was only planned whenever the pressure was at or near 10^{-7} torr, it was not felt to be necessary.

Moreover, it was only intended to turn the high voltage on while taking measurements, not leave it on continuously. It was impractical to keep the liquid N_2 trap continuously filled - it was only kept filled while testing was carried out. (This was a mistake as will be apparent later).

Any one channel of the seven filter sections then corresponds most closely to the basic partial discharge circuit of Figure 21b), but not exactly, because of the 100 Megohm resistor between the two 1100 pf condensors. The calibration pulses that were injected at the low voltage end of the coupling

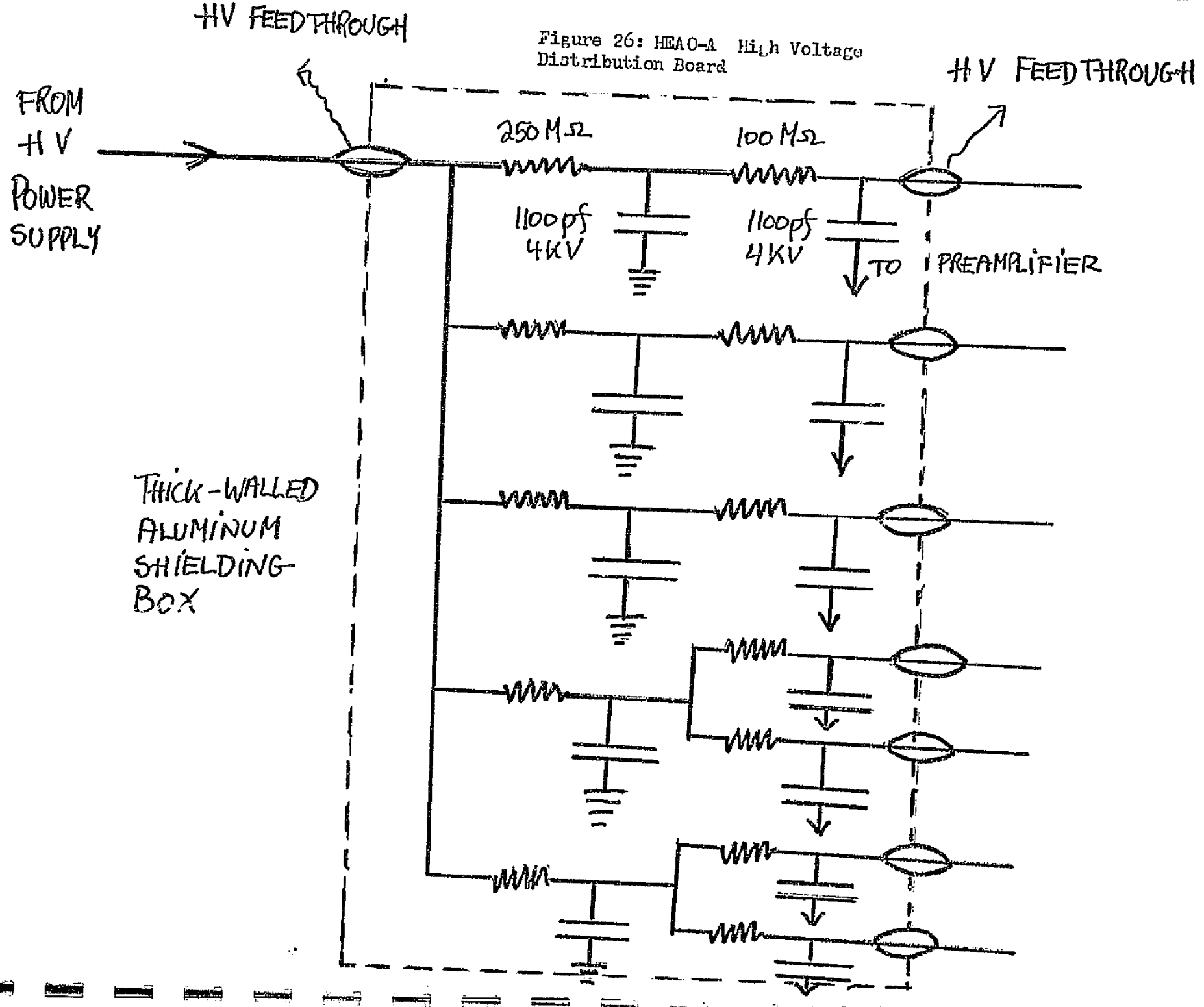

Figure 26: HEAO-A High Voltage Distribution Board

condensor were 0.2μsec rise time, 5μsec decay time, 50/sec rep rate. Actually these are somewhat longer than the expected discharge signals, according to several references[25,30] and as shown in Figure 27. Also, the rise time of the calibrating pulse should be "by a factor of 10 or more, faster than a quarter cycle of the highest frequency to be sensed by the amplifier. Rise times of the order of 2×10^{-7} seconds or faster are recommended"[26].

Table VI shows the testing history of the HEAO-A circuit board. Not all channels were tested at each date. What happened was as follows:

1. August 13, 1976: Testing begun on channel 3, in vacuum at 10^{-6} to 10^{-7} torr. At 2500 volts D.C. count rate was fairly low, namely 30,1.
2. August 15: This same channel has only 1,0 counts at 2500 volts D.C. The vacuum system was let up into the corona region of pressures, about 100-200 microns, to see if the high voltage was getting to the system. Yes it is, because there are thousands of counts. But this damaged the Hewlett Packard preamplifier. It now is noisy and counts without anything on the detector input.
3. September 10: Repaired. Count rate is quite low again.
4. September 15, 16: Channel 7 is tested and has low count rate.
5. Then this high voltage distribution board is taken out of the vacuum system, and one potted with sandfilled 93-500

silicone rubber is placed in the vacuum system. This one, reported in Table V, broke down into thousands of counts at about 1800 volts. The Hewlett Packard preamp is damaged again !

6. September 18, 19: The Rockett preamp is used to test channel 1 - very low count rate of 4,0. This is reasuring since there is an area of visibly poor adhesion on the circuit board near this feedthrough.
7. October 2: The Hewlett Packard has been repaired again and is used to test all channels. Very low count rate on channels ,2,3. Count rate of 121,4 on channel 4; 47,1 on channel 5; 59,0 on channel 6. Channel 2 retest without liquid nitrogen on the high vacuum line trap now tests at 35,0. Unfortunately no particular notice was taken of this.
8. October 9: More data taken on Channel 2 - still 35,5. Channel 1 is somewhat higher than before at 16,3. Then 5 ft of Reynolds cable is inserted with connector between the power supply and the high voltage distribution board. At first there are more of the big counts than before, but after 1/2 hour in vacuum we have 10,1. <u>So the Reynolds cable and connector can be said not to introduce extra counts as per short term testing</u>.
9. October 16: Channel 1 is very beautifully quiet at 1,0. It was decided to leave the <u>high voltage on continuously</u> at 2500 volts, starting at 5:30 pm. Upon return at 8:45 <u>3-1/3 hours</u> later, the count rate on Channel 1 was up to 111,2; on Channel 4 up to 200,5; Channel 7 up to 370,1.

Upon removal from the vacuum system and inspection it is noticed that the exposed sintered milk-glass insulation on the feedthroughs has turned yellowish in color-, most yellowish on pins 4,5,6,7, exactly where the count rate has increased the most. It is also noticed that there is liquid diffusion pump oil on and around the feedthroughs. Unfortunately, during the entire test history the side with the exposed, unpotted feedthroughs had been pointing downward, and the pins 3,4,5,6 had been directly over the port to the trap and diffusion pump. Between tests there had been no liquid N_2 on the trap. Evidently, there had been backstreaming of diffusion pump oil, and it deposited on the underside of the high voltage board where the feedthroughs were. The continuous application of 2500 volts D.C. then must have caused some sort of tracking. Objections that the diffusion pump oil is a silicone oil can be countered by the fact that investigators* in electron spectroscopy always find characteristic carbon spectra from backstreaming diffusion pump oil, even when great care has been taken to avoid this. There apparently are organic fractions in diffusion pump oil.

The most yellow feedthrough had the highest count rate. The surface contamination could not be rubbed off or washed off. It was decided to vapor hone (sandblast) the contaminated insulation.

10. November 18: The feedthroughs have been sandblasted. The insulation on numbers 1,2,3,4 are coated with Epon 828-Versamid 140; numbers 5,6 are coated with a new silicone

*Private communication with Dr. Leslie Speller, Howard University

rubber-polyimide conformal coating NT 114 of NT industries, which cures upon exposure to the water vapor in the atmosphere. Number 7 is not coated at all. Measurements show:

Channel 1 - no improvement

Channel 4 - improvement-count rate down by 1/3

Channel 5,6 - have become worse. Count rate 632,122.

Channel 7 - improvement; count rate down by 4/5

Consultation with Mr. M Karageorge of Code 663.3 who has worked with the same circuit board. He states that in his experience vapor honed insulation on these particular feedthroughs has generally been more noisy than the untouched glazed insulation. This is thought to be due to many "cavities large enough to accommodate 200 water molecules." Moreover, there is now the question whether the NT 114 coating is inherently noisy if cured by just exposing to the normal room air for 24 hours.

11. It is decided to dig out the 7 spoiled feedthroughs, replace them with new ones and repot the seven cavities thus created.

12. January 7,9,11, 1976: Channels 5,6,7 noise count is much better, but not as quiet as before the mishaps. Channel 1 is now much worse, in fact at 1700 volts it has 868,2 counts. There is a visibly enlarged area of poor adhesion on the circuit board near the feedthrough. This was probably made worse by the digging out of the number 1 feedthrough.

End of Test Run.

Some Conclusions From Test 1:

a. Insulation on high voltage feedthroughs should always be solid potted to protect it against deposition of foreign matter that might lead to tracking.

b. Areas of poor adhesion near a high voltage terminal do not necessarily contribute to electrical noise, but might enlarge later due to mechanical stresses, and then become problem spots.

c. Vapor honing or sandblasting of insulation needs to be checked for electrical noise before it is routinely used for cleaning off impurities or to improve adhesion. The physical structure of the material under the removed surface layer might actally absorb water vapor and make the device more noisy.

d. The new NT 114 silicone rubber-polyimide conformal coating needs to be investigated for partial discharge tendencies. Perhaps the curing has to be done at elevated temperatures in a moist oven.

Test 2: Sand-filled 93-500 silicone rubber potting of a two channel high voltage distribution board. Test in vacuum at 10^{-6} to 10^{-7} torr. Two channels of HEAO-A filters were potted by filling the shielding box with clean, previously baked out mica sand and pouring Dow Corning 93-500 silicone rubber resin on it in vacuum. The vacuum was then released, and the atmosphere pushing down on the liquid resin would help to push it down into the evacuated crevices between the grains of sand. The unit was then cured as usual for 93-500.

The testing connections were made just as with the previous circuit. As seen in Table VII catastrophic breakdown occurred variously between 1800 and 2000 volts, as signified by thousands of counts.

After cutting through the top layers of silicone-rubber-

encased sand it was found that underneath there was nothing but loose sand. In other words the 93-500 had not penetrated deeply, and the high voltage buss wires were just lying in loose sand. Upon closer examination it was found that the shielding box was not vacuum tight. Screws through the bottom of the box leaked gas along the threads.

Conclusion:

1. Filled, non-transparent potting jobs must have their integrity examined by partial discharge testing.
2. Vacuum impregnation of fillers will only be successful if the potting container below the liquid resin level is absolutely vacuum tight. Otherwise, when the atmosphere is expected to push the resin down into the crevices, it will not be able to do so if the crevices are at one atmosphere too due to rapid leaking in of air into the bottom of the container.

Test 3: Attempt at long-term testing-high voltage on continuously-of 5 ft-long Reynolds cable and connector in vacuum at 10^{-4} torr. This was instrumented too late, on March 14, 1976. It was hoped to let the test proceed for 6 months or so, to test for diffusion outward of gas in the center strand of the cable into the surrounding vacuum, to see if there would then be more partial discharge counts as the pressure inside the center strand would go through the corona region. But the test was cut short after 6 weeks when the laboratory was ordered to be cleared. During the 6 weeks that the test did run the count rate decreased. This agrees with findings on

an earlier reported test[24] for about that length of time, on a much shorter piece of cable. But on the diffusion effects on internal pressures in the center strand the test was not long enough and therefore totally inconclusive.

Test 4: Capacitors from different manufacturers, tested at atmospheric pressure.

Here the connections were made according to Figure 21b). The coupling capacitor used was a 500 pf; 10 kv, Aerovox, since this was by far the most corona-free capacitor in the investigator's possession, up to 5000 volts applied. This was ascertained both on the presently described equipment and also with James G. Biddle Co. equipment. With the latter the 500 pf, 10 kv Aerovox capacitor did not show observable D.C. partial discharge pulses at sensitivity of 2 picocoulombs until about 7.5 kv, although corona started on A.C. applied voltage at about 5 kv.

The tables are headed by the descriptor "raw" calibration, which means the uncorrected setting of the dicriminator to minimum observable charge. Then follows the descriptor "corrected" sensitivity, which means the "raw" calibration multiplied by the correction factor $\frac{C_{cc} + C_t}{C_{cc}}$ to give the actual circuit sensitivity, which gets poorer the greater the sample capacitance C_t is compared to the coupling capacitance C_{cc}. Again, a data recording of 58,3 means 58 total counts, and 3 of these were "biggies" above the upper boundary of the window.

Table IX compares several types of CRL capacitors. The CRL-RF 345C ±10%, 1000 pf, 4 kv, D.C. variety already has many pulses

at 3/4 rated voltage at the stated sensitivity. If one wanted very quiet performance of a circuit at this sensitivity 3×10^{-14} coulomb, one would only use these up to 1/2 rated voltage. On the other hand the CRL 2 x 620 pf, 2 kv, is very quiet at 2000 volts D.C. and could be used to 3/2 rated voltage. The same is true for the CRL X5U, 910 pf, 2kv. The CRL Z5U, 820 pf, 3 kv looks good to rated voltage. (Tests at 5000 volts on the Aerovox 500 pf, 10 kv were interspersed to make sure that the beginning of noise at 3000 volts of the CRL's discussed above was not due to the high voltage power supply, and it was not). The total count on all of these capacitors lies mostly in the lowest decade of charge. These seem to be somewhat reducible in number by alcohol wash. This means that some of these lowest energy pulses are due to surface leakage. On the other hand, dropping one of the condensers inadvertantly caused a marked increase in both little and big counts. So these ceramic disc capacitors must not be used after dropping them. There is more data on this dropping effect in a later table.

Table X presents data on these same capacitors and on some other manufacturer's condensers, all measured at a later time, after several replacements of the FET transistor in the HP.P. preamp, and at a less sensitive calibration. The earlier and later data on the CRL capacitors correlates very well. The Aerovox, 500 pf, 10 kv is seen to be very quiet, at 5000 volts and the Maida capacitors are very noisy, in fact 10 to 100 times noisier at 5000 volts than the Aerovox.

It is of interest that on observing the Maida partial discharge pulses on the oscilloscope there were two distinct shapes

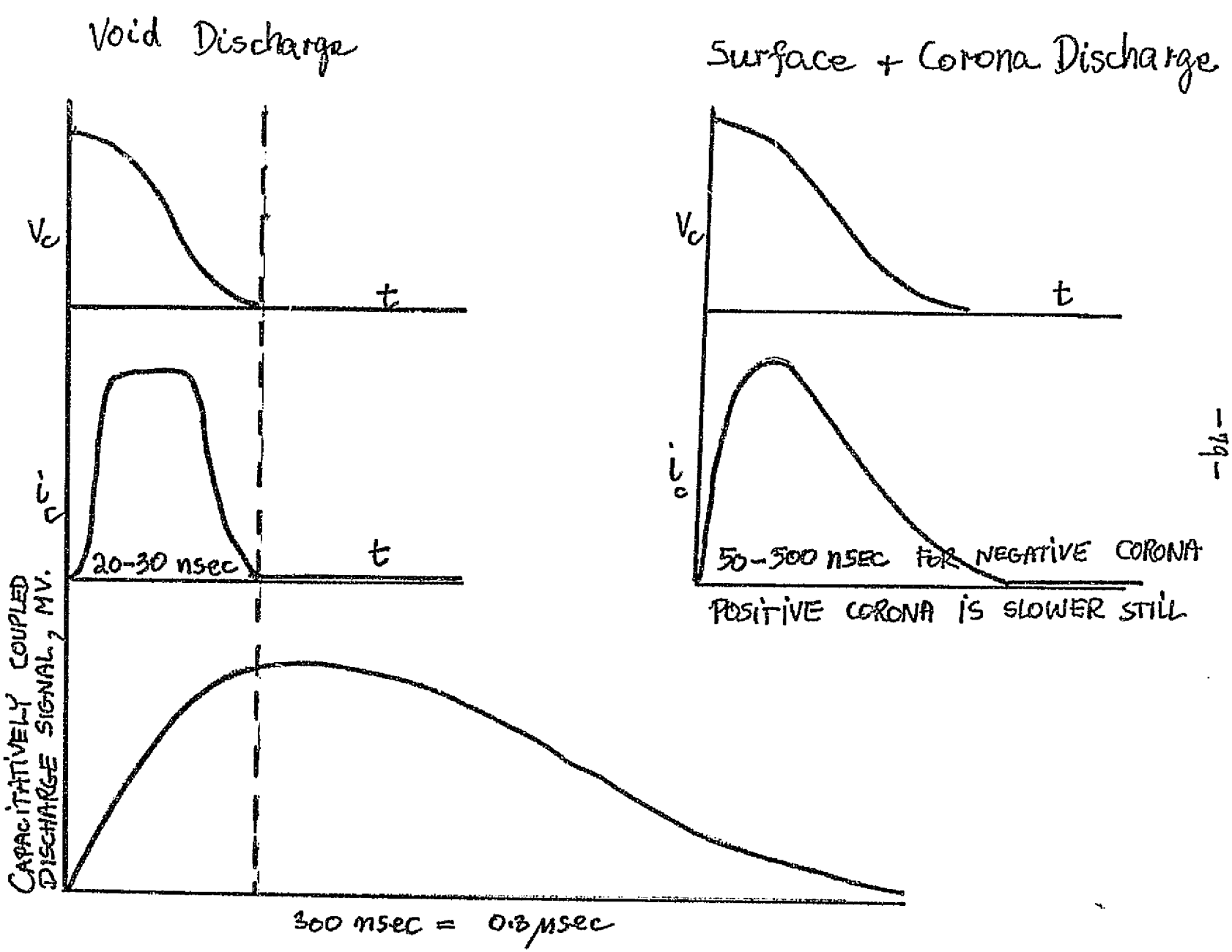

Figure 27: Different types of discharge versus length of output signal, from Literature.

of pulses common among the big ones: the usual S-shaped ones that looked like the calibrating pulses after going through the pulse shaping of the post amplifier: The other type had inverted polarity and was much wider:

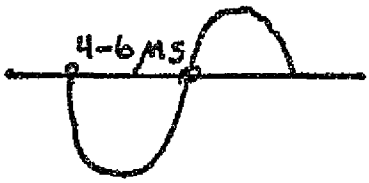

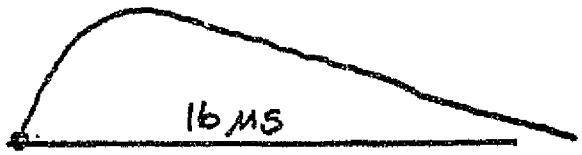

This probably indicates two different origins of pulses. Perhaps the wide, long duration ones are discharges from the electrode edges onto the disc surfaces whereas the shorter pulses might be from voids? Compare Fig. 27.

Table XI shows some data obtained on a few of the same capacitors on Biddle equipment at G.E. Space Systems Center at King of Prussia, Pa. The sensitivity of this equipment does not permit testing down to as low charge levels as the instrumentation used for most of this report. It is from 2 picocoulombs on up. On the other hand, it permits going up to 40 kv D.C. or 60 kv A.C. applied voltage. Nevertheless, the data snow that the Maida 15 kv already has some D.C. corona at 5 kv and that the CRL RF 345 C 4 kv has a sharp upswing in numbers of counts around 3000 volts, which agrees with data in the previous tables. Of great interest is to see how the histogram of the Maida condenser changed to many more and much more energetic counts after being dropped. Also the fact that the CRL capacitor th. had marked corona increase at about 3000 volts on D.C. showed corona inception at 600 volts on A.C. agrees with data obtained earlier at the Biddle Company, as to start of observable pulses on D.C. versus A.C. applied voltage.

Table XII gives some measurements on 1100 pf, 6 kv CRL capacitors when potted in plain Sylgard 184, in sand-filled Sylgard, and not potted. The fact that stands out is that whereas not much difference was noted up to 3500 volts, at 4000 volts there are markedly more counts from the sandfilled pottings than from the plain Sylgard or unpotted samples.

General Conclusions:

It is evident that up to an applied voltage of 5000 to 6000 volts D.C. this method and apparatus is successful in revealing the presence of partial discharge pulses and thus the integrity of the insulation to a sensitivity of the order of 2×10^{-14} coulombs, both at atmospheric pressure and vacuum. If one wishes to go to higher applied voltages, one then faces the ever more difficult problem of making sure that the equipment itself, that is, the power supply, the coupling capacitor, the interconnections themselves be partial-discharge-free. This has been accomplished to a sensitivity of 2 picocoulombs in certain commercially available units, such as the partial discharge equipment made by the James G. Biddle Company. If a correlation between partial discharge histograms near corona inception voltage and the subsequent long-term life at rated voltage could be established, then tests on such equipment would certainly be useful in predicting future performance of high voltage components and circuits.

TABLE VI

Test of HEAO-A High Voltage distribution board, in vacuum at 10^{-7} torr.

"Raw calibration: 1×10^{-14} coul; 1 -- 10 x 10^{-14} coulomb window

Corrected Sensitivity: 2×10^{-14} coul; 2 -- 20 x 10^{-14} coulomb window

Channel #1

(This has some poor adhesion on the circuit board nearby)

Sept. 18, 1975: "Rocket" preamp

0 v	2400 v	Net at 2400 v
11,0	10,1	0,1
	10,0	0,0

Sept. 19, 1975:

3,0	7,0	4,0

Oct. 2, 1975: H.P. preamp has been repaired and is used after this date on all channels.

12,3	16,0	0,0
15,4	14,0	0,0

Oct. 9, 1975

27,0	50,2	23,0
	30,4	3,4
	41,2	14,2
	52,1	25,1

Add Reynolds cable and connector in series: splice <u>not</u> potted at center strand or shielding.

20,4	29,11	9,7
	28,8	8,4
	33,4	13,0
	35,2	15,0
	35,1	15,0
20,1 18,1	39,8	11,7
16,2	27,2	9,1
	28,2	10,1

So, after the Reynolds cable has been in vacuum for about 1/2 hour it does not add detectable counts to the system.

Channel #1, continued

Oct. 16, 1975	0 v	1700 v	2400 v	Net at 2400 v
	10,0		11,0	1,0
			6,0	0,0
		At 5:30 pm	4,0	0,0
Left high voltage on				
Continuously until 8:30 pm			121,2	111,2
	10,0		122,0	112,0
Something bad must have happened.				
Nov. 18, 1975 Sandblasted all insulation on feedthroughs, coated with epoxy on Channel #1				
	109,2		205,2	108,0
			=184,2	
	No improvement		170,1	
Jan. 7, 1976 The feedthroughs have been replaced, but without vacuum bake-out				
	55,1	65,2	407,6	
	44,1		493,2	390,3
			430,3	
				Worse
Jan. 11, 1976	49,1	868,2		Worse
	43,1			

Channel #2

Oct. 2, 1975, H.P. preamp

	0 volts	1400v	2400v	Net
	25,4		26,3	0,0
Oct. 2, 1975	Repeat after testing all other channels, without N_2 in trap.			
	22,2		57,1	35,0
	39,0		85,2	46,2
Oct. 9, 1975				
	44,0	39,0	75,5	35,5
	After sandblasting, coating with epoxy			
Nov. 18, 1975				
	76,0	75,0	164,2	88,2

Channel #3, H.P. Preamp

Aug. 13, 1975	100v	1250v	2500v	Net
	34,0	32,0	54,1 76,1	33,1
		1,0 0,0	31,1 31,3 29,2	30,2
Aug. 15, 1975		0,0	1,0	1,0

Put system into corona region to test the system--counts like mad. After test trouble with preamp--it is now noisy by itself.

Sept. 10, 1975 Preamp quiet by itself.

35,0	33,0	36,0	2,0
		43,0	9,0
		38,0	4,0

Oct. 2, 1975

0 volts	2400 v	NET
25,1 29,1	20,0	0,0

Channel #4

Oct. 2, 1975

0 V	1400v	2000v	2400v	Net
22,1			143,5	121,4
21,1	15,1		167,6	145,5
			132,2	110,1

Oct. 16, 1975, After 3-1/4 hours at H.V.

14,1	Quiet	106,2	320,5	
			200,4	200,5
			225,6	

After sandblasting, coating with epoxy

Nov. 18, 1975

73,13!			197,16!	124,3
			171,12!	

Channel #5

Oct. 2, 1976

	0 volts	1700v	2400v	Net
	53,0		100,1	47,1

Dec. 2, 1975 — After sandblasting, coating with NT 114

110,1	205,10	742,123	632,122

Jan. 9, 1976 — Replacing feedthroughs, but no vac-bake out.

42,0 40,0	48,1	166,9	124,9 Better
80,3 88,2	155,0 150,3	230,5	150,2

Channel #6

Oct. 2, 1976	0 V	1700v	2400v	Net
	28,4!		87,0	59,0

After sandblasting, coating with NT 114

Nov. 18, 1975				
	55,1	63,5	611,20	!! 556,19

After replacing feedthroughs, but no vac.-bake out

Jan. 11, 1975				
	49,0	55,13 ! 36,2 ?	103,5	54,5
	110,0	30,5 ?	125,17	25,14
	93,0		124,11	

Channel #7, H.P. Preamp

Sept. 15, 1975

	O v	1700v	2000v	2400v	Net
	1,0			6,0	5,0
				5,0	4,0
				6,1	5,1
	41,1			45,2	4,1
Sept. 16, 1975	0,0			5,2	5,2

Then tested the sandfilled HV tray, got Breakdown; preamp trouble after test.

Oct. 16, 1975 After 3-1/4 hours with HV on

18,1	90,2	388,1	370,1

Feedthroughs yellow; 4, 5, 6, 7 most yellow, wash with alcohol.

9,1	22,0	54,0	240,3	230,1
			371,5	362,4

Nov. 18, 1975, After sandblasting, no coating

65,1	81,4	140,2	75,1 Better

Dec. 2, 1975	144,0	222,3	262,5	116,5
	155,2	200,3	250,3	95,1
			225,5	70,3

Replacing feedthroughs, but not doing vac. bake-out

Jan. 7, 1976

	O v	1700v	2400v	Net
	82,0		123,3	53,3
	69,0	Better		

Jan. 9, 1976

97,0		130,6	113,10	
	87,0	98,1	111,10	24,10
75,0			109,11	

Jan. 11, 1976

83,6		187,7	35,3
93,4		115,8	

TABLE VII

September 16,

Sand-Filled Circuit

HP 5554C Preamplifier

"Raw" Calibration: 5×10^{-14} Coulombs

Large Counts: Those above 2×10^{-13} Coulombs

I. Pressure: Atmospheric

This unit suddenly shows thousands of counts at 1800 volts.

II. Pressure: 10^{-4} Torr

	Total counts 5 mins.	Large counts 5 mins.
1900 volts:	3910	852
2000 volts:	Thousands of counts on both	
	Breakdown	
0 volts:	Now the preamp is noisy at 5×10^{-14} coul. Changes raw sensitivity to 8×10^{-14} coul.	
2000 volts:	Breakdown again	

Something is wrong.

TABLE VIII

5 ft. length of Reynolds Type "L" cable with connector, at 10^{-4} torr, at 2400 volts D.C.

Attempt at long term test using Hewlett Packard preamp 5554C

Raw calibration 1 x 10^{-14} coul; 1-10 x 10^{-14} coul window

Corrected sensitivity 2 x 10^{-14} coul; 2 - 20 x 10^{-14} coul win.

March 14, 1976

Net counts just after installation	171, 1
	105, 1
	208,0
	130,2

April 28, 1976

Net counts	82,0
	99,2
	118,3

Lab ordered cleared, inconclusive test. NOT long enough.

TABLE IX

Capacitor Testing on H. P. Preamp 5554C.

Raw Calibration: 1×10^{-14} coul minimum
1×10^{-14} coul --- 10×10^{-14} window.

A) CRL - KF 345C ±10% 1000 pf, 4kv.

Corrected Sensitivity: 3×10^{-14} coul --- 30×10^{-14} window.

# at	OV_r Ov	$1/2V_r$ 2000v	$.63V_r$ 2500v	$3/4V_r$ 3000v	$7/8V_r$ 3500v	V_r 4000v
1				58,0 53,1 75,0 93,2 117,0		
2		2,0	25,0 30,0	382,33 309,9		
3				390,		
4				547,		
5				360,		
6			Alcohol wash	400,10 220,5		
12				275,10		
13				105		
14				205,10		
16				350,0		

B) CRL 2 x 620 pf 2kv

Corrected Sensitivity: 2.2×10^{-14} coul --- 22×10^{-14} window

# at	$0V_r$	$1/2V_r$	V_r	$3/2V_r$	$7/4V_r$	$2V_r$	$5/2V_r$
1	O	1000v	2000v	3000	3500	4000	5000 volts
2	0,0	5,0	2,1	3,0		300,0	
3	7,0	7,0		71,2		157,0	
4	1,0		1,0	36,0			
5			0,0	105,0	155,0		
6						250,20	

C) CRL X5U 910pf 2kv

Corrected sensitivity: 2.8×10^{-14} coul --- 28×10^{-14} window

1	0,0	1,0	88,0	322,8
2	0	2,0	120,0	327,13
3	Dropped inadvertently	67,1	224,1	588,73!!

Don't Drop These!

TABLE IX (continued)

C) CRL X5U 910 pf 2 kv rating D. C.

Corrected sensitivity: 2.8×10^{-14} coul;
$2.8 -- 28 \times 10^{-14}$ coul window

#	at OV_r Ov	$1/2V_r$ 1000v	V_r 2000v	$3/2V_r$ 3000v	$7/4V_r$ 3500v	$2V_r$ 4000v	$5/2V_r$ 5000v
1	0,0		1,0	88,0		322,8	
2	0,0		2,0	120,0		327,13	
3	Dropped 0,0 inadvertently		67,1	224,1		588,73:	Don't drop these:

D) CRL Z5U 820pf 3 kv rating D. C.

Corrected sensitivity: 2.6×10^{-14} coul; $2.6 -- 26 \times 10^{-14}$ coul window

#	at OV_r OV	$2/3V_r$ 2000v	V_r 3000v	$4/3V_r$ 4000v	$5/3V_r$ 5000v
1	0,0	4,3	49,0	80,1	138,5
2	0,0	5,0	54,0	109,6	151,25 177,40
3	0,0	4,0	35,0	117,2	234,38 164,24
4	0,0	2,0	47,3		445,85 210,55 254,32

TABLE X CAPACITOR TESTING

Using HP preamp 5554C

Raw Calibration: 2×10^{-14} coul; $2 - 10 \times 10^{-14}$ coul window.

A) CRL - RF 345C ±10% 1000pf 4kv rating D.C.,

Corrected Sensitivity: 6×10^{-14} coul; $6 - 30 \times 10^{-14}$ window

#	At	$0V_r$ 0	$1/2V_r$ 2000	$.63V_r$ 2500	$3/4V_r$ 3000	$7/8V_r$ 3500	V_r 4000	$5/4V_r$ 5000
A		0,0	13,0		19,1	73,9 90,2	193,27 264,23	
F					16,0	76,9		
G					26,2			
B							118,17	
E							505,70	
D							115,14	
C				148,23	Lots of counts		- - -	

B) CRL 2 x 620 pf 2kv rating D.C.

Corrected Sensitivity: 4.4 X 10-14 coul; $4.4 - 22 \times 10^{-14}$ window

#	0 0	$1/2V_r$	V_r 2000	$3/2V_r$ 3000	$2V_r$ 4000
A			13,0	5,0	28,10
B			2,2		66,10
C			370,100	Must be a bad one	

C) CRL X5U 910pf 2kv

Corrected Sensitivity: 5.6×10^{-14} coul; $5.6 - 28 \times 10^{-14}$ coul

#	0 0	$1/2V_r$	V_r 2000	$3/2V_r$ 3000	$2V_r$ 4000	
1	0,0		1,1	19,2		
2	7,7		21,2	31,5		
3	0,0		91,8	70,29		The dropped one

D) CRL Z5U 820pf 3kv

Corrected Sensitivity: 5.2×10^{-14} coul; $5.2 - 26 \times 10^{-14}$

#	$0V_r$ 0v	V_r 3000v	$5/3V_r$ 5000v
	0,0	14,0	96,14

E) CRL 1100 x 2 1100pf 1kv

Corrected Sensitivity: 6.4×10^{-14} coul; 6.4 -- 32 x 10^{-14}

$0V_r$ 0	$1/2V_r$ 500v	V_r 1000v	$3/2V_r$ 1500v	$2V_r$ 2000v
20,0	26,0	38,0	21,0	105,1
27,0		27,1		23,0

F) CRL X5U 1100pf 4kv HEAO-A

Corrected Sensitivity: 6.4×10^{-14} coul; 6.4 -- 32 x 10^{-14}

$0V_r$ 0v	$.63V_r$ 2500v	$3/4V_r$ 3000v	V_r 4000v
0,0	15,1	52,8 44,3	216,42
		57,4	258,44

G) Aerovox 500pf 10kv

Corrected Sensitivity: 4×10^{-14} coul; $4 -- 20 \times 10^{-14}$

#	$0V_r$ Ov	$3/10V_r$ 3000	$4/10V_r$ 4000v	$1/2V_r$ 5000v
1	0,0			9,0 0,0
2	0,0			24,0

H) Maida X5R 500pf 10kv

Corrected Sensitivity: 4×10^{-14} coul; $4 -- 20 \times 10^{-14}$

1	0,0	9,2 10,0	168,18 102,17
2	0,0	104,6	83,15

I) Maida Z5U 1000pf 20kv

Corrected Sensitivity: 6×10^{-14}; $6 -- 30 \times 10^{-14}$

# at	$0V_r$ 0	$3/20V_r$ 3000v	$4/20V_r$ 4000v
	0,0	43,3	72,6
	0,0	24,2	45,4

K) Maida X5R 1000pf 15kv

Corrected Sensitivity: 6×10^{-14}; $6 -- 30 \times 10^{-14}$

$0V_r$ 0	2000	3000	4000	$1/3V_r$ 5000
0,0	10,0	22,2	217,32	1326,96
00,		40,2	112,17	1118,160

G) Aerovox 500pf 10kv

Corrected Sensitivity: 4×10^{-14} coul; $4 -- 20 \times 10^{-14}$

#	0 0	$1/2V_r$ 5000v
1	0,0	9,0 0,0
2	0,0	24,0

TABLE XI

Testing done with Biddle Co. equipment at G. E. Space Systems Center, King of Purssia, Pa.

April 21, 1976

Sensitivity: 2 picocoulombs on up. Sampling time: 200 seconds

1000 puff, 15kv, X5R, Maida

A) 5kv: 4 pulses total

1 at 17 pc

1 at 15

2 around 2 pc

10kv DC: 18 pulses total count

1 at 30 pc

1 19

2 8

14 around 2

12kv DC: 27 pulses total count

1 105 pc

1 60 pc

1 19 pc

24 around 2

15kv DC: 39 pulses total

1 105 pc

1 72

1 46

1 29

1 17

34 around 2 pc

B) Dropped some onto metal strip on floor from 7 ft. height.

10kv DC: 66 pulses total

33	105 pc
1	90
1	11

15kv DC: 200 pulses total

3	at	950 - 1000 pc
3	at	900 - 900
3	at	850 - 900
1		750 - 800
2		700 - 750
2		550 - 600
1		513 - 550
4		450 - 500
8		400 - 450
7		350 - 400
12		300 - 350
23		250 - 300
21		200 - 250
16		150 - 200
2		100 - 150
1		50 - 100
96		1 - 50

C) CRL RF 345C 1000pf 4kv

2000v: 5 counts total

1 at 16 pc

4 around 2 pc

3000v: 53 counts total

1 105 pc

1 18

1 8

50 3 pc to 0.8 pc

4000v: 81 counts total

5 105 pc

1 50

1 24

1 16

1 12

72 5 pc

AC corona inception at 600 volts

TABLE XII

Sandfilled vs Plain Sylgard

Using HP preamp 5554C

Raw Calibration: 2×10^{-14} coul; 2 -- 10 x 10^{-14} coul window

Corrected Sensitivity: 6×10^{-14} coul; 6 -- 30 x 10^{-14} window

CRL 1100pf 6kv	2000 V	3000 V	3500 V	4000v
Sandfilled Sylgard 184		81,12 66,5		745,224
#1			214,30	540,143
#2	11,0	331,63		3425,344
#3		25,4		179,36 105,28
#4				1965,108
Plain Sylgard 184		37,6	225,43	476,156
#0	22,0	92,30		574,118
Alcohol wash	8,0	12,0		145,41 140,38
#5		20,4		792,26
Not Potted		88,5 44,3	240,37	216,42
	24,0	57,4		258,44

CHAPTER IV

SOME ASPECTS OF POTTING

The subject of potting and encapsulation has certainly previously been written about, both under NASA auspices and otherwise. Examples are the NASA publication "Potting Electronic Modules" by R.E. Keith[1] which in itself gives 120 references through the year 1969; also the book by J.J. Licari on Plastic Coatings for Electronics[31] and many others listed in the references[24,32,33,34,35,]. A Goddard Space Flight Center document # X-752-74-247[38] by E. Tankisley is also available.

Potting or encapsulation of an electronic circuit should be taken very, very seriously in the original design stage, especially when high voltage is involved. The potting should accomplish protection against the space environment and against the vibration environment during launch. It also must serve to en hance electrical insulation, but if the design is such that the potting compound breaks away from the components, the insulating properties will be worse than if no potting were used at all. The idea that potting is the simple job of pouring the liquid resin into the mold, and then one is finished, is totally erroneous. Projects have been delayed for months over the seemingly simple task of potting.

Let us agree that materials experts have already selected a limited number of polymer systems from a large list of available ones, selected because of superior electrical characteristics, low cure shrinkage, and low outgasing in vacuum. As examples, four approved potting compounds in use at Goddard Space Flight Center are listed again in the the table below:

TABLE XIII

Four high voltage potting compounds. Proportions by weight.

EPON EPOXY	Shell, Epon 828 resin, 50% Miller Stephenson V-40 hardener, 50% (or General Mills Versamid 140; 50%)
STYCAST EPOXY	Emerson & Cuming, Stycast 3050; 100 parts; Catalyst 9 hardener, 8 parts.
SOLITHANE (Polyurethane)	Thiokol C113 resin; Thiokol C113-300 hardner. Various proportions to give various formulations.
SILICONE RUBBER (Elastomer)	DOW CORNING SYLGARD 184 or 185 resin; 10 parts Dow Corning Sylgard 184 or'185 curing agent, 1 part.

That is not to say that alternates can never be considered. Adiprene, for instance, could be used instead of Solithane 113. Of the three general chemical types listed above the epoxies have many superior characteristics, but they are difficult to cut into for repairs, and they develop enormous compressive stresses upon cooling. The Solithane has many good qualities, but it has a tendency to crack, especially the softer formulations. The Silicone rubber has superior corona degradation resistance, but it has relatively poor adhesion[24] and is quite permeable to gases and water vapor. Poor adhesion seems to be a general characteristic of the rubbery state. So there is no one ploymer system that has all the desirable characteristics in one.

Obviously, this chapter can not address itself to all the problems that arise. nor is it a review of the more recent literature. This could be done if it was desired. Instead, a few selected topics that this investigator has had experience with during the last two years are discussed:

a) Surface preparation to enhance adhesion.

b) Internal stresses which try to pull the potting compound away from the surfaces.

c) Partial discharges or corona in voids created by detachments or by air bubbles.

Surface Preparation

This has partly already been presented in last year's report[24] because the major portion of adhesion measurements was performed then. Some of this will be repeated again here.

If one tries to get one substance to adhere to another, the forces that come into play are the essentially weak Van der Waals forces between neighboring molecules, those of the substrate and those of the adhesive. If the type of chemical bonding between the organic polymer and the most often inorganic substrate is compatible, then there will be inherently good adhesion. An example of this are the epoxies. The highly polar and surface-active nature of the epoxy structure provides both a chemical and mechanical interlocking with the substrate. The many available electron pairs from the oxygen atoms on the epoxy molecule provide sites for hydrogen bonding with adsorbed hydrogen atoms on metal or other surfaces. Other authors state that the hydroxylated metal oxide surfaces of the substrate supply sites on which the organic portions of the epoxy molecule can be attached. Now, however before all of this can be brought into action the liquid resin must be able to wet the surface. So, no grease, wax or scale should be present on the surface. The question arises as to the severity

of the cleaning process that is suitable for the device that is going to be potted. Let us first pretend the device is something entirely made of glass. The most commonly recommended cleaning here would be a chromic acid bath, followed by a mild sodium hydroxide rinse, followed by successive rinses with deionized water, then thorough drying. Or, something as drastic as letting a high voltage gas discharge impinge on the surface in a vacuum system, could be used.

However, most electronic circuitry can not be subjected to such drastic cleaning methods. Much more conservative approaches must be used, with solvents that will not damage or corrode the various types of materials, such as solder, beryllium copper, nickel, ferrite, glass-epoxy circuit board ect., ect. Here, one needs solvents that will remove ionic or salt contaminants and also grease and oil. The former would be attacked by hydrophylic solvents, the latter by hydrophobic. See Table XIV .

Freon TF is, of course, an excellent solvent for grease. A slab of solder-coated berylium copper rinsed with ethyl alcohol will still let water stand up in droplets, whereas one rinsed in Freon TF will let water spread out completely and be wetted completely.

As a minimum cleaning procedure I would recommend a series of agents:

1) Clean with deionized water,
2) Dry in oven at 70°C,
3) Clean with ethyl alcohol, 200-proof,
4) Dry in oven at 70°C,

5) Clean with Freon TF, particulate-free,

6) Dry in oven at 70°C.

Freon TF does cause silicone rubber to swell up, so no residue of it must be left on or in the module to be potted. Also, keep the Freon TF out of plastic bottles.

Table XIV Cleaning Solutions and Solvent Types[31]

Chemical Type	Examples
Hydrophobic	
Organic solvents	Naphthas, Xylene, Toluene,
Fluorocarbons	Freon TF, Freon TMC
Chlorinated Hydrocarbons	1,1,1,-trichloroethane, Perchloroethylene, Trichloroethylene
Hydrophylic	
Organic Solvents	Acetone, Methyl Ethyl ketone, (MEK) Methanol, Ethanol, Isopropalol
Ionic	Alkaline, Acid, Detergent water solutions
Nonionic	Detergent water solutions
Water	Tap, Deionized, distilled
Hydrophobic-Hydrophylic	Alcohol Naphtha (50:50 mix), Fluorocarbon-water emulsion containing a surfactant: Azeotropic mixture of fluorocarbon and acetone, blends of fluorocarbon & ethyl alcohol

The words "clean with" can mean several processes. Ultrasonic cleaning with the solvents selected has been found convenient by this investigator. Another alternative is vapor-degreasing with inhibited trichloroethylene or with inhibited trichloroethane, or now it is also possible to vapor degrease with Freon TF. Vapor degreasing is highly recommended for metals and should always be done with them as a first step, regardless of what other surface preparations are planned. One must of course check that the vapor degreasing temperature of the particular solvent used does not hurt the active devices in the electronics, or that the agitation of ultrasonic cleaning is not harmful. Strong sprays or stiff bristle brushing may sometimes be preferred to the fancier cleaning methods.

In many cases, but not in all, a sandblasting with sharp grits or a more gentle vapor honing with glass balls will greatly improve the adhesion. One has to be sure that after this process moisture is then kept away from the circuitry. "Laminates such as those used in printed circuits are much more readily affected by moisture after they have been sanded and processed than before."[35] This was also found true with the sintered glass high voltage feedthroughs used in the HEAO-A circuit distribution board.

If one wishes to do surface cleaning for maximum adhesion and for minimum water retention and minimum electrical noise then a more involved procedure described by Mr. Karageorge of Code 663.3 should be used; this involved a glass-epoxy circuit

board with resistors and condensors and high voltage feed-throughs with sintered glass insulation. This circuit fitted into a thick-walled brass box:

A) Clean the brass with undiluted, strong detergent. Vapor hone the brass with glass balls.

B) The glass epoxy circuit board, as delivered, has mold release on it. Therefore scrub it with toluene with stiff bristle brush. Place in ultrasonic bath of toluene for 1/2 hour. Follow this with an ethyl alcohol scrub and ultrasonic ethyl alcohol bath for 1/2 hour.

C) Repeat this routine after the electronic components have been soldered on.

D) Next subject the entire unit to a vacuum bake-out at 80°C (no active devices in this circuit) at 10^{-3} torr or better for 24 hours. The really first layer of absorbed water vapor does not leave until one goes to 10^{-5} torr. But this would immediately be reabsorbed upon exposure to air and so was not thought worthwhile doing.

E) The unit now has to be stored and carried about in a moisture free environment, such as a plastic bag with dessicant. Testing must be done in a dry-box.

F) Primer is applied with an airbrush or just by pouring and dipping. After curing of the primer according to manufacturer's directions the circuit is placed into a vacuum chamber. The potting compound is deaereated and placed into the vacuum system for one hour before pouring under vacuum. (The primer here was Dow Corning 92-019

the potting compound was Dow Corning 93-500 silicone rubber). Curing is done at atmospheric pressure, at 145°F as per manufacturer's specifications. It is allowed to anneal in the oven as the oven cools.

Some improvements could be:

1. It would be best if after vacuum bake-out the circuit could stay in the vacuum system and the potting compound be introduced through some sort of funnel and valve arrangement.

2. The vacuum system should have adequate sorption traps and slowly opening valves so that there will be no backstreaming of oil into the vacuum chamber.

3. The exhaust fumes from the mechanical vacuum pump should be vented directly to the outside, not into the general air of the potting shop.

Obviously, even after the most meticulous cleaning process one still needs a primer when potting with silicone rubber. In other words, cleaning will not improve upon the inherent adhesive strength of the types of atoms of the adhesive to the types of atoms of the substrate. In the case of silicone rubber and in the case of other compounds as well a chemical bridge is needed between the adhesive and the substrate, and that is the function of primers.

INTERNAL STRESSES:

One must understand that in a potted module there is a battle between the adhesive forces and internal stresses that might be acting in such a direction to tend to tear the polymer away from the components or from the potting case. For example, if one heats a potted module above the temperature at which it was cured and at which there zero stresses, then if one goes above the potting material will want to expand much more than the other materials and it will tend to tear away from the embedded components. The thermal coefficients of expansion of the potting polymers are approximately 10 to 100 times larger than for the ordinary substances like metals, glass, ceramics ect. Cooling will cause contraction and pulling away from the potting case. The fact that the potting compounds are rubbery does not help since these are also the ones that have weak adhesion. Potting cases, if possible, should be made of flexible, thin walled material that can move in and out with the changes in volume of the polymer. If thick-walled, unyielding casing has to be used then one can play some games by placing perforated epoxy circuit board pieces at regular intervals throughout the volume of the potting compound and cemented to the walls with epoxy. This serves to break up the long lengths of polymer into shorter ones and give more surface area to adhere to. However, sooner or later the body of cured resin will seek stress relief by detaching itself somewhere anyhow. Distributing circuit components fairly uniformly throughout the potted volume is helpful by permitting uniform stress relief. Fillers such as glass balls or mica sand can be looked at as millions of stress relief centers, the average effect being a reduction inthe aggregate thermal expansion coefficient of the filled potting compound. But then, one can no longer visually inspect for poor adhesion spots and has to use X-rays. Also, when fillers are used the internal compressive stresses are high because the Young's modulus is high, and the material is hard to cut into for repair.

PARTIAL DISCHARGE or CORONA:

This has already been discussed in Chapter III. The point here is that poor adhesion, if it has to be tolerated, should be encouraged to occur

where the elctric field is weakest, at the grounded case, far away from high voltage wires and electrodes and not near any sharp point or edges. A gaseous gap caused by poor adhesion will not have partial discharge pulses occurring init, if the potential drop across it is below the corona ignition voltage of the gap at the prevailing pressure within it. So it would do no harm, if it exists where the elctric field is very weak. One has to watch closely, of course, that the area of poor adhesion does not spread into areas where the elctric field is strong, or serve as crack initiation centers. Water vapor not completely baked out from filler sand may also cause intermittent discharge pulses, and for that reason bake-outs prior to potting are important.

In the final analysis it is the number of partial discharge pulses per unit time and their energy distribution that give a comparative clue to the quality of a given potting"job" and so should stand as the final test for acceptance or rejection. At present this can be used as a comparative tool. To establish absolute criteria in terms of pulse rate and energy content requires more experimental investigation.

REFERENCES

1. R.E. Keith, Potting Electronic Modules, NASA SP-5077 Technology Utilization Division, 1969, NASA Washington, D. C.

2. Kimmel, M., Technique for the Elimination of Thermal Stresses in Welded Electronic Components, Brief 68-10307, Tech. Util. Office, Marshall SFC, Alabama, 1968.

3. Isleifson, R.E. and Swanson, F.D., How to Measure Internal Stress in Resin Embedments Modern Plastics, November 1965.

4. Smith, M.H., Measurement of Embedment Stresses in Electronic Modules, National Electronic Packaging Conference, New York, N.Y., June 1966.

5. Heise, R.E., Jr., Residual and thermal Stresses in Potting Resins and the Development of Strain Gage Instrumentation for their Determination. Navord Report 5767 U.S. Naval Ordnance Laboratory, White Oak, Md.

6. Frankland, H.G., Sawyer, N.J. and Sanderson, I.S., Solder Joints 2/Measuring the Stresses in the Joints; Insulation/ Circuits, February 1971.

7. Bush, A.J., Measurement of Stresses in Cast Resins, Modern Plastics, February 1958.

8. Steele, D.V., Internal Stresses Developed in an Epoxy Resin Potting Compound During Long-Term Storage (AD-411514) Naval Ordnance Laboratory, White Oak, Md., 1962.

9. Sulouff, R.E., Properly Applied Strain Gauges Determine Uniaxial Stress on Component Leads, Insulation/Circuits, October 1974.

10. Wittenbert, A.M. and Malec, L. F., Mechanical Stresses Induced on Encapsulated Components Proc. 9th Elec. Insul. Conf. September 1969, p.101-104.

11. Dallimore, G., Stucki, F. and Kasper D., Measurements of Internal Stress in Electronic Encapsulating Resins with a Small Solid State Transducer, SPE Journal, June 1964.

12. Stucki, E.F., Fuller, W.D., Carpenter, R.D., Internal Stress Measurement of Encapsulated Electronic Modules. Electronic Packaging and Production, February 1967.

13 Bryant, Paul, Measuring Stress You Could Never Measure Before in Materials Engineering 8-72.

14 Noshay, A., How to Test and Improve Thermal Shock Resistance of Epoxies. Insulation/Circuits, May 1973.

15. Dauksys, R.J., and Kuhbander, R.J., Reduction of Thermal Coefficient of Expansion of Epoxy Potting Compounds, A74-35800, 1971

16. Dewey, Glenn H., and Outwater, John O., Pressures on Objects Embedded in Rigid Cross-Linked Polymers, Modern Plastics, February 1960.

17. Baker, Earl, Calculation of Thermally Induced Mechanical Stresses in Encapsulated Assemblies, IEEE, Transactions on Parts Materials and Packaging, December 1970

18. Frankland, H.G., Sawyer, N.J. and Sanderson, I.S., Solder Joints 1/Determining Causes of Cracking in Conformally Coated Solder Joints, Insulation/Circuits, January 1971.

19. Kerlee, Clarence, Selecting Encapsulants and Potting Compounds for Electronic Modules, Proceedings of the 10th Electronic Insulation Conference, 1971.

20. Lundberg, C.V., Correlation of Shrinkage Pressures etc. Industrial and Engineering Chemistry Vol. 6 June 1967, p. 92-100.

21 Sampson, R.N., and Lesnick, J.P.. Evaluation of Casting Resins Employing Strain Gage Technique, Vol. 35, February 1958, Modern Plastics.

22 Milligan, R. V., The Effects of High Pressure on Foil Strain Gages, Watervliet Arsenal, Watervliet, N.Y., 1964, (AD-611211).

23 "Epon Resins for Castings" Shell Chemical Company Catalogue 1967.

24. Renate S. Bever, Investigation of Problems Associated with Solid Encapsulation of High Voltage Electronic Assemblies; also Reynolds Connector Study. Final Technical Report. April 15, 1974 - April 15 1975, NGR 09-053-003, NASA Tech. Inform. Ctr , College Park MD or Goddard Space Flight Center Document X-711-75-221, GSFC, Greenbelt, MD.

25. Discharge Detection in High Voltage Equipment by F. Kreuger, American Elsevier Publishing Co., Inc., 1968.

26. "Corona Detection in Insulation Systems." Biddle Technical School, Plymouth Meeting, February 1970.

27. Detection and Measurement of Discharge (Corona) Pulses in Evaluation of Insulation Systems, ASTM D1868-73.

28. IEEE Recommended Practice for the Detection and Measurement of Partial Discharge (Corona) During Dielectric Test. IEEE Std. 454-1973

29. "Partial Discharge (Corona) Detection in Electronic Systems" P.H. Reynolds and C.J. Saile, 11th Electrical Insulation Conference, 1973, p. 341-343.

30. "Wide-Band Partial Discharge Detector" by E.A. Franko and E. Czekaj, IEEE Transactions on Electrical Insulation, December 1975, Vol. E 1-10, #4.

31. J.J. Licari, Plastic Coatings for Electronics, McGraw Hill, 1970.

32. Dan Grzegorczyk and George Feineman, Handbook of Plastics in Electronics, Reston Publishing Co., 1974.

33. E.W. Tankisley, Recommended Practices for Encapsulating High Voltage Assemblies X-752-74-247, Goddard Space Flight Center.

34. Industry Experts Answer Questions on Potting, Coating, Encapsulating Insulation/Circuits, p.55, September 1974.

35. Encapsulation of Electronic Devices and Components by Leonard Buchoff, The Center for Professional Advancement, Somerville, N.J.

36. Lee and Neville, Epoxy Resin Adhesives, p.21-10

37. Final Technical Report, April 15, 1974 - April 15, 1975, NASA Grant NGR-09-053-003 by Renate S. Bever.

38. Transient Diffusion through a Membrane Separating Finite and Semi-Infinite Volumes by James A. Barrie, H. Garth Spencer and Alexander Quig, Journal of Chemistry, England, p.2459, 1975.

39. Diffusion in Polymers, Crank, Academic Press, 1975.